TWO DIMENSIONAL COMPUTATIONAL FLUID DYNAMICS MODEL OF POLLUTANT TRANSPORT IN AN OPEN PIT MINE UNDER ARCTIC INVERSION

By

William B. Collingwood

RECOMMENDED:

Advisory Committee Chair

Chair, Department of Mining and Geological Engineering

APPROVED:

Dean, College of Engineering and Mines

Dean of the Graduate School

Apr 3, 2012

Date

TWO DIMENSIONAL COMPUTATIONAL FLUID DYNAMICS MODEL OF POLLUTANT TRANSPORT IN AN OPEN PIT MINE UNDER ARCTIC INVERSION

A

THESIS

Presented to the Faculty

of the University of Alaska Fairbanks

in Partial Fulfillment of the Requirements

for the Degree of

MASTER OF SCIENCE

By

William B. Collingwood, B.S.

Fairbanks, Alaska

May 2012

Abstract

A better understanding of the microscale meteorology of deep, open pit mines is important for mineral exploitation in arctic and subarctic regions. During strong temperature inversions in the atmospheric boundary layer—which are common in arctic regions during the winter—the concentrations of gaseous pollutants in open pit mines can reach dangerous levels. In this research, a two dimensional computational fluid dynamics (CFD) model was used to study the atmosphere of an open pit mine. The natural airflow patterns in an open pit mine are strongly dependent on the geometry of the mine. Generally, mechanical turbulence created by the mine topography results in a recirculatory region at the bottom of the mine that is detached from the freestream. The presence of a temperature inversion further inhibits natural ventilation in open pit mines, and the air can quickly become contaminated if a source of pollution is present. Several different exhaust fan configurations were modeled to see if the pollution problem could be mitigated. The two dimensional model suggests that mitigation is possible, but the large quantity of ventilating air required would most likely be impractical in an industrial setting.

Table of Contents

Page

List of Figures

Page

List of Tables

Acknowledgements

I would like to thank the National Institute for Occupational Safety and Health (NIOSH) for the financial support that allowed me to conduct this research. I especially wish to thank Mr. Chris Pritchard at NIOSH for his helpful suggestions. I also wish to acknowledge the support of my industrial partner, who generously agreed to share much of the operational and meteorological data used in developing numerical models for this project. I want to thank the members of my advisory committee: Dr. Sukumar Bandopadhyay, Dr. Rajive Ganguli, Dr. Nicole Mölders, and Dr. Michael Nelson. I also wish to thank all other parties who reviewed this thesis and provided constructive criticism. Finally, I especially wish to thank my advisory committee chair, Dr. Sukumar Bandopadhyay, for his advice and encouragement throughout my research and the writing of this thesis.

Chapter 1: Introduction

1.1 Scientific Rationale

The Arctic is the portion of the world underlain by a continuous layer of perennially frozen ground. The Arctic region also contains vast mineral resources. Mining of these resources is both an important and a major activity in the Arctic regions of several countries, particularly the United States. One of the challenges for deep open pit mining in a cold climate are atmospheric inversions. Inversion occurs when through some act of nature (there are several possibilities) the temperature of the air over the mine increases with altitude, and the cold, heavy, surface air is trapped in the pit (Bandopadhyay and Izaxon, 2005). In itself, an inversion is not hazardous. However, due to the presence of gases and particulates from diesel emissions, blasting, and other pollutants created by the mining process, the air within the pit can be severely and sometimes quickly contaminated, leading to serious health and safety consequences. To maintain and enhance the health and safety of the miners, effective measures are necessary to both minimize dust emissions and adequately ventilate the pit to dilute, disperse, and remove toxic pollutants (Bandopadhyay and Izaxon, 2005).

With the advancement of open pit mining technology, the depth to which minerals can be profitably mined has increased, resulting in deeper pits than ever before. In extreme climatic conditions, such deep pits tend to trap pollutants at the pit bottom due to air inversions and have presented a considerable challenge for the mining community to keep the pit adequately ventilated. Mine operators in cold regions are very familiar

with the problem, the severity of which can be gauged from Figure 1.1 and Figure 1.2. Several arctic or sub-arctic mines have reported the occurrence of air inversions, including the Kinross Fort Knox gold (Fairbanks) and Teck Cominco Red Dog lead-zinc mines in Alaska, BHP Billiton Ekati diamond mine in Canada, Boliden Aitek copper mine in Sweden, and the Mirni and Udachini diamond mines in Russia (Bandopadhyay and Izaxon, 2005). Even Rio Tinto's Bingham Canyon mine in Utah has reported local air inversions from time to time.

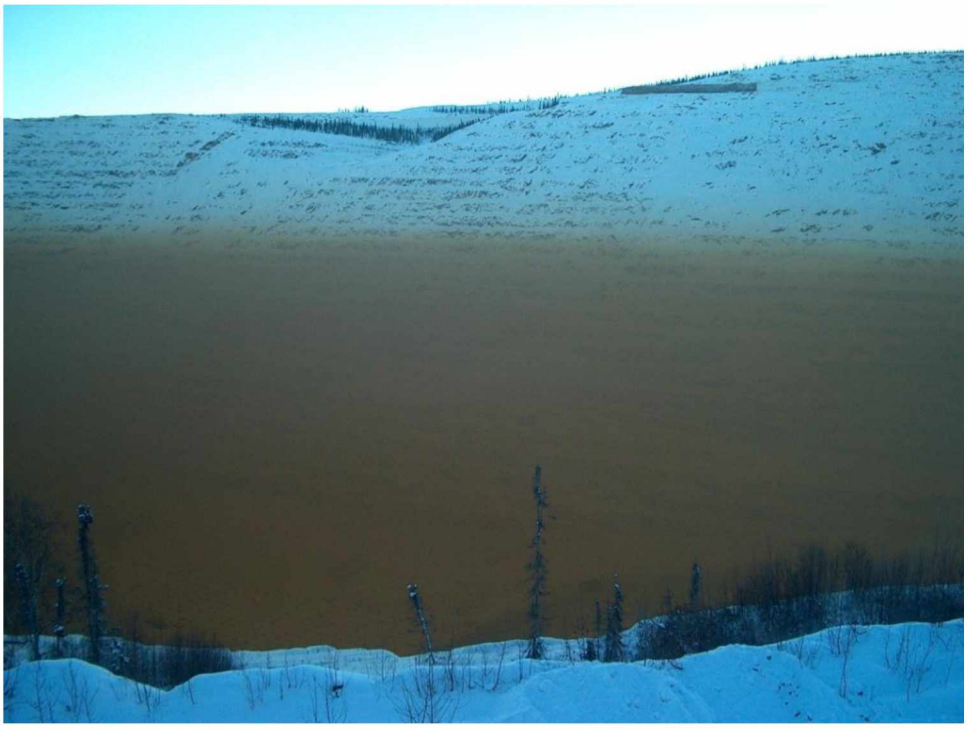

Figure 1.1: Typical Air Inversion at an Open Pit Mine, View 1

Figure 1.2: Typical Air Inversion at an Open Pit Mine, View 2

Minimizing the effects of air inversions has been recognized as an important aspect of healthy and safe environmental conditions (Bell et. al, 2003). Extreme cases of unsafe respirable atmospheres have been associated with air inversions in both large urban areas such as Los Angeles, California; Mexico City, Mexico; Sao Paulo, Brazil; Santiago, Chile; Mumbai, India; and Tehran, Iran, and in smaller cities like Oslo, Norway, Salt Lake City, Utah, and Boise, Idaho. During a severe inversion, trapped air pollutants form a brownish haze that can cause respiratory problems. The Great Smog, one of the most serious examples of such an inversion, occurred in London in 1952 and was blamed for thousands of deaths (Bell et. al, 2003).

Natural ventilation is the preferred means to deal with pollutants in open pit mines. The wind flow pattern in open pit mines is generally of recirculatory type (Collingwood et. al, 2012). The wind flow in the bottom of the pit is recirculatory and decoupled from the prevailing wind field, and conditions for natural ventilation are far from ideal. Increased wind speed is useful for the dilution and dispersion of air pollutants in open pit mines, but, even in ideal natural convection conditions, there may be an accumulation of pollutants at the bottom of the pit, thus necessitating artificial remedial measures. Temperature inversion can be expected to exacerbate this naturally occurring phenomenon. Further, the benches and overall pit slope generally impede natural ventilation (i.e., the dilution and removal of contaminants via natural windflow) in an open pit mine. Thus, a detailed examination of the cause-effect relationship leading to a predictive model for air inversion and mitigation of pollutants in arctic open pit mines is necessary. The phenomenon of temperature inversion and atmospheric pollution has been studied by such government agencies as the EPA (Winges, 1990) and other researchers (Baklanov, 1984). Unfortunately, the direct application of these studies and models to open pit mine ventilation or the specific situations in arctic or subarctic mines is site specific.

Natural ventilation, in general, has been the primary mode of dilution and elimination of pollutants in shallow open pit mines. Natural ventilation comes into an open pit from the windward side of the pit and flows in to the pit as a turbulent jet. This jet has two effects: (1) it re-circulates and redistributes the concentration profile of

pollutants already existing within the pit; (2) it may introduce substances (dust, for example) into the pit that do not originate in the pit.

To understand and analyze air inversions, the process by which such inversions and the consequent entrapment of pollutants take place must be investigated thoroughly. To solve the problem of air inversion in arctic open pit mines, the flow of air through an open pit mine must first be examined. The airflow through the mine geometry has several demarcated zones. An understanding of these regions can help to understand the flow phenomena and transport of advective contaminants; finally, it also determines the final concentration profile in a steady state situation.

Since pollution in a mine is anthropogenic and often emitted from fixed or mobile sources, any proposed solution must include consideration for these factors in addition to the atmospheric boundary layer (ABL) problem. In atmospheric science, the ABL is defined as the portion of the atmosphere that is most affected by the earth's surface (Wallace and Hobbs, 2006). The ABL typically ranges from 1 km-2 km in thickness. Above the ABL is the free atmosphere, the region in which surface friction is generally not felt.

Ventilation design for open pit mines requires the knowledge of the quantity of the pollutants that are liberated into the pit by various sources. The most important items in the total balance of pollutants in open pit mines are the stationary point sources (drilling rigs, excavators, loading machines) and moving sources (such as trucks). The transport of admixtures of pollutants (e.g., CO, NO_x, diesel particulate matter (DPM),

etc.) from these sources in an open pit mine is directly related to the aerodynamics of the airflow in the open pit. Evaluation of the atmospheric conditions in an open pit mine requires a determination of the concentration of admixtures. Therefore, it is necessary to predict the intensity of continuous point sources of pollutants and determine the regularities of the dissipation of admixtures from sources located at different aerodynamic regions in the pit.

The ABL can be defined as the part of the troposphere that is directly influenced by the presence of the Earth's surface and responds to surface forcings with a time scale of an hour or less (Stull, 2003). During daylight hours, a portion of the incident solar radiation is absorbed by Earth's surface. This radiation is partitioned into sensible and latent heat flux into the atmosphere and a comparatively small amount of heat that is conducted into the ground. The sensible heat flux from the surface heats the air immediately adjacent to the ground. This air then rises in convection currents to the top of the ABL, resulting in well-mixed air throughout the boundary layer (Figure 1.3).

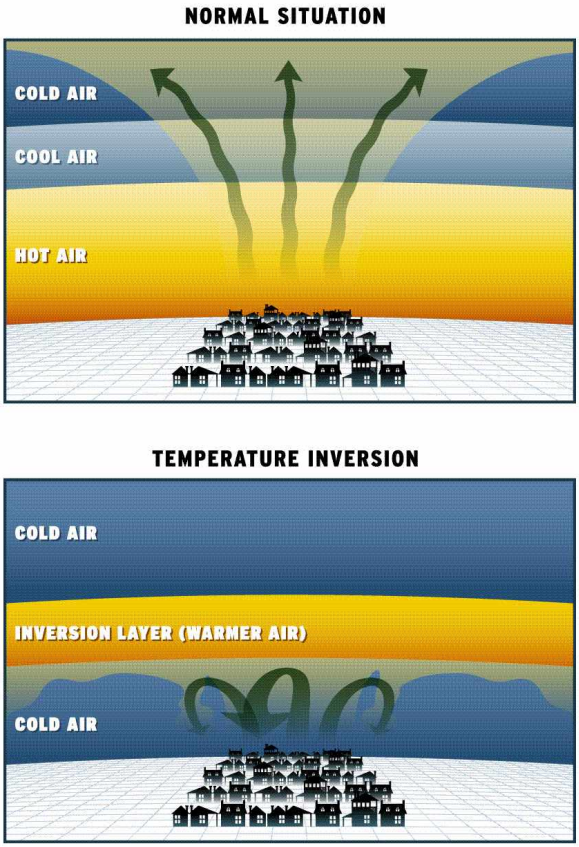

Figure 1.3: Convection Currents in the Atmospheric Boundary Layer

During an atmospheric inversion air, temperature will actually increase with height to the tropopause. In the arctic, lengthy periods of atmospheric inversion can occur in the winter months when days are short due to radiative cooling (Tran and Mölders, 2011). The deficit in solar radiation results in heat flow from the air to Earth's surface, cooling the air near the ground. The convection currents that normally occur during daylight hours cease, and the air in the boundary layer is no longer well mixed. If a source of air pollution is present—such as emissions from diesel equipment—the air

close to the pit bottom can quickly become contaminated with harmful levels of noxious gases.

Aerodynamically, the air current prior to its separation from the upper edge of the pit wall is a boundary turbulent layer, which is known in meteorology as the surface layer (Wallace and Hobbs, 2006). Concepts of direct flow ventilation systems applied to open pit mines has been cited in mine ventilation literature (Skobunov, 1962; Belousov, 1985; 1990). This ventilation system is distinguished by flow, without separation, around the leeward (i.e., downwind) wall of the pit (Figure 1.4). The flow of air masses and the transport of the admixture are determined by the aerodynamic parameters that become established before the flow around the open pit, as well as by the parameters, which are characteristics of the purely direct-flow ventilation system. Under actual conditions one would expect the airflow in the surface layer to stabilize prior to the separation of the flow from the top edge of the pit.

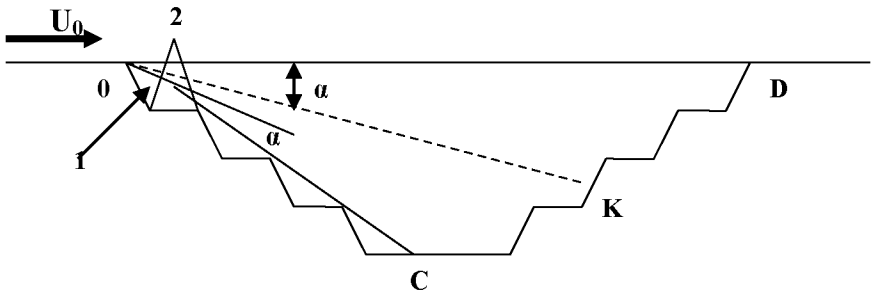

Figure 1.4: The Angle of Expansion of an Air Jet in an Open-pit Mine (Belousov, 1990)

The estimation of concentrations of fugitive dust or gas for an open pit mine has traditionally been done using EPA models such as the Industrial Source Complex model (TRC, 1985). Since the dust-producing operations in an open pit mine may occur at depths up to several hundred meters below grade, only a fraction of the fugitive dust generated inside the pit escapes to the surface, where it may then be transported beyond the mine boundaries. The two mechanisms occurring simultaneously that contribute to the pit retention phenomenon are: (1) the decoupling of the wind field in the pit from the wind field at the surface, and (2) the disposition and settling of particulates on the mine pit surface and along the pit walls. A dispersion model that does not account for the influence of pit retention may over-predict the downwind concentrations (Lowndes et al., 2008). The topographical impediment imposed by a mine pit disrupts the airflow above and inside the pit, so that the plume of gas and dust may not have the Gaussian distribution used in many dispersion models (Reed, 2005). Furthermore, most of the Gaussian plume dispersion models used for regulatory purposes have been developed to model downwind dispersion of dust from sources across a flat or undulating terrain, so these models cannot be directly applied to study the complex flow regimes that exist within open pit mines.

Published accounts of open pit mine ventilation, particularly with respect to air inversion, are practically non-existent in English literature. Researchers at the Kola Mining Institute, Murmansk region of Russia, and Yakutsk Mining Institute of the North, Soviet Academy of Sciences, have done some research in open pit mine ventilation.

Published research from these research institutes, mostly available in Russian, has been collected and translated into English.

The following sections contain a brief review of available literature describing air inversions as related to open pit mines. The literature cited in this chapter focuses on the phenomenon of temperature inversions in the atmosphere, the movement and quality of air in open pit mines as related to air inversions, and possible remediation measures that have previously been attempted in Russia.

1.2 Air Inversion

Air inversion is a specific instance of fluid inversion, which can take place in any fluid contained in or confined by a topographic trough. The word inversion, in this case, refers to the inversion of the normal vertical temperature profile seen in any large mass of fluid, such as air or water, in a natural containment. For water, such natural containments may be ponds or lakes, which are topographic traps within which water would naturally accumulate due to gravity. For air, natural containment takes the form of low-lying valleys between mountain ranges, lateral containment between pressure/temperature gradients, or even artificially created troughs like open-pit mines. Air inversion is significantly more discernible than water inversion in lakes, in terms of its extent in area and severity, its effects and consequences. Thus, further elucidation of the concept of temperature inversion will be undertaken with the specific phenomenon of air inversion in mind.

The lower atmosphere of the earth displays a definite temperature profile with increase in altitude. Jacob (1999) gives an example of such a natural temperature profile, as reproduced in Figure 1.5.

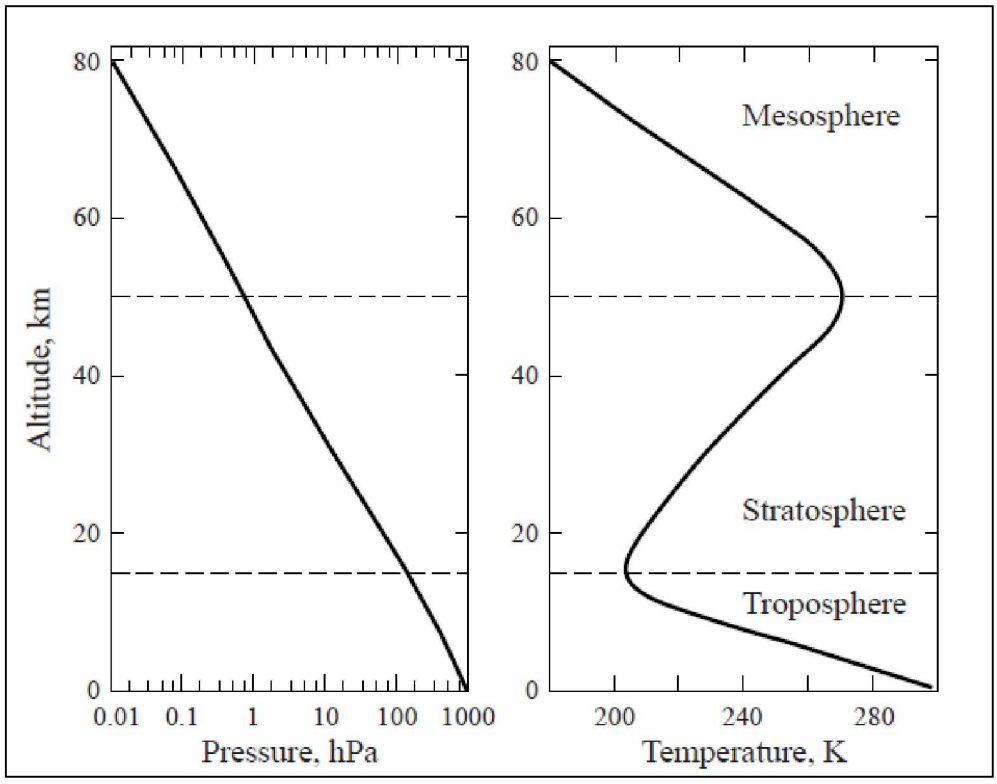

Figure 1.5: Mean Pressure and Temperature vs. Altitude at 30° N, March (Jacob, 1999)

Figure 1.5 shows the three principal layers that make up the earth's atmosphere: the troposphere, the stratosphere, and the mesosphere. The troposphere extends from the surface of the earth to between 8 and 18 km, depending on the season and the latitude. The upper limit of the troposphere is called the tropopause. The stratosphere extends from the tropopause to the stratopause, for about 50 km. The mesosphere, the next

layer above the stratosphere, extends from the stratopause up to a height of 80 km (Jacob, 1999).

Figure 1.5 also shows that within the troposphere, the temperature decreases with increase in altitude. Beyond the tropopause, however, the temperature increases in the stratosphere as altitude is gained, due to absorption of solar radiation by the ozone layer (Jacob, 1999). In the mesosphere, the temperature gradient again reverts to the negative. Figure 1.5 depicts the normal temperature profile that exists in the atmosphere, without the presence of anomalies such as an inversion.

Most human activity is confined to the envelope of the troposphere. The pollutants generated by activities such as motoring or mining are confined largely to the troposphere. This is because neither gaseous nor particulate pollutants have enough energy to climb to altitudes (greater than 20 km), and because the tropopause limits the transfer of pollutants to higher altitudes (Jacob, 1999). Jacob also notes that the primary effect of surface based inversion is seen only in the troposphere. Thus, it would be worthwhile to examine the characteristics of inversion in the ABL (i.e., the layer) closest to the earth's surface.

As stated before, the temperature gradient in the troposphere is negative under normal circumstances. Normally this gradient is maintained by the presence of sufficient solar radiation during the day to heat the earth's surface. This heat, which is first incident on the ground, is then re-radiated from the ground into the atmosphere, causing the layer of air immediately above to the ground to heat up. The higher a layer

of air is above the ground, the less re-radiated energy it receives, and its rise in temperature is proportionally less. This phenomenon gives rise to the temperature profile in the troposphere, as depicted in Figure 1.5.

A temperature inversion occurs when this natural cycle is interrupted due to lack of re-radiated heat from the ground. Since the primary source of the heat that the ground re-radiates is the sun, the relative position of the sun and the consequent characteristics of the solar radiation are the principal cause for surface based inversions. The most common change in the quantity of solar radiation reaching the ground occurs due to the motion of the earth around its axis. During the day, the surface of the earth exposed to the sun is heated, but after sunset the same ground cools down rapidly, interrupting the re-radiation of heat. This mechanism renders the layer of air closest to the ground cooler than the layers above, reversing the normal temperature profile described in Figure 1.5. During this time, a cap of temperature-inverted air settles on the land, trapping the layer of cold air next to the ground. This layer cannot rise by convection, nor can it readily mix with the layers above it, so all the pollution generated in the area is trapped within this layer, thus decreasing the quality of breathable air. Jacob (1999) noted that this phenomenon might contribute substantially to the pollution problems experienced in an urban area, more so if that area is located in a topographic trough like a valley. While this diurnal phenomenon is ubiquitous and detrimental to air quality, it is not a cause for urgent concern, because the period of its existence is usually

comparatively small, the situation being alleviated next morning as the sun rises. In arctic and sub-arctic areas, however, the problem takes on different characteristics.

In arctic and sub-arctic regions, solar radiation must travel through a significantly larger thickness of the atmosphere before reaching the ground, and it is incident on the ground at a flatter angle. Both factors contribute to reduce strength and effectiveness of solar radiation in supplying primary heat to the ground. In these regions, there is less daylight in the winter, leading to less effective heating of the ground. Cold winters in high latitudes depress the temperature of the air and the ground to a very notable degree, exacerbating the problem. These factors, working in unison, create conditions that generate inverted layers of air during the night and during the day, with durations of several days at a stretch (Mölders and Kramm, 2010).

The city of Fairbanks, Alaska, is located in a valley at 64.34°N, 147.87°W. The city thus has an extremely cold climate, and inversion is common here during winter (Tran and Mölders, 2011). Holty (1973) noted one such instance at the Fairbanks International Airport. The data were collected on December 17, 1969, at 2:00 P.M., and is depicted in Figure 1.6.

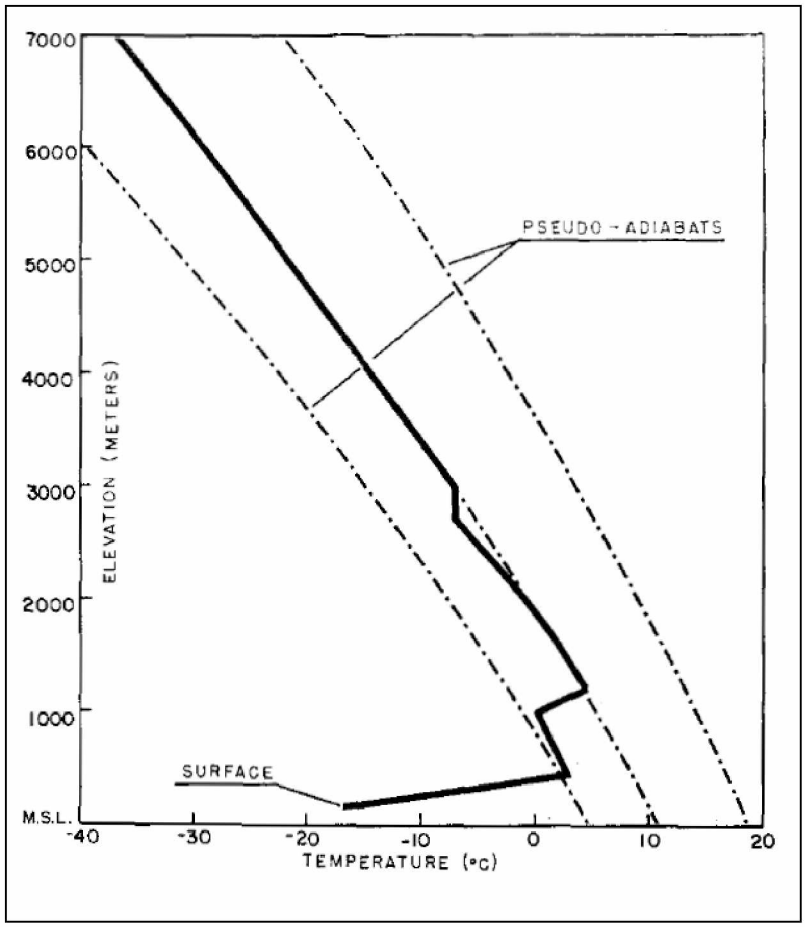

Figure 1.6: Temperature vs. Elevation at the Fairbanks International Airport on December 17, 1969, at 2:00 P.M. (Holty, 1973)

Figure 1.6 shows that inversion took place wholly within the troposphere. The inversion started at the surface and the inversion cap extended upward for a little more than 1,000 m. This inverted column was measured in the daytime, showing that inversions in the arctic and sub-arctic regions are not limited to the nighttime hours. Holty also notes that during the winter in Fairbanks, particularly under inverted caps of air, the CO and particulate concentrations in the breathable layers of air often exceeded the current EPA standard by as much as five times. He also noted that lead aerosols

have a much longer residence time in such cold air than is normally seen. All of this shows that, in arctic and sub-arctic areas, inverted air columns contribute significantly to the quality of air and pollution characteristics.

Hartmann and Wendler (2005) used the National Climatic Data Center Radiosonde Database, which has been recording twice daily radiosonde data from Fairbanks starting in 1957, to analyze the trends in surface based inversion in Fairbanks from December 1957 to February 2004. They classified the data into 'surface inversion' and 'no surface inversion' cases, the 'no surface inversion' cases being those in which incident solar radiation lifts the surface inversion, but an elevated inversion may still be observed. They reported no appreciable trends in the overall frequency inversions for the entire winter. However, it was seen that December and January had a slight decrease in the frequency of inversions, while February had a slight increase. When a surface-based inversion was detected, Hartmann and Wendler also determined the inversion's mean depth and its mean temperature gradient. Their findings are displayed in Figure 1.7 and Figure 1.8.

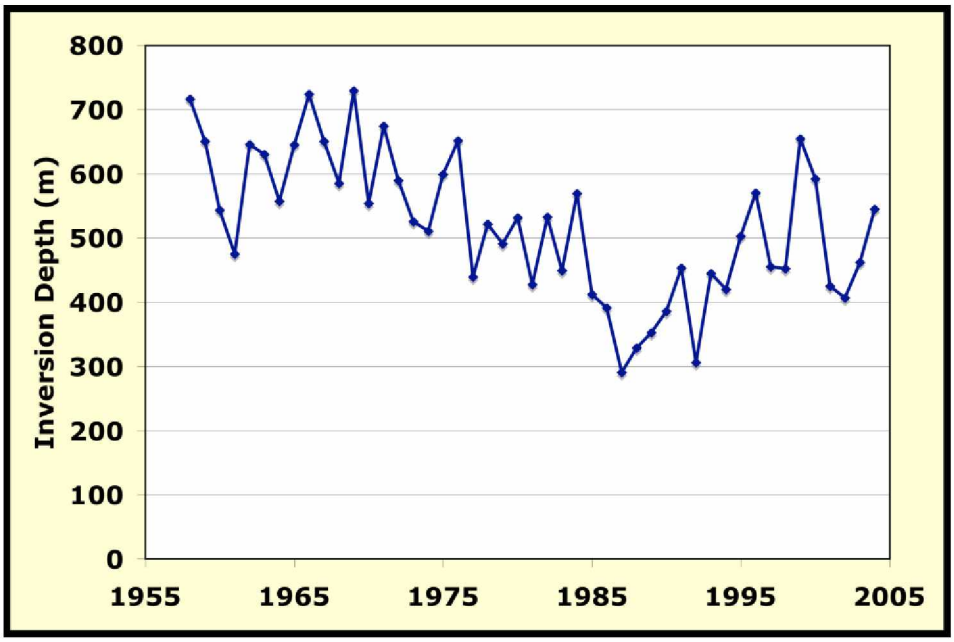

Figure 1.7: Time Series of Mean Winter Surface-Based Inversion Depth (Hartmann and Wendler, 2005)

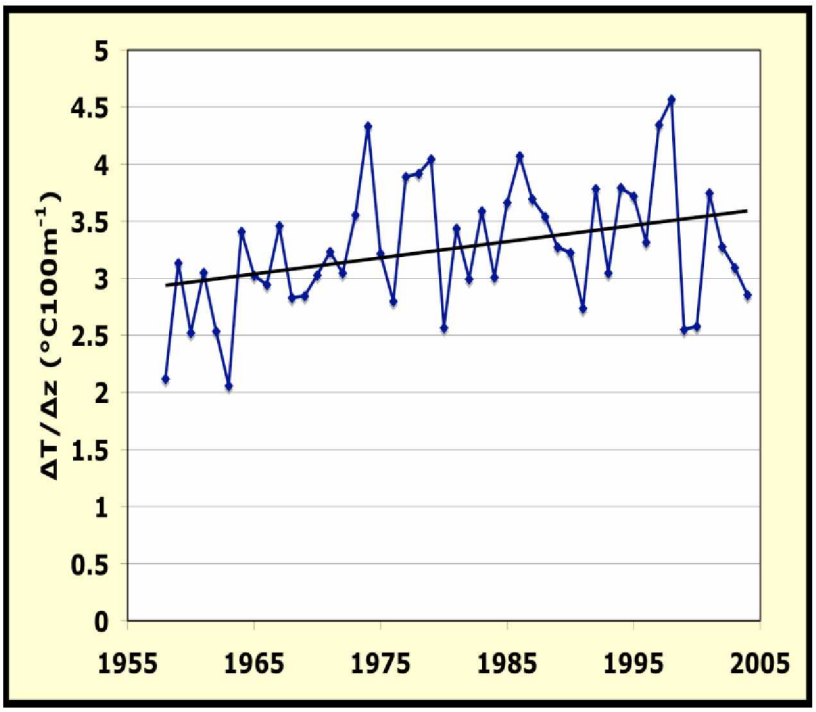

Figure 1.8: Time Series of the Mean Temperature Gradient of Surface-Based Inversions (Hartmann and Wendler, 2005)

Hartmann and Wendler reported that they observed a decrease in the mean inversion depth of 212 m, as depicted in Figure 1.7. They also observed an increase of 0.7° C per 100 m in the in the mean temperature gradient of the inversion along its altitude. The trends identified by Hartmann and Wendler may indicate that since the depth of inversion is decreasing and the temperature gradient along that depth from the surface upwards is increasing, the difference in temperature between the surface and the top of the inversion layer will tend to remain constant. Thus, the strength of the inversion may in future remain constant. At the same time however, the decrease in the depth of inversion signifies that the same strength of inversion occurs over a smaller altitude from the surface. The miscibility between the inverted layer of air and the layer overlying it depends on the strength of the inversion, and more specifically on the difference in temperature between the top and the bottom of the inverted layer. Thus, a thinner inverted layer could possible trap the same amount of pollution, with no change in the probability that miscibility characteristics may favorably increase. This behavior would make the quality of breathable air at ground level progressively worse, contributing to the already acute pollution problem. Hartmann and Wendler also noted that the most common direction from which wind flows in the Fairbanks area during inverted conditions is the northeast quadrant.

Reichardt and Reidy (1980) studied the concentration of polycyclic aromatic hydrocarbons (PAH) in Fairbanks in the winter of 1976-1977. They reported high values of PAH between December and February, and found an increase in PAH concentrations with an increase in the strength of inversions. They characterized a strong inversion as one in which the temperature gradient is greater than or equal to 7° C for the first 100 m altitude and a weak inversion as one in which the temperature gradient is less than 1° C for the same distance, with all readings being taken at 2:00 A.M. During strong inversions, the measured PAH concentrations ranged from 15.8 to 154.7 $\mu g/m^3$, with a mean of 86.2 $\mu g/m^3$. During weak inversion events, the PAH concentration were between 8.9 $\mu g/m^3$ and 48.3 $\mu g/m^3$, with a mean of 25.0 $\mu g/m^3$. Thus, it can be clearly concluded that pollutants are more effectively trapped in the inverted layer under strong inversion conditions.

More specific information regarding the effect of solar radiation in the formation of inversions and thus pollutant accumulation was given by Bowling (1986). She listed all possibilities by which solar radiation can affect pollutant accumulation in the high latitudes, and observed that the total daily solar radiation incident on the ground may heat up the ground and destabilize the lower atmosphere. This effect would promote mixing within and between the layers of air just above to the ground, and also lift the inversion cap due to the re-establishment of convection, thus aiding in the dispersion of the pollutants. The timing of the sunrise and the sunset as related to the daily variation in pollutant generation (morning and evening commuter traffic) may also play a part in

pollutant accumulation. During peak winter in Fairbanks, the nighttime inversion remains strong during the morning peak hour, is attenuated about noon, and is re-established before the evening commuter traffic begins. This behavior has led to extremely high concentrations of CO (15 ppm or more) being recorded in Fairbanks. The rate of change of incident solar radiation after sunrise and before sunset, and the intensity and wavelength distribution of the radiation around noon, are also major contributing factors to pollutant dispersal or accumulation. In particular, some pollutant molecules are likely to dissociate photo-chemically in the presence of sunlight, thus transforming into less harmful substances.

It was also noted by Bowling that in many high-latitude areas, the presence of surface winds prevent the formation of strong inversions, although weaker inversions may still persist. However, Fairbanks is situated at a valley bottom, which imposes restrictions on wind. In addition, wind speed in Fairbanks during winter is known to be low (typically less than 2 m/s). As a result, large eddies can be found over the Fairbanks valley. Such eddies, while aiding in dispersion, may be confined vertically by atmospheric stratification, and simply move the pollutants around within the same layer of air rather than mixing them vertically.

Dimitriev and Shadrin (1973) noted that apart from dust and individual species of gases (like CO, CO_2, NO_x and SO_x), the chemical mix present in an open-pit mine may react in the presence of an appropriate amount of solar radiation to form what is known as photochemical smog. A photochemical smog includes photochemical aerosols and

toxic photo-oxidants like aldehydes, ketones, organic and nitrogen peroxides, ozone, etc. Aerosols are known to cause respiratory and ocular problems.

The presence of strong solar radiation may help chemically transform some species of contaminant molecules present in the open-pit air. Such transformations may increase or decrease the noxious potency of the resultant molecules with respect to the original. The reactions are, however, strongly dependent on the concentrations of the reactant molecules. During winter months in the arctic, low insolation conditions result in limited time during which these transformations can take place. Reaction rates also tend to be lower due to cold temperatures during the winter months. Photochemical smog is a markedly visible aberration from acceptable breathable air quality.

1.3 Previous Modeling Approaches

Meteorological and tracer experiments have been conducted to investigate the dispersive characteristics of valley atmospheres (Allwine et. al, 1997). These and other studies have led to the identification and more complete understanding of key physical processes governing dispersion of pollutants in valleys. The important physical processes include up and down valley wind speeds, up and down slope winds, turbulent diffusion, convective boundary layer growth, temperature inversion decent, nocturnal temperature inversion breakup, tributary flows, cross-valley circulations, and interaction with above-ridge top winds. Studies on the flow and dispersion of diesel exhaust in underground airways, from point and moving sources, have also been conducted by

Bandopadhyay and Ramani983, 1984, 1985, 1988). However, while application of these models is limited—because the geometry of and airflow characteristics in open pit mines are much different than those in underground mines—the findings are still relevant to the study of the mine ventilation conditions in an open pit mine.

In an open pit mine, the upward heat flux also develops a convective boundary layer (CBL) over the pit surfaces, but, in contrast, the heated pit slopes cause warmed air parcels to flow up-slope. These up-slope flows remove pollutants from the base of the temperature inversion and maintain the mass continuity, which results in a general circulatory vertical movement over the center of the open pit (Allwine et al., 1997). The CBL growth and descent of the inversion are both functions of sensible heat flux, atmospheric pressure, air density, solar flux, pit potential temperature lapse rate at sunrise, and the warm-air advection rate above the pit.

The subject of natural airflow in open pit mines has been under study for some time, particularly in the former Soviet Union (USSR). Researchers have worked on the mechanism of wind flow, along with a study of the factors that influence such flow. Some of these studies are described below.

Vershinin (1976) compared the effectiveness of two schemes for ventilation of open pits, using either upward or downward air motion to remove contaminants. Vershinin's work is notable as an early, physical model of open pit ventilation. He assumed a contaminant level of 5 to 6 times greater than the permissible level and calculated the time required for the contaminant level to reach the permissible level, given an initial

flow pattern of a given velocity and diameter. The source of the assumed flow was not specified, but Vershinin briefly mentions the use of artificial heating devices, turboprops, and turbojets for such purposes.

Vershinin states that, all other things being equal, the upward ventilation scheme is preferable because the pit sides will be swept by pure air, with the contaminated air being removed by flow up the center of the pit. Vershinin's solution for both cases is based on the basic equation of discontinuity, in which the rate of descent of the boundary between the contaminated and uncontaminated zones, ω, is given by

$$\omega = \int_F \frac{\rho u dF}{\rho_n S_q} \qquad (1)$$

Where:

F = cross-sectional area of the current,

$\tilde{n}$ = density of the air,

u = rate of airflow within the current at a given level z,

$\tilde{n}_n$ = air density in area around the current at cross-section F, and

S_q = cross-sectional area of the pit at level z.

When the current is isothermic and the temperature gradient in the pit is adiabatic, the expression is simplified to

$$\omega = Kz/S_q, \qquad (2)$$

Where:

K is a proportionality constant, defined by Abramovich as

$K \approx 0.31(W_0 d_0 \cos\alpha)$, where

Q_0 = initial flow rate of the current, and

d_0 = initial diameter of the current.

From these equations, Vershinin derived solutions for $\tau\uparrow$, the ventilation time required with upward airflow, and $\tau\downarrow$, the time required with downward airflow. The integrated equations were solved by computer for two simple truncated cones, one with a wall slope of 14°20', the other with a wall slope of 35°25'. A table was prepared showing the relative efficiencies of the two ventilations schemes for pit (cone) volumes ranging from 100×10^6 and 600×10^6 m^3 and contamination volumes ranging from 50×10^6 and 550×10^6 m^3. In general, when the volume of the contaminated zone was relatively small, upward motion cleared the pits faster, but the results were far from clear.

This model has two serious shortcomings. First, no field data is presented to verify the model. Second, the model assumes that current is isothermic and the temperature gradient in the pit is adiabatic. The latter shortcoming is particularly acute for the present study, which seeks to analyze situations (inversions) where the temperature gradient is specifically non-adiabatic.

An early study by Aloyan et al. (1982) describes the use of a three-dimensional, nonstationary numerical model for open pit ventilation. The primary challenge in this study was adapting the standard method to microscale atmospheric processes, which required accurately accounting for the surface relief. This goal was accomplished by describing the surface (the open pit) using a grid of rectangles, which could be altered to

achieve the desired configuration and accuracy. The following problems were solved with this model:

1. Simulation of the winds in a quarry under various thermal conditions (stable, unstable, and equilibrium stratifications) and examination of the effects of an external wind on the temperature inversion in a quarry.
2. Estimation of the time interval for ventilation of a quarry with constantly acting pollution sources and after instantaneous large-scale rock blasting, the study of the time dependence of the ventilation in the presence of various factors (temperature stratification, external wind, geometrical parameters of quarry, and source output).
3. Determination of maximum quarry depth from the viewpoint of ventilation.
4. Simulation of air motion in the quarry due to the temperature inhomogeneity at the surface, with estimation of the effects of solar radiation and the diurnal temperature variation on the ventilation.
5. Dependence of the ventilation processes on the absorbing properties of the surface for various pollutants.
6. Examination of the scope for artificial ventilation under various meteorological situations and various locations of the sources and sinks.

The authors showed the results for natural ventilation of a typical quarry in northern latitudes with characteristic dimensions R (radius) = 600 m and H (depth) = 300 m (Figure 1.9). The figure shows the concentration of pollutants in the pit after three, six, and nine hours. The figure shows reasonable results.

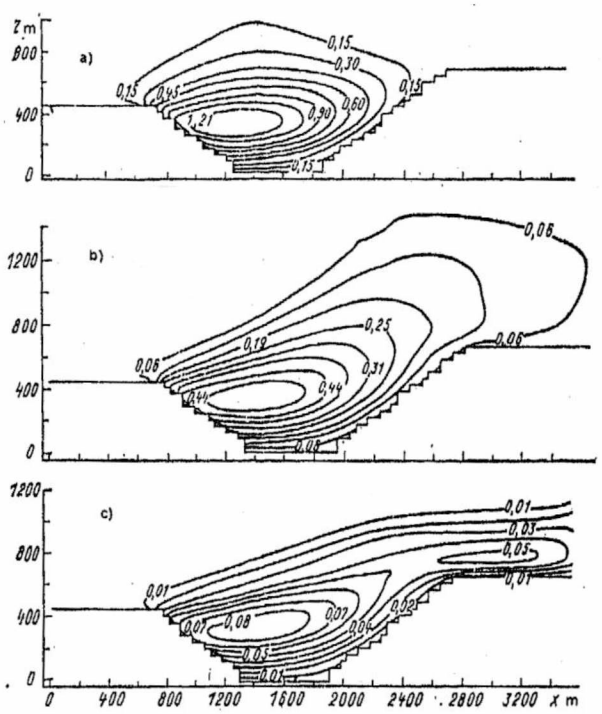

Figure 1.9: Lines of Equal Concentration for a Pollutant in a Propagating Aerosol Cloud in a Quarry, at 3-hour Intervals (Aloyan et al., 1982)

Measurements were made in the Saam and Olenegora pits in the Kola Peninsula, and there was "...good qualitative agreement between the calculated distributions and actual measurements." However, the actual data was not presented.

Baklanov (1984) constructed a model similar to that described by Aloyan et al. (1982), with the goal of solving the following problems:

1. Propagation of an initially specified cloud or impurities in a pit over time.
2. Atmospheric contamination with local or point contamination sources acting steadily or temporarily.

3. Estimating the time interval of ventilation with a specified discharge for the cases of natural or artificial pit ventilation.
4. Studying the propagation of impurities as a function of the absorbing properties of the surface and the interaction between the impurities.
5. Estimating the background contamination of the atmosphere and immediate surroundings with the release of a gas/dust cloud from open pits.
6. Suppression and neutralization of the extraneous impurity cloud using chemical reagents and moisture jets.

Baklanov's results for propagation of an aerosol cloud were almost identical to those of Aloyan. He also considered emanation of impurities from a point source, and diffusion of impurities in under stagnant conditions. Again, field measurements were made, and "…sufficiently good agreement" was found between those measurements and the model results. Also again, no data to support the study were presented.

In 1986, Baklanov established a thermodynamic model of the dynamics of open pit ventilation systems. The model can simulate the diurnal change that takes place during the differential solar heating of the surface during the day and the release of this energy during the evening. In the 1986 model, the volume of the pit was interpreted as a system where the kinetic energy of a directed movement of the air is lost to forces of friction (mainly turbulent friction). For the air movement in the pit to be maintained naturally, external energy sources are necessary to supplement the reserve of kinetic energy. These include factors such as the energy of background currents and the influx

of solar energy. With regard the energy flux through the surface of the region under study the main factors forming the natural ventilation of pits were said to be the flows of kinetic and thermal energy of background processes through the boundary with the outer air mass and the thermal energy flux through the ground surface.

The heat flux from the pit surface into the atmosphere is in many cases (especially in the absence of winds) was defined as the main source forming the microclimate and the atmospheric circulations in the pit. It is affected by several factors and is determined by the radiative and thermal balance on the discontinuity surface between the atmosphere and the ground. The hydrometeorological regime of the pit atmosphere, therefore, was described in combination with the energy exchange of the ground and the atmosphere. The mathematical models describing the dynamics and the atmosphere in the pits were combined with the system for calculating the thermal and radiative balance on the surface and the model for the thermal regime of the ground. The problem of microclimate in the pit has been reduced to a description of the energy interactions in the "atmosphere-surface-ground" system. The integral identity and the energy balance equation were thus written for the entire "atmosphere/surface/ground" system. In 1995, Belousov noted that because the air above the pit cools slower than the air above the ground at the same altitude, there is a resultant horizontal flow of air toward the pit. He also noted that the air above the pit in such cases would rise, due to the standard adiabatic process, to a maximum height of:

$$H = \Delta t_h / (\gamma_a - \gamma) \qquad (3)$$

Where

H is the maximum height air above the pit top can rise (m),

Δt_h is the horizontal temperature difference (degrees),

γ_a is the adiabatic vertical temperature gradient (degrees/m), and

γ is the actual vertical temperature gradient (degrees/m).

This rise in the air could result in the removal and mixing of pollutants from the pit, provided the pollutants generated at the pit bottom reach the top layers of the air in the pit. In very cold climates, the movement of pollutants from the bottom to the top of the pit is severely restricted due to lack of energy in the bottom layers and possible inversion caps in place. Belousov noted that it has been observed that the surface flow at the very top of the pit is coupled with flow from the surface adjacent to the mine, while the air mass at the bottom of the pit is decoupled from the airflow at the top of the pit. Such decoupling and lack of energy in the bottom layers of the air in the pit will actively hinder removal of pollutants from the bottom of the pit, which is where most of the pollutants are generated. This finding underlies the need for an artificial ventilation schemes to introduce fresh air into and remove pollutants from the lower reaches of the mine.

In earlier papers, Belousov (1985, 1990) noted that the ventilation of open pit mines is affected by the relief of the surface near of the mine over which the wind flows before it approaches the pit, as well as the geometric properties of the pit itself. The model scale chosen in the study was 1:1,000. The study also used “air walls,” which the author

defined as a system of vanes or wings on the windward side of the model pit that were used to direct the natural flow of wind toward the pit-bottom. The author found that the removal of pollutants from the bottom of the mine was aided by the placement of air walls. Such removal was also aided by the removal of ordinary waste dumps from the leeward side of the mine because such dumps increase the effective depth of the pit, decreasing the reach of either the turbulent of the laminar flow zones into the mine. The author has also reported a close agreement with observed results of velocity profiles in mines. However, the incident air velocity in the model that was used to solve the problem was much greater in magnitude that can be reasonably supported. The model scale being 1:1,000, the air velocity used for solving the problem was roughly the same as the observed velocities in actual mines. It would be more reasonable to scale down the velocities used to numbers more representative of the scale in which the model was placed. In addition, the author predefined the expansion angle of the air jet entering the mine (primarily based on the wings placed on the windward side of the flow) to $\alpha = 15°$. This behavior is schematically described in Figure 1.4.

In Figure 1.4, α is the opening angle of the free plane (expansion of the jet), set at 15°; *1* indicates the position of the shield (wing); *2* indicates the position of the mast on to which the shield is attached.; U_0 is the incident velocity of wind across the pit in m/s.

In the 1990 paper, Belousov regarded the presence of the vanes as an aid to the natural circulation occurring in mines. He stated that in the absence of the vanes or shields, the air entering the pit with a velocity U_0 would directly ventilate the volume of

the pit marked *OKDO* on the cross section in Figure 1.4. The section *OCKO* would be ventilated by recirculation. With the presence of the vanes, however, the lower boundary *OK* is moved downward, and converges with *OC*, thus ventilating almost the entire pit.

There are several problems with this approach. As described before, there is hardly any crosswind registered when capping inversions are in place, or in extremely cold weather, even without a capping inversion. This fact negates the possibility that such natural winds may be marshaled to aid in removal of pollutants. Setting of the angle α at 15° may also be erroneous.

In a 1995 study, Belousov analyzed the conditions under which surface breezes would induce circulation in an open pit. Such breezes result from temperature differentials, which lead to heat and mass transfer, and horizontal temperature and pressure differentials, ultimately resulting in airflow toward the lower-pressure sections. The flow velocities, depending on the magnitude of the pressure drop and the scale of the surfaces of the sections, may be as great as several meters per second.

The probability of a breeze is determined by radiation and circulation factors. The natural conditions under which breezes will develop are either clear or slightly cloudy weather, little or no baric wind, a generally stable state of the atmosphere in the particular district, and the presence of sufficiently large horizontal differentials of air density, determined mainly by the air temperature. The stability of a breeze will depend on the rate of heating of the air mass of the low flow to a certain temperature in the

region of the relatively warm section; with an inadequate rate, the circulation may either die out or pulsate.

The difference in radiation conditions between the pit itself and the adjacent territory is responsible for the existence of significant horizontal differences of temperature. For example, many years of data from atmospheric probes at the Sibai mine have shown that a temperature difference as great as 7°C may exist between the air above the center of the pit at the surface level and on a meteorological platform at a level of 2 m located 100 m from the pit. With above-freezing temperatures at night and in the morning, the density gradient is usually directed toward the pit. The magnitude of the gradient decreases toward midday, and the direction of the gradient changes. During the cold period of the year, the gradient is very nearly zero. This behavior indicates that a breeze between an open pit and the adjacent territory is most likely to be observed in the warm part of the year, when the amplitude of the diurnal variation of air temperature and the difference in radiation conditions are at their greatest.

Belousov calculated the minimum temperature differential, between the air above the pit and the adjacent air mass, required to generate a stable, recirculating breeze. For above-pit temperatures (T_p) ranging from 233 to 313 °K, and actual temperature gradient (γ) from 0 to –0.04 °K /m, these differentials varied from 2.33 to 6.33 °K, increasing with increasing T_p and decreasing γ. The magnitude of this temperature differential is also affected by the ratio of pit depth to pit radius, and the ratio of the

distance through which the air mass or breeze over the pit will pass when heated sufficiently to create a convective rise to the pit radius.

Peng and Lu (1995) constructed a 1:1,000 scale model of a surface mine located in southern China. Their study focused on the movement and circulation of wind in deep open pit mines. An important part of their work consisted of conducting experiments to verify the claim made by Belousov and others that the angle α was approximately 15°. They reported a wide variation of the angle, from 6° to 32°, and observed that the angle was not only influenced by the topography surrounding the mine, but that it was also related linearly to the pit depth. They reported the relation to be:

$$\alpha = -1.234 + 0.0172H \qquad (4)$$

Where:

α is the angle of expansion of the jet (degrees), and

H is the height or depth of the pit in (m).

Peng and Lu concluded that most of the pit would be ventilated by recirculation under natural ventilation conditions. To augment natural ventilation and recirculation, they used natural ventilation guides in the form of trumpet-shaped air walls or vanes, to simulate the Venturi effect. They reported that the recirculation area in the deeper regions of the pit disappeared with the introduction of the vanes. This mitigation technique, however, had the same drawback described previously: In the absence of a crosswind, there is no possibility of natural circulation to aid in removal of pollution.

When the concept of the angle α is examined thoroughly, two significant problems can be noted. Firstly, the reach of the vane or wing system to influence the angle expansion may have been overestimated. All of the models described in the literature so far have been scaled-down models. The problem with this approach lies in the nature of the interaction between the wind and the model environment. Turbulent or laminar airflow, when injected into a model space, would be influenced by the dimensions of that space. In a scaled-down model, the airflow would be shaped by a much smaller space in all three dimensions, thus restricting its movement and creating more turbulence, but on a smaller scale. While this situation might be claimed to reflect actual conditions in mines, there are two significant problems.

First, many of the models used natural or near natural wind velocities as an input. This approach creates a huge disparity in scales between the velocity and the volume on which it would work. Thus, the eddies and the recirculation zones that are formed in the models are grossly over-scaled. When an eddy is observed in the model, its location, approximate dimensions, and area of influence are noted, and then scaled up according to the model scale. Thus, the resultant (scaled-up) eddy would be very large and would likely never form under natural conditions.

Additionally, when a scaled-down model is used, there is very little or no control over the timescale on which processes take place in the model. For example, if a small source of gaseous pollutant is placed at a location in the model, the gas emitted from it will diffuse according to the diffusivity constant, which can be expressed dimensionally

as [L^2/T], where L is length and T is duration. This ratio indicates that the gas, whether or not carried by convection, will travel at roughly the same rate in a model that it would in the natural environment, with minor adjustments for temperature, pressure and concentration gradient. The resultant concentration profile in the model would not be realistic in that case.

The second significant problem with the application of the angle α lies in the nature of the resistance that inflowing air faces once it enters the pit. A detailed examination of the concept of α in the literature, along with the diagrammatic representations of the same, suggests that it was assumed that the inflowing air would have a momentum sufficiently large to displace the existing air in the pit with little compression of the inflowing air. The inflowing air would thus be able to flow wherever its momentum directed, without interference. This appears not to be the case in reality. The air toward the bottom of the pit is cooler, therefore denser, and contains pollutants in both gaseous and particulate form, so it has a high inertia. If the inflowing wind does not have a sufficient velocity or mass, it is quite possible that the inflow will be compressed and, on meeting a more massive and denser body of air, the path of its momentum will deflect. Such deflection, coupled with turbulent mixing, will induce the formation of recirculation or eddy zones in the upper reaches of the pit (where the inflow wind meets the in-situ air). These turbulences will destroy the linear motion of the inflow wind assumed in the formulation of the angle α, mixing the sharply delineated boundary layers, and invalidating the angle as an indicator of ventilation.

Peng et al. (1995) presented a series of wind tunnel tests conducted on a scaled open pit mine. The geometry of this model was complex. It was based on an actual open pit mine located in southern China. As in other studies, a recirculatory wind profile was observed in the pit bottom. This recirculation increased with increasing pit depth. The 'wind expansion angle' that separates the recirculatory region from the region of uniform flow was found to vary between 6° and 32° Smoke concentration (here used to simulate the concentration of irrespirable gases and harmful dusts) increased with increasing recirculation in the pit. Finally, the application of vanes to guide the wind into the bottom of the pit was found to be an effective means of ventilating the pit.

Meroney and Grainer (1992) presented another wind tunnel test of an open pit mine. In this particular situation, an open pit coal mine in an inverted position was modeled. Accumulation of harmful gases related to spontaneous combustion of coal and shale is of particular concern in this situation, especially under conditions of atmospheric inversion. In the wind tunnel, conditions of atmospheric inversion were simulated by capping the open pit with a false roof and creating temperature variations using resistance heaters, using a 1:600 scale model of a typical open-pit coal mine. The study focused on the dispersion pattern occurring in the presence of clearly-defined and stable stratified zones in the atmosphere above the mine. The scale model was placed on the roof of the Monash Environmental Wind Tunnel. Vertically and horizontally spaced heating elements were placed upwind of the model, so air flowing in the wind

tunnel would pass over the heating elements resulting in differential heating and the resultant stratification sought in the modeling effort. The scaling of the flow was achieved by considering the Froude number for the scaled down mine and adjusting the gravitational component of the Froude number for temperature due to heating. The behavior and movement of contaminants in the pit by was studied by placing visible contaminant sources in the pit. The penetration of flow into the pit was found to be a function of Froude number and the magnitude of the inversion. The "…general behavior of the flow was found to agree with previous atmospheric experience, salt-water drag tank models, linear perturbation analysis, and computational-fluid-dynamics models."

This approach can generate a multitude of problems. The stratification achieved by preheating the air before it reaches the mine pit, presumably generates the stratified layers, while the air at the pit bottom, unaffected by the heat remains cooler. The heated air is then swept past the model pit by momentum imparted by the fan in the wind tunnel, which, with limited mingling with the air at the pit bottom, preserves the stratification. However, the momentum, otherwise expressed as the velocity head of the fan would have to unrealistically high for the scaled down model (even with the Froude number adjustment), to achieve this. Thus the stratification in the model may not reflect actual conditions, and the actual boundary layers between the dynamic and static layers of the wind-flow may not correspond to those predicted by the model. Additionally, the scenario modeled seems unrealistic: it seems unlikely that a flow of such warm air with high lateral velocity would enter the stable atmosphere of a mine pit

during the night. The Froude number adjustment would be difficult to make in this case.

The Froude number depends on the hydraulic length of the system, which in this case would amount to the mine profile. As posited by the investigators, the full length of the mine profile is not in use by the flowing air as in does not affect the lower reaches of the pit. This fact, coupled with the observation that the boundary layer between the static and the dynamic layer of air is spatially variable, would indicate that the effective length for the Froude number would be significantly variable, and thus very difficult to evaluate.

Moreover, the placing of the scaled down model in an inverted position on the roof of the wind tunnel may cause additional problems. After heating, the airflow is pushed by momentum on to the mine pit. Of course, warm air tends to rise. When on top of the pit, even with the momentum impetus, the air will tend to rise. In the present case, this rise will take it into the pit, rather than out of it, as is naturally valid. This behavior will destabilize the inverted layer that the experimental setup attempted to create. Contaminant transport would also be affected by this phenomenon. In the contaminant distribution contours shown in the investigation, it is clear that contaminants from sources placed on the downwind slope of the mine display a tendency to expand into the mine. This expansion would only happen if the prevalent convection currents were forcing the flow of the contaminants towards the bottom of the pit.

Fomin (1996) conducted a thorough investigation of the nature of convective flow in deep open pit mines. The mathematical model generated during his investigation took into account various factors that affect the flow of air and contaminants in a mine in the absence of a forced convective system. Because a forced convective system could also include inflow of air into the mine by atmospheric convective processes, Fomin assumed that there was no airflow near the mine, and that only convection from the heated walls of the pit could impart energy and therefore velocity to the wind. In the model, the contaminants (O_2, N_2, and CO_2) were injected into the pit uniformly from the sides and the bottom of the pit. This injection also carries heat into the model, as exhaust gases are hot. Fomin defines the Grashof number (for heat) as follows:

$$Gr_q = \frac{g\beta q h^4}{\lambda \upsilon^2} \qquad (5)$$

Where:

g = acceleration due to gravity,

β = volumetric expansion coefficient,

q = heat flow due to exhaust gas,

h = depth of the pit,

λ = coefficient of thermal conductivity of air, and

ν=– kinematic viscosity coefficient of air.

He also defines the Grashof number for mass balance as follows:

$$Gr_R = \frac{gR_i h^4}{\rho D \upsilon^2} \qquad (6)$$

g = acceleration due to gravity,

R_i = rate of mass injection of a particular gas (i varies from 1 = 4 for the four contaminants,

h = depth of the pit,

p = density of the composite gas (assumed to be constant),

D = Diffusivity constant of the contaminant gas in air, and

v = kinematic viscosity coefficient of air.

The Grashof number is a measure of the ratio of the buoyant forces to the viscous forces in a natural convection situation. In this case, however, the investigator set the depth (h) of the model to 500 and 600 m. This means that the buoyant force experienced by any quantum of air will always be the same as if it were at the bottom of the pit. The buoyant force will decrease as the air moves up (considering an adiabatic and mass-impermeable boundary around the quantum of gas in question). Therefore, the ratio of the buoyant force in the Grashof number is exaggerated, and will result in dramatic upward convective velocities. This behavior is probably the reason why the model results show a veritable chimney effect at the center of the model.

The boundary conditions and the initial conditions used by Fomin (1996) are standard and often used. He considered the pit walls to be impermeable to mass or momentum and the pit top and sides to be open boundaries. This assumption allowed for (convection permitting) a quasi-laminar flow state in the model and greatly simplified the flow patterns. Fomin observed that the air seemed to roll down the sides

of the hot walls of the pit before being taken upwards at the center of the pit by upward convective flows. He explained that while it could naturally be expected for the hot injected gas to rise immediately, after a certain time, the convected heat would be conveyed beyond the horizon of the mine and a stable convection current established. This would create the vertical convective column that draws all air from the vicinity along the contour. He used several temperature gradients upward from the floor of the mine, so that the temperature on the vertical axis increased with height, which effectively established an inversion cap on the system. This setup, along with a fixed pit-bottom temperature, ensures that the convective column was established and stable. The force of convection upwards, however, is not only controlled by the heat injection, but also by the momentum balance of the buoyant air, which is exaggerated.

1.4 Solution Approaches

Shi et al. (2000) noted that that local air quality is closely related to the ABL in complex terrain. They pointed out that many numerical ABL models have been utilized to study meso-scale or micro-scale systems over complex terrain, such as land-sea breezes, mountain-valley and river valley winds. Special micro-scale terrains, such as open-pit mines, have not attracted much attention.

Shi and associates constructed a high-resolution, nonhydrostatic, three-dimensional ABL model. They considered the characteristic features of an open-pit mine, which is only 2 km by 2 km wide and more than 100 m deep. Physical processes such as shortwave radiation of the sun and its uneven distribution on the ground, longwave

radiation of earth-atmosphere systems, sensible and latent heat fluxes and heat flowing into the substrate of the earth, were involved in the model. Using this model ABL structures over this kind of micro-scale concave terrain (an open-pit mine) were fully studied.

The results showed that the most important characteristics of the stationary ABL were the recirculation, which has a closed structure and high turbulent kinetic energy. This structure of the stationary ABL was consistent with the results of wind-tunnel experiments conducted earlier. The depth of the pit, the slope angle of the pit wall, the incident airflow velocity, and the indicating shear of the initial velocity profile all influenced the structure of the ABL greatly. It was found that thermal forcing and mechanical forcing were equally important mechanisms in the evolution of the ABL.

Some difficulties in the simulation arose from the complex forcing mechanisms that induce turbulence at night. In addition, there were some difficulties in deciding how to choose the parameters for the closure model. Nonetheless, the results were considered relatively significant and useful for the forecasting and control of the local air quality in open-pit mines. The numerical results showed that strong turbulence exists in the pits of the type modeled, possibly caused by the interaction between the non-linear and diffusion terms in the governing equations. It was thought that the local topography of the terrain also had an effect on the turbulence.

Sharan and Modani (2006) developed an analytical model for estimating the crosswind concentration of a pollutant released from an elevated source. The analytical

model developed by the authors is logically superior to the existing Gaussian model developed by Doran and Horst (1985), for two reasons. First, the authors use a power-law function to estimate wind speed, which tends to increase with height. Existing models assume that wind speed is constant with height. Second, the mathematical model developed by the authors calculates eddy diffusivity as a function of downwind distance from the source. Existing models assume that eddy diffusivity is constant. The authors go on to compare their model to actual data collected at three different sites. For two of the three sites, the model formulated by the authors performs as well as or better than existing models. For the third site, the model did not perform as well as existing Gaussian models.

Lowndes et al. (2008) proposed that optimal modeling of open pit emissions might be more accurately achieved by the use of a multi-scale, predictive modeling approach. They suggested using computational fluid dynamics (CFD) methods, for high resolution near source dispersion, and conventional Gaussian based methods for far field dispersion modeling. They presented a numerically-based flow and dispersion analysis of a typical open pit using CFD in conjunction with a conventional Gaussian, plume-based methods. Typical operating emissions and meteorological conditions are obtained from long-term data records collected at a large operating quarry extraction operation in the UK. Emissions were modeled using a Lagrangian framework within conventional ABL profiles expressed as functions of turbulence and velocity parameters

under assumed neutral conditions. Results were presented in terms of the impact of site topography on in pit retention as compared to the Gaussian based method.

In this paper, Lowndes and associates summarized a series of recent CFD studies on fugitive dust conducted by a team of researchers from the University of Nottingham, UK. These studies were validated using field meteorological and dust deposition data collected at a large limestone quarry in the UK. All studies were validated with field data.

The terrain immediately surrounding the quarry is undulating farm grazing land. The in-pit topography is characterized by a complex series of interconnected ramps, vertical faces and working benches. Detailed site elevation survey data at 4-m grid spacing were used to delineate the detailed topography of the working pit and surrounding terrain. These data were used to construct the surface topography of the model domain within the Gambit pre-processor model used by the commercial Fluent software, which in turn was used to construct the flow and dust dispersion simulations. The size of the total model domain constructed was approximately 4 km $\times$ 4 km. The model could be rotated to allow for the ease of simulation of the direction of the simulated ABL to represent the mean average wind speed and direction. The rectangular domain mesh was divided into four primary flow boundaries, a background flow inlet and outlet and two boundary walls to define the flow across the quarry opening.

For the dust, four particle sizes 2.5, 10, 30, and 75 μm, at mass fractions of 0.05, 0.45, 0.3, and 0.2 respectively, were used to simulate fugitive dust emission sources

within the quarry. The quantities of dust released from each individual or collection of fugitive dust emission events modeled (bench blasting, loading, truck haulage, etc.) were calculated using the emission factors defined by the US EPA AP-42 fugitive dust emission models. Detailed analyses were made of the influence of pit topography, and factors influencing in-pit dispersion and deposition of dust.

Lowndes and associates suggest that a number of recent research studies have concluded that the use of the US EPA AP-42 dust emission models for large open pit and quarry operations, together with conventional Gaussian plume dispersion models, can produce over-predictions of off-site emission and deposition. They go on to state that these studies have also concluded that the EPA methods are unable to replicate the true nature of the in-pit fugitive dust emissions, dispersion and deposition. They suggested that the use of an appropriate, three-dimensional, field-validated computational model might allow for improved simulation of these events, which could allow the mine operator to predict the occurrence of in pit reduced visibility.

The authors then suggest the development of a three component modeling approach:

1. Improved dust emission models to represent more accurately the emission characteristics of stationary and mobile in pit fugitive dust sources.
2. More complex three-dimensional computational fluid dynamic models, for more accurate prediction of the influence of the in-pit microclimate on the dispersion and deposition of fugitive dust within the pit.

3. A method for determination of an areal emission factor for dust through a defined area across the mine opening, and the transference of the determined areal dust emission to the background atmospheric boundary layer, with the resultant far-field, downwind dust dispersion to be solved by a conventional, Gaussian-plume dispersion model.

The research presented by Shi Yong et al. (2000) is of particular interest for this project. In this study, the authors used non-hydrostatic equations to develop a numerical model for an open pit mine with dimensions of approximately 2 km $\times$ 2 km $\times$ 295 m in depth. Upon running the models, the authors observed a pronounced recirculation in the center of the pit. This recirculation was validated by wind tunnel experiments. After creating additional models, the authors discovered that the magnitude of this recirculation increased with increasing pit depth, slope angle, and initial wind velocity. The shear of the initial wind velocity also influenced the recirculation. One weak area of this study is that the authors have not validated their numerical models with real world observations of conditions in an actual open pit mine.

Tandon and Bhaskar (1998) developed a two-dimensional, finite element model of open pit mines using FIDAP 7.5 (Fluid Dynamics Analysis Package) software package. The authors considered three different cases in this study: (1) the geometry of an actual open pit mine in the western United States, (2) an idealized trapezoidal pit geometry, and (3) an idealized rectangular geometry. "Neutral" atmospheric conditions and a wind speed of 6 miles/hour were assumed in the models. Under these conditions, the

authors observed air recirculation in both of the idealized pit geometries. This recirculation is consistent with wind tunnel tests conducted by the EPA. However, no recirculation was evident in the case of the actual pit geometry. The authors concluded that the presence or absence of recirculation is largely a function of pit geometry, and suggested that future research comparing these fluid dynamics models to actual field conditions was warranted.

Aloyan et al. (1982) proposed a novel scheme to solve the flow of air into a mining pit. The scheme of equations solved took into account not only the mass and momentum balance equations that would be solved in the normal course of such a solution, but also external planetary parameters like the Coriolis force. The effects of temperature and the resulting stratification of the air above the pit, the effects of pressure, and the contours of the pit were also taken into account, as were external sources of heat flow into the system, whether artificial or natural, such as solar radiation. Pollutant sources were placed in the model to account for the generation or inflow of pollutants in the model. The system of equations was then solved using a novel technique called the use of "fictitious" regions in the model space. In this technique, the irregular topography of the actual mine could be approximated as a set of rectangular parallelepipeds. The mass and momentum equations could then be re-specified for the new boundaries that are generated. The regions of the mine that are compliments to the parallelepiped were then simply continuations of the same boundary and domain conditions as the approximated rectangle.

This system brings forth a generalized model that can theoretically be applied to any mine topography and thus is very flexible. The numerical experiments provide an interesting correlation among the feasible depth of an open pit mine that can be ventilated, the behavior of contaminants under different thermal conditions, and an estimate of the time it would take to ventilate the pit after a major pollutant dispersion event (such as a blast).

Very few data were presented from the experimental results. The results that were presented indicate that the escape of pollutants from the pit is directly proportional to the velocity of the influent air. However, at high influent velocities, the lower regions of the pit will be affected by turbulence, and the contaminants would be subject to remixing with the local air, thus altering their concentrations and possibly chemistry. This turbulent zone mixing should be clearly visible in contaminant contours. The data presented, however, show no sign of turbulent mixing, even with high velocities of 16 m/s, and contours drawn indicate laminar, stratified flow. The same lack of turbulent mixing is observed in the work of Baklanov (1984).

A scheme very similar to that of Aloyan et al. (1982) will be used in the present research. The model will be further complicated by the addition of any given number of contaminant components. Each of these contaminants can be modeled with respect to its characteristics. The boundary conditions employed state that the contaminant starts with a background value within the pit, after which the injection of pollutants inside the pit and the convection resulting from the mass and momentum balance equation for

the flow changes the concentration values in the model space. The top of the pit is capped with a concentration gradient equal to zero, which implies that any contaminant mass reaching the top boundary will encounter no further concentration gradient and will not be taken any farther. This boundary condition is specified by:

$$\frac{\partial \vec{c}}{\partial z} = 0 \qquad (7)$$

Where:

z = H,

c = concentration vector field, and

H = height of the model from the pit-bottom to the top boundary.

The concentration values at the X and Y extremities of the model are set to the original background concentration. The application of the concentration gradient limit on any boundary of the model may give rise to a problem. If the concentration gradient is zero, it implies that the mass will not have any impetus to travel beyond that boundary due to lack of a favorable concentration gradient, unless convected by force. Such convection would be the only way to take mass out of the system. Since, in these models, such atmospheric boundaries are normally defined as no-slip walls, the chances of such forced convection are minimal. This means that for lack of movement, the mass coming into contact with the boundary will accumulate at the boundary, and, if a high enough boundary concentration is achieved, will try to diffuse back into the model space, even against the flow gradient.

It may be noted that during the entire model runtime contaminants are being added to the model from individual and diffuse sources. Though the intention of the boundary conditions is to take a certain amount of contaminants out of the system (based on the model physics) so that some mass balance can be achieved, it has just been shown that the model will fail to do so. This failure may lead to a major source of disruption in the mass balance resulting at the worst in a failure to achieve convergence, or in an unintended, unspecified, and undesirable addition to the concentration contours. A more appropriate boundary condition for concentration would be to set the *concentration itself*, rather than the *concentration gradient* equal to zero concentration itself rather than the concentration gradient to zero. This way, the boundary condition will correctly assume infinite dilution when the pollutant mass meets the top boundary of the open pit.

1.5 Proposed Remediation Measures

There have been several approaches to ventilation of open pit mines in Soviet Russia. Baklanov and Rigina (1993) presented their research into the application of cascade ventilation to the dilution of contaminants in large, open pit mines. A number of open pit ventilation configurations were simulated using numerical models. Most of the models were executed under conditions of atmospheric inversion with no wind. In this study, pits ranging from 420 to 750 m in depth, with ventilation configurations ranging from two to seven individual fans, were simulated. The only cascade ventilation system that was effectively able to remove contaminants from the pit was a system of

seven units applied to a pit of 450 m in depth. The power consumption for this scenario was 3.4 X 10^5 kW. The authors of the study concluded that cascade ventilation is not an effective means of ventilating open pits. No specific details were given as to the construction of the numerical models used in this study or the assumptions made in applying the cascading ventilation systems to the models.

Belousov (1990) discussed how improved ventilation in open pit mines could be achieved by the installation of "aerodynamic foils" (wings) on the windward sides of open pits. The author conducted 210 wind tunnel tests with a 1:1,000 scale model of an open pit coupled with an aerodynamic foil. Mathematical relationships were developed from the wind tunnel tests that relate the required geometrical parameters of the wing to wind speed and the dimensions of the open pit. The author suggested that additional benefits could be realized by combining aerodynamic foils with combinations of fans and pipes located in the pit. The author claimed, "when wings are installed with optimal parameters, virtually the entire pit is ventilated by direct flow." The effectiveness of this technique requires, of course, that a constant wind of suitable velocity is flowing over the open pit.

In an example where the method was employed to create rarefaction on the windward side for an open pit in a plain land terrain with a pit 1,000 m long and 250 m deep, with a wall slope of 30°, the minimum critical wind velocity required for effective air exchange without accumulation of toxic impurities was 2.8 m/sec. To intensify the ventilation requirements, a perforated pipeline 200 m long was installed along the

windward side of the pit. According to the model, the total quantity of air to be pumped out was 105 m^3/sec. This flow rate of pumping was achieved by connecting to the pipeline centrifugal fans, installed beneath it on the slope every 20 m. The air from the fans was ejected through flat sleeves with an output cross section of 0.5 m $\times$ 6 m along the slope. According to the model, this method would double the air exchange efficacy.

In general, the model showed that, in pits where the ratio of depth to length (or radius) and the pit wall angle are large, the efficacy of ventilation by air pumping on the windward side could be increased by a factor of 3 to 4. Controlling the boundary layer of the wind stream makes it possible to improve the environmental conditions in an open pit.

Belousov (1995) also discussed yet another approach to ventilation of an open pit mine, and examined the ventilation of open pits due to thermodynamic processes, such as temperature differences. This form of air exchange is referred to as "breeze circulation." In open pit mines, breeze circulation tends to develop naturally in warm months when there is a temperature gradient between the center and the edges of the pit. In cold months, this temperature gradient trends towards zero, and breeze circulation typically is not present.

The author developed mathematical relationships for the development of stable breeze circulation based upon thermodynamic first principles. Relationships were developed for both circular and elongated pits. The magnitude of breeze circulation

was greater in elongated pits for the same initial conditions than for circular pits. The relationships developed show that stable breeze circulation can develop when a temperature gradient of 5 to 10° C is present. The efficiency of this circulation can be improved by "turbulizing" the flow by the installation of air vanes above the pit.

1.6 Scope of This Research

Little research into open pit mine ventilation has been performed. Published literature on atmospheric modeling rarely addresses the problems associated with open pit mining under conditions of atmospheric inversion. A number of contemporary studies on dust liberation and retention in open pit mines have been performed (Lowndes et al., 2008). However, the models used in these studies were generally run under the assumption of neutral atmospheric conditions. This condition is an inappropriate simplification for deep open pit mines that are subject to night time and winter inversions. Additionally, most of these studies focused on the downstream concentrations of dust liberated from the pit. The concentrations of pollutants within the pit are a concern to worker health and safety, but this issue has received little attention in the published literature.

The majority of the research that specifically addresses open pit mining under conditions of atmospheric inversion has been conducted in the former USSR. Unfortunately, most of this research is not available for peer review. Little of this research was published in peer reviewed journals.

Most of the Russian research into open pit mine ventilation was performed prior to 2000. This research was generally performed using proprietary software, as few commercial CFD codes were in existence at that time. Commercial CFD codes have been extensively validated by third party researchers prior to their acceptance by the scientific community. The validation process for the proprietary software used by the Russian researchers is not transparent. It is difficult to comment on the validity of the Russian studies without independent validation of the software used to perform the studies.

Most of the software used in Russian open pit mine ventilation is based on a finite difference discretization of the problem domain. Unlike the finite volume and finite element methods used in most modern CFD codes, the finite difference method does not allow for mesh refinement in critical areas (e.g., the pit bottom). The inability to refine the mesh is a major flaw in the Russian studies, as mesh refinement in critical areas is essential to obtaining an accurate solution.

The computing resources available to modern researchers are vastly superior to what was available to Russian scientists researching open pit mine ventilation. In order to obtain model convergence in a reasonable amount of time, Russian models were forced to use an extremely coarse mesh size (compared to modern standards for CFD codes). Since a higher mesh resolution generally yields a more accurate solution, it is worth revisiting these studies with modern computing and software tools.

Given the limited computing and software capabilities available at the time of the Russian studies, it was extremely difficult to capture the topographical intricacies of an actual open pit mine. Most of the Russian numerical models are based on crude idealized pits. This idealization is problematic, as a number of researchers have found that mine geometry is critical in determining the characteristics of the local wind field (Tandon and Bhaskar, 1998.) Open pit mine ventilation is a site specific problem, and using an idealized pit geometry does not lead to accurate results.

In reviewing the existing literature, a wide variety of opinions seem to exist on the efficacy of the proposed remediation measures. Some researchers claim that none of the proposed solutions have been effective, and others claim that several of the proposed solutions have proven to be quite useful. Since few of the results of this research are available in the public domain, it is virtually impossible to verify any of these claims. Clearly, more research is needed.

The scope of research is as follows: (a) investigate air inversion process in mines; (b) identify and categorize the factors influencing air inversion and air pollution; (c) review literature and select available mathematical modeling approach to study the air inversion problem in active open pit mines; (d) collect data from an operating open pit mines in Alaska and validate the model; (e) analyze potential mitigation measures.

1.7 Work Plan

It is clear from the above discussion that it is essential to analyze the wind flow patterns that significantly affect the dispersion of pollutants within deep open pit mines.

The dispersion equations developed within the deep pit boundary may provide a reasonably accurate estimate of pollutant dispersion within the deep open pit mines. The fundamental equations of continuity and momentum describe the in pit dispersion mechanisms within the atmospheric boundary layer (ABL). In addition, the meteorological conditions within the deep open pit mine are significantly affected by temperature (stability) and roughness conditions, which ultimately generate complex dispersion phenomenon including separation of atmospheric boundary layer, recirculation and transport. Further, the simulation of transport and dispersion of pollutants using the fundamental governing equations may require modifications to incorporate the in pit microclimatic effects on the flow regimes. Therefore, it is essential to analyze and evaluate microclimatic parameters including the wind turbulence and shear in order to simulate the dispersion of pollutants in an open pit mine. The problem is complex and any solution approach would require a good understanding of the interaction of the aerodynamic movement of air, air inversion process, meteorology, pollutant sources, and application of air movers in open pit mines.

The mathematical modeling effort proposed here is to solve the coupled conservation equations of mass, momentum, and energy with appropriate initial and boundary equations. Advanced technology has made computers faster and more powerful, which allows computational fluid dynamics (CFD) procedures to be applied to many airflow problems. CFD modeling has been used in atmospheric pollution studies

in urban areas (Baklanov, 2000). However, none of those models or studies including those models has addressed ventilation design for deep, open pit mines in general and especially in arctic or sub-arctic conditions. The problem is complex and any solution will require a good understanding of the interaction of the ABL, heat transfer in cold regions, aerodynamic movement of air, air inversion processes, meteorology, pollutant sources, and application of fans in open pit mines.

The atmosphere in an open pit mine is highly dependent on the mine geometry, mesoscale meteorological processes, the air inversion process, pollutant sources, and the application of fans or other mitigation measures. In this study, field data from a selected mine will be used to create and validate the numerical models.

Different dispersion models of Eulerian and Lagrangian type can be used with CFD for modeling pollutant transport in open pit mines. In this research, an Eulerian 2-D model of pollutant transport will be used. The actual topography of an open pit mine in the arctic or subarctic will be used to define the computational domain. The CFD model will include physical processes, such as solar radiation, latent and sensible heat fluxes and the heat flowing into the pit surface, and meteorology.

Parametric studies will be performed to determine the relative effect of wind velocity on the atmosphere in the open pit. The inversion process will be modeled, and the effect of the inversion on the contaminant distribution within the pit will be discussed.

In order to mitigate the pollution problem, several remedial measures will be considered. The layer of air closest to the ground requires energy to restart the convective cycle and dissipate the pollutants. This energy can be imparted to it either kinetically or thermally. A kinetic solution would entail placing a fan in the mine pit or at the top of the pit, thus resulting in dilution ventilation.

The 2-D model will determine the flow parameters, including the influence of relief, thermal in-homogeneity of the atmosphere and the surface, influence of the radiation effects upon the open pit microclimate, and forming of local temperature inversion and local winds. The 2-D model with adequate accuracy can be applied to open pit mines elongated in one direction (surface mines, for example) on the assumption that the relief of the area is two-dimensional. Ventilation problems in an open pit mine are a 3-dimensional problem. Although there are some issues in simulating a 3-D problem in a 2-D model owing to the complex mechanical turbulence the 3-D model can generate, a 2-D model is a good first approximation of the problem. A 2-D model provides valuable insight into the general trends and important variables in the problem while avoiding the complexity of a full 3-D modeling effort. The insight gained and obstacles overcome in 2-D modeling can be applied to an on-going 3-D modeling effort.

Chapter 2: Data Collection

Ventilation design for open pit mines requires the knowledge of the quantity of the pollutants that are liberated into the pit by various dust and gas sources. The most important items in the total balance of pollutants in open pit mines are the stationary point sources (drilling rigs, excavators, loading machines) and moving sources (such as the trucks). The spreading of admixtures from these sources in an open pit mine is directly related to the aerodynamics of the airflows in the open pit space. Evaluation of the atmospheric conditions in an open pit mine requires a determination of the concentration of injurious mixtures. The problem is complex and any solution approach would require a good understanding of the interaction of the aerodynamic movement of air, air inversion process, meteorology, pollutant sources, and application of air movers in open pit mines. An array of data is required to create and validate open pit mine ventilation numerical models. The meteorological conditions within the deep open pit mine are significantly affected by temperature (stability) and roughness conditions, which ultimately generate complex dispersion phenomenon including separation of atmospheric boundary layer and recirculation.

The meteorological inputs needed to determine the contaminant concentration are the wind speed and direction as a function of time at one height, the nocturnal temperature inversion characteristics at sunrise, the heating rate of the pit atmosphere after sunrise, and the turbulent eddy diffusivities as function of atmospheric stability.

The wind speed and direction observations at one height will be used to determine the advection term.

Among others, the following information need be collected during the data gathering and CFD model building phases: (a) Mean diurnal wind velocity (mean values for each month); (b) Number of calm days, their distribution both daily and monthly, the mean and maximum duration of clam weather; (c) Number of foggy days according to the months and their duration (mean and maximum); (d) Mean monthly humidity of the atmospheric air (for the warm period of the year); (e) Duration of the period with freezing soil temperature (below 0 deg. C); (f) Mean monthly air temperature with absolute maxima and minima; (g) Sources of air pollution, volume and rate of contaminants for each point source; (h) Air inversion frequencies and durations ; (i) Air quality values during air inversions, and required standards that need to be met.

Data are needed from an operating open pit mine regarding the number of stationary equipment in place (shovels , generators, drills, for example), and number of moving equipment (dozers, graders, trucks, for example), their locations, and status of operation (ready hours, delay hours, and stand by hours). Data is also needed on moving sources (such as trucks) from shift reports and status reports to develop the duty cycles of the trucks so that reasonable pollution loading information can be developed for model application. Engine make, model, specification of equipment, numbers and types of equipment in the pit, diesel exhaust information from pre-test, if available for diesel powered equipment in the pit. Topographic parameters including

the slope angle (α) and the azimuth (β), and the solar azimuth B on the distribution of solar radiation on the ground, the mine depth, the angle of the terrain, the initial air velocity and its vertical shear, air quality data (air samples) at various open pit benches. Particularly, concentrations of NO_X, CO and DPM, and dust at various working or active benches. Pit geometry (depth, slope angles, bottom width, bottom length, elevation of various benches, widths of working benches), and in electronic format (Auto-cad files, for example)a and Digital pictures of the pit, (f) air inversion frequencies and durations; (g) air quality values during air inversions, and required standards that need to be met.

Meteorological data was compiled from the Cleary Summit Weather Station (Figure 2.1), which is located approximately 7.7 kilometers from the mine site.

Figure 2.1: Cleary Summit Location

Operational data was collected from an operating mine. This data includes the number of stationary equipment in place (shovels, generators, drills, etc.), number of moving equipment (dozers, graders, trucks, etc.), the location of the equipment, and the status of operation (ready hours, delay hours, and stand by hours). Data was also collected on moving sources (such as trucks) from shift reports and status reports to develop the duty cycles of the trucks so that reasonable pollution loading information could be developed for model application.

To validate the models, it was necessary to collect air quality data at various open pit benches. Concentrations of NO_X and CO at various working or active benches during inversions was collected (Table 2.1). Figure 2.2-Figure 2.7 provides a representative sample of the data collected during the research.

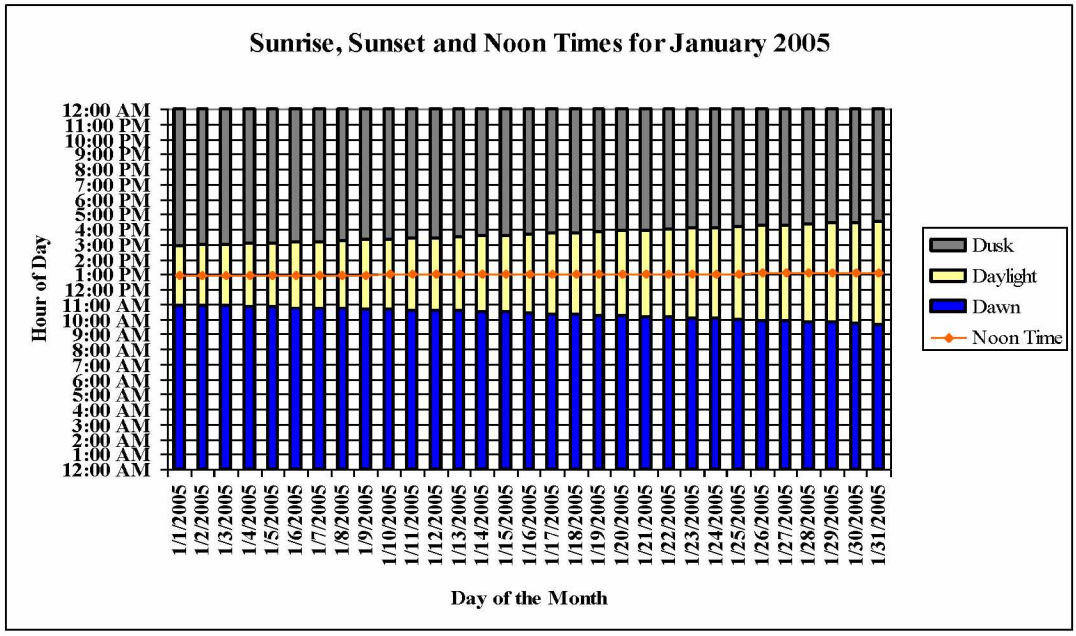

Figure 2.2: Sunrise, Sunset and Noon Times (January 2005)

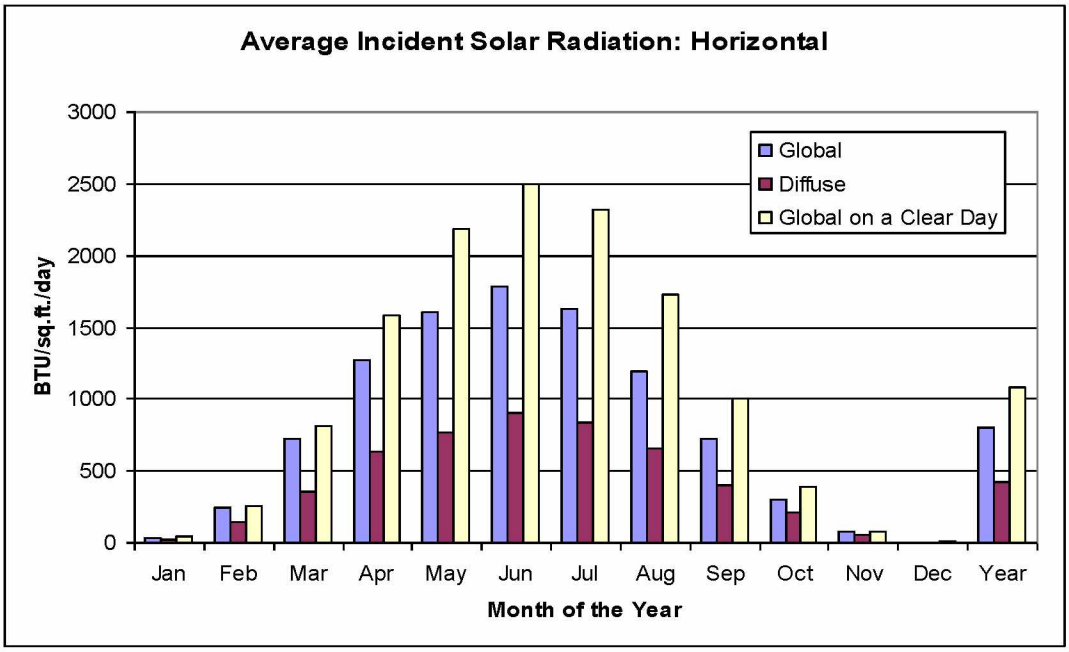

Figure 2.3: Average Incident Solar Radiation for 2005 (Horizontal)

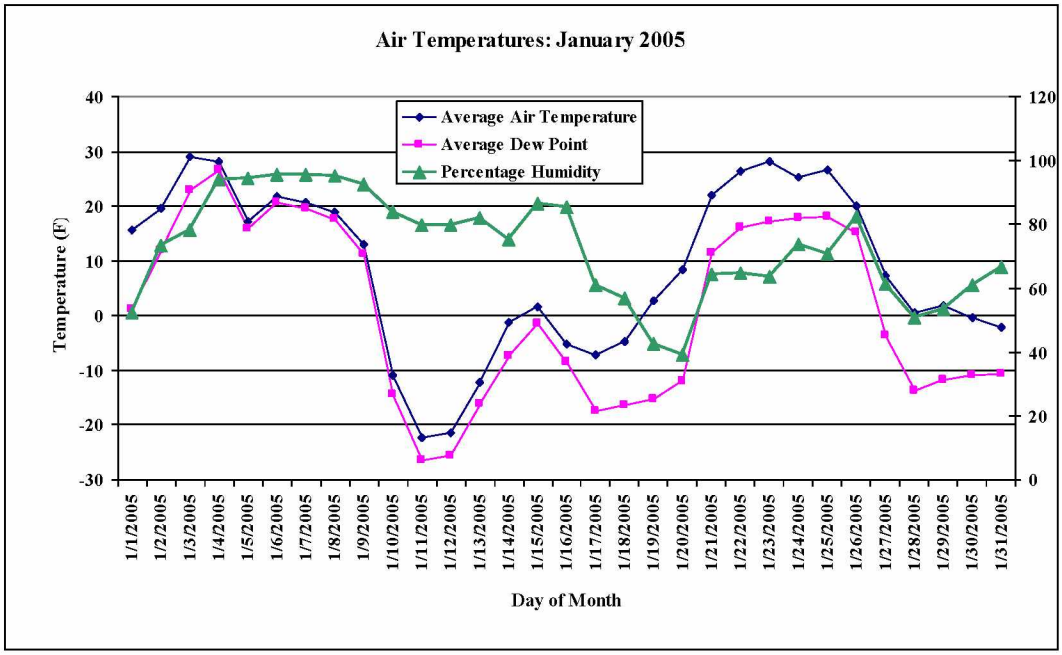

Figure 2.4: Average Temperature and Dew Point (January 2005)

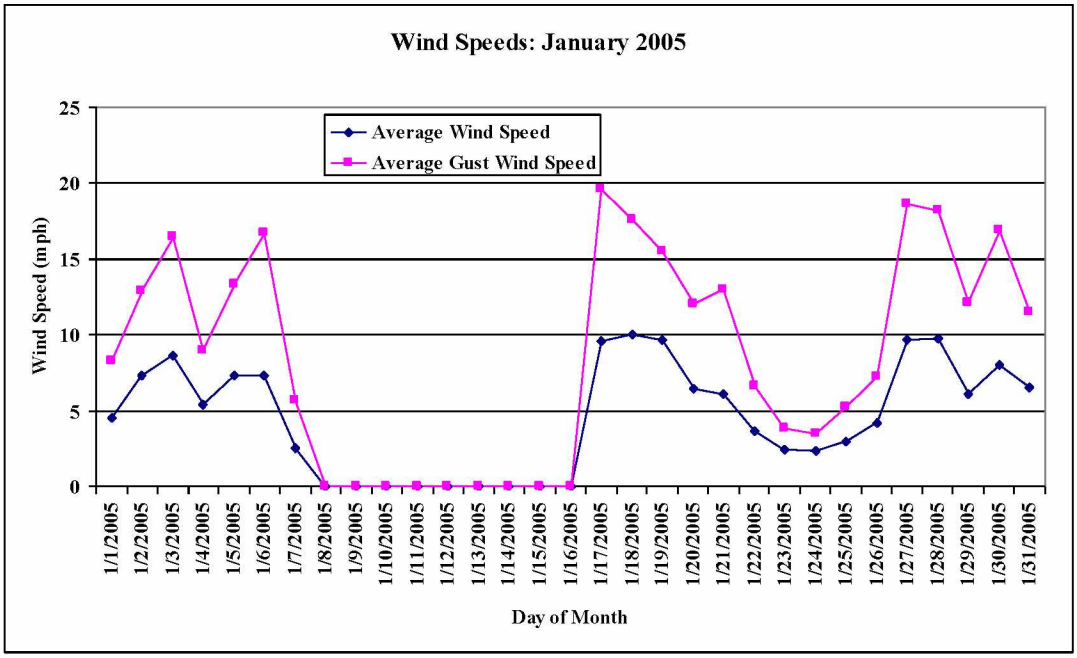

Figure 2.5: Average Wind Speeds (January 2005)

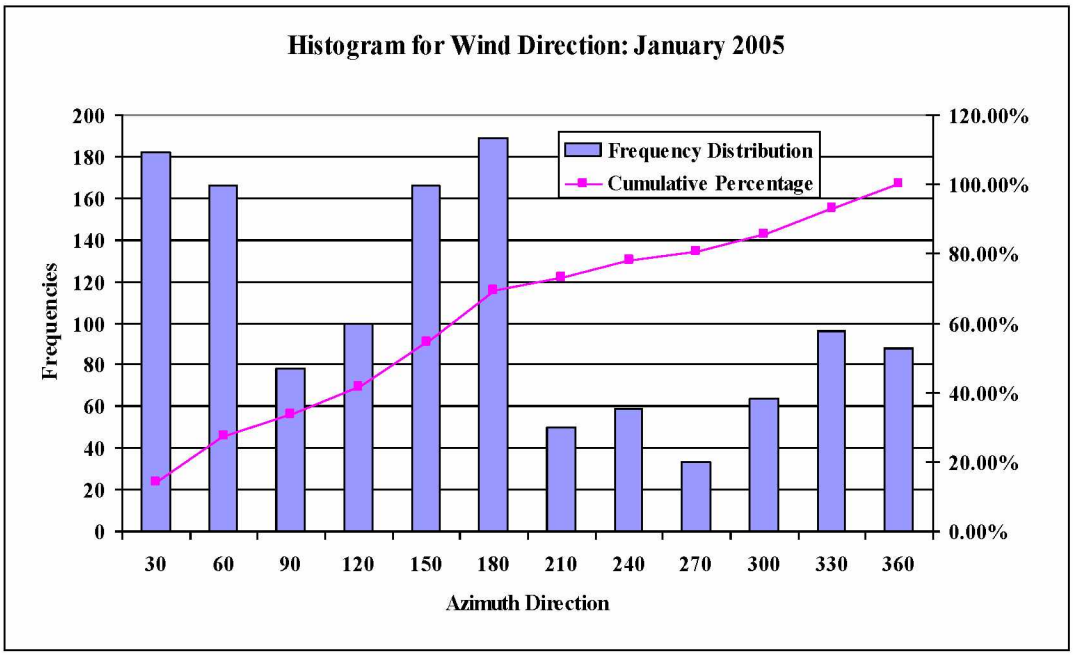

Figure 2.6: Histogram of Wind Direction (January 2005)

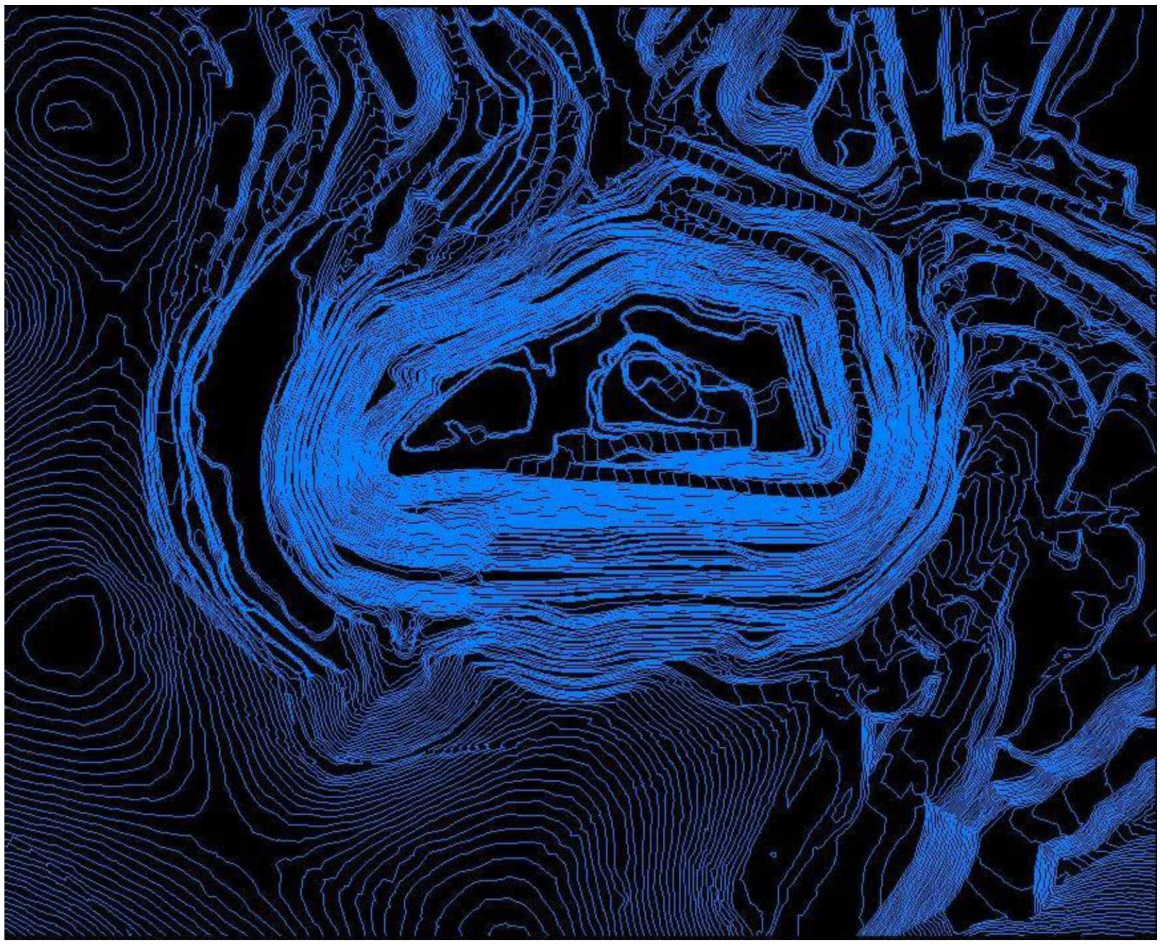

Figure 2.7: Contour Lines for the 2010 Pit Configuration

Table 2.1: Air Quality Data Collected From an Open Pit Mine during an Inversion

	Airport Temp					Pit Temp		1090 Bench (ppm)				1120 Bench (ppm)			
Date	High	Low	Precip(in.)	Day Avg	Time	Top	Bottom	O2	CO	NO	NO2	O2	CO	NO	NO2
1/1/2005	4	-11		-4	900							20.7	0	2	1.9
					1609							20.6	0	0	1.8
					2100							20.9	0	0	2.1
1/2/2005	13	-4	0.03	5											
1/3/2005	26	2	0.01	14	232							20.9	18	3	1.9
					800	35	24					20.7	8	4	2.1
					1000	35	25					20.9	10	4	2.1
					1216	38	33					20.7	4	2	1.6
					1600	40	31					20.9	2	0	0
1/4/2005	28	23	0.43	26	830	26	30					20.9	0	0	0.2
					1600	23	26								
1/5/2005	30	19	0.18	25	702	21	20								
					1600	25	27								
1/6/2005	33	27	0.11	30	4:15	26	26					20.9	0	0	0
1/7/2005	29	22		26	7:27	29	29								

Chapter 3: Model Development

3.1 Fundamental Transport Equations

The wind flow patterns significantly affect the dispersion of pollutants. It is therefore essential to analyze the wind flow patterns in order to simulate the pollutant transport and dispersion in deep open pit mines. The fundamental equations of continuity and momentum describe the in pit dispersion mechanisms within the atmospheric boundary layer (ABL). The transport equations developed within the deep pit boundary provide a reasonably accurate estimate of pollutant dispersion within the deep open pit mines. In addition, the meteorological conditions within the deep open pit mine are significantly affected by temperature (stability) and roughness conditions, which ultimately generate complex dispersion phenomenon including separation of atmospheric boundary layer and recirculation. Further, the simulation of pollutant dispersion characteristics using the fundamental governing equations may require modifications to incorporate the in pit microclimatic effects on the flow regimes. Therefore, it is essential to analyze and evaluate microclimatic parameters including the wind turbulence and shear in order to simulate the dispersion of pollutants in an open pit mine.

For the pollutant transport and dispersion calculation, Gaussian, Eulerian and Lagrangian models are typical choices. The Gaussian model is based on the analytical solution of the dispersion equation under very restrictive assumptions. The model is not applicable for complex terrain and non-uniform wind fields, as well as for changing

source strength conditions. Eulerian models, which numerically solve the advection diffusion equation on a grid, show a rather high numerical diffusion. Lagrangian models do not have this disadvantage. As long as nonlinear chemistry is not involved or the consideration of non-uniform background and a large number of sources are to be considered, the Lagrangian approach is well suited for the dispersion calculation for any desired scale. Additionally, the model execution can be easily accelerated by using parallel computation platforms.

The basic concept of Lagrangian models is the observation of individual particles. For this reason, these models are also referred to as Lagrangian particle dispersion models (LPD) or as trajectory models. In the case of atmospheric dispersion the term *particle* denotes any air pollutant or any buoyant substance in the air. For physical reasons the particles are assumed to have no spatial extension so that they can follow every flow. However, they are assumed to show certain characteristics. Together with the motion of a particle, the modifications of these characteristics will be registered. Gases or evaporating liquids are also represented by particles, whereas for example the density of the gas components are considered as characteristics. If a uniform mass is assigned to the particles the density of the particles is proportional to the concentration.

Lagrangian models use given wind fields and take into account fluctuation caused by turbulence to predict the pathways of individual particles or air volumes and register modifications in their characteristics for each time step. The definite form of a

Lagrangian model is mainly determined by the chosen scale, affecting for example, the types of turbulences simulated. Particles or air volumes, respectively, may be released from any number of locations. The type of source (e.g. point or line source) has no influence.

In contrast to Gaussian models, Lagrangian trajectory models are appropriate for the description of dispersion in complex meteorological situations and/or structured topography. The underlying basic methodology of the model can be described as the position of a particle is given by its previous position (in the first step the position of its source) plus a term describing the motion by advection processes and by turbulence. The advective wind is completely determined by the velocity and the direction of the wind, while the fluctuation or turbulent component describes the actual fluctuation. The simulation of turbulence is based on the statistical theory of Taylor for diffusion effects (Taylor, 1921). The velocity fluctuation is simulated by a Markov sequence of first order where the random component describes the coincidental effects in diffusion.

The Eulerian method treats the particle phase as a continuum and develops the conservation equations on a control volume basis and in a similar form as that for the fluid phase. For studying the pollutant dispersion in the selected mine, an Eulerian 2-D model will be developed in this chapter.

All fluid flow problems require that three fundamental equations be discretized and solved. These equations serve the basis of modeling transport phenomena in deep open pit mines. These equations include the conservation of mass (Eq. 4), conservation

of momentum (Eq. 5), and conservation of energy (Eq. 6). From these three fundamental laws, the velocity, pressure, and temperature can be found at each point within the domain. In Eulerian form, these equations can be expressed as:

$$\frac{\partial \rho}{\partial t} + \nabla \cdot (\rho \boldsymbol{V}) = 0 \qquad (4)$$

$$\rho \frac{d\boldsymbol{V}}{dt} = \rho \boldsymbol{g} + \nabla \cdot \tau_{ij} \qquad (5)$$

$$\rho \frac{dh}{dt} = \frac{dp}{dt} + \nabla \cdot (k \nabla \boldsymbol{T}) + \boldsymbol{\Phi} \qquad (6)$$

Where:

ρ density.

$\boldsymbol{V}$ velocity.

t time.

$\boldsymbol{g}$ acceleration of gravity.

τ_{ij} stress tensor.

h enthalpy.

p pressure.

k thermal conductivity.

$\boldsymbol{T}$ absolute temperature.

$\boldsymbol{\Phi}$ dissipation function.

Density, enthalpy, viscosity, and thermal conductivity are functions of pressure and temperature; consequently, the values of these variables can be determined after the pressure and temperature have been found from the conservation laws. Buoyancy

driven flow occurs when density differences within a fluid drive the fluid flow. Modeling buoyancy driven flow is very important for problems in open pit mine ventilation. In a fully compressible model, density is determined from pressure and temperature by the ideal gas law. Fully compressible models are computationally expensive, and convergence can be difficult to achieve. If pressure differences in the model are not extreme, the incompressible ideal gas law can be used in place of the ideal gas law. The incompressible ideal gas law is expressed as follows:

$$\rho = \frac{p_{op}}{\frac{R}{M_w}T} \qquad (7)$$

ρ density.

p_{op} a constant operating pressure.

R universal gas constant.

M_w molecular weight.

$\boldsymbol{T}$ absolute temperature.

3.2 Cell Zone and Boundary Conditions

Proper specification of the boundary conditions is crucial in numerical modeling. With respect to open pit mine ventilation, five different regions are of interest. These regions are illustrated in Figure 3.1. These regions include a so called ABL Wall Boundary, a Velocity-Inlet Boundary, an Outflow Boundary, an Interior Region, and a Pit-Bottom Wall Boundary. The ABL Wall Boundary is a solid boundary that represents the inversion cap

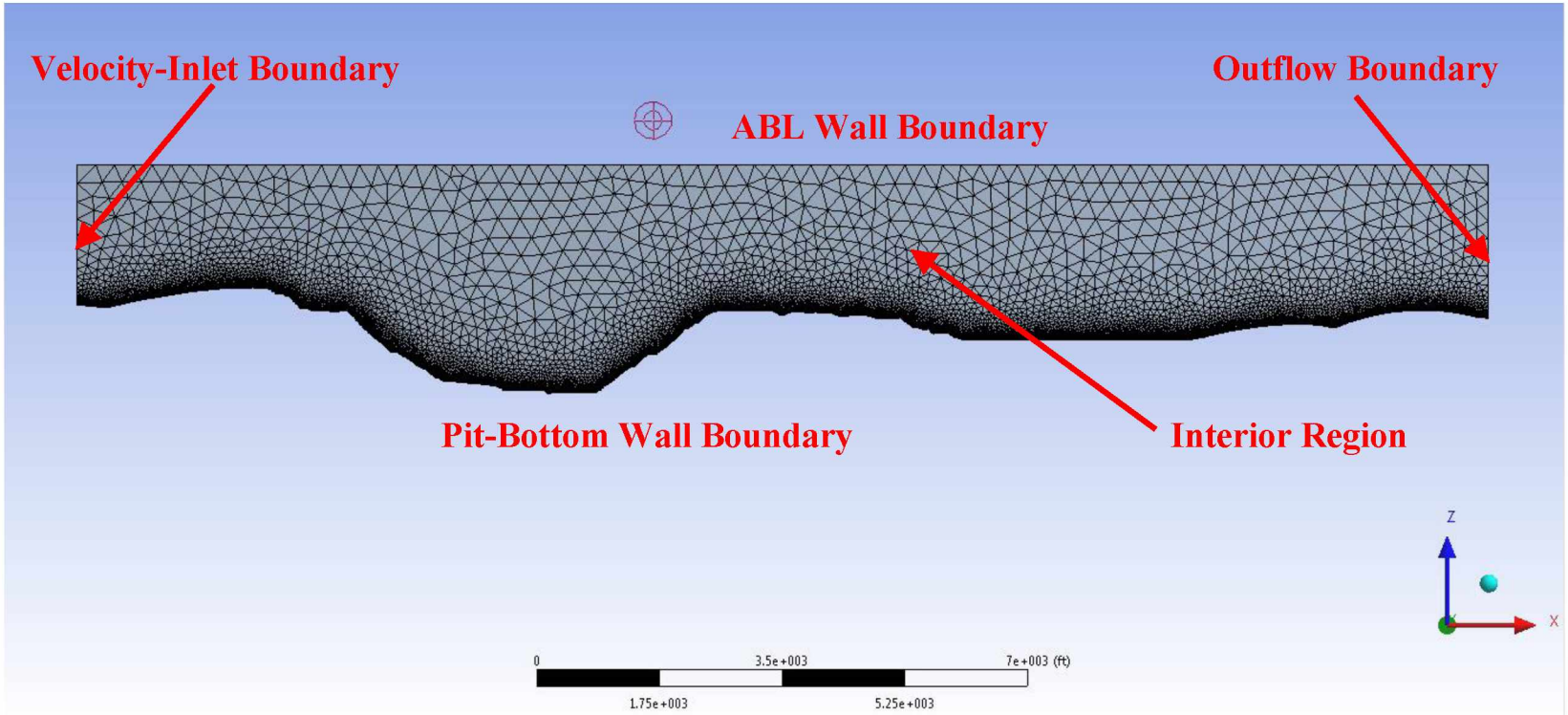

Figure 3.1: Boundary Conditions for a Fluent Model of an Open Pit Mine

or the top of the atmospheric boundary layer. The required user inputs for the ABL Wall Boundary include shear and thermal parameters.

The Velocity-Inlet Boundary is the location where wind flow enters the model domain. Required user inputs at this boundary include the velocity, pressure, temperature, turbulence parameters, and species parameters. The Outflow Boundary is the location where mass flow exits the pit. Since it is assumed that the flow is fully developed at the outflow, no user inputs are required. To avoid spurious results, it is best to place the Outflow Boundary as far from the region of interest as possible.

The Interior Region of the model represents the air inside the pit. Necessary inputs for the Interior Region include contaminant source and sink terms. If the incompressible ideal gas law is used for density, it is also necessary to input an operating pressure for the interior region (Eq. 5). Finally, the Pit-Bottom Wall Boundary represents the floor of the open pit mine. Necessary inputs at this boundary include wall roughness, thermal, and species conditions.

In Fluent, wall roughness is expressed in terms of the sand-grain roughness height. Sand-grain roughness has physical meaning; it represents the average height of a uniform sand grain above an aerodynamically smooth wall. The concept of sand-grain roughness was originally formulated by researchers performing experiments with sand roughened pipes and channels. In turbulent pipe flow, the coefficient of drag increases with increasing sand-grain roughness (White, 2006). In atmospheric science, aerodynamic length is a commonly used expression for surface roughness. The

aerodynamic length represents the altitude value where—in a logarithmic plot of velocity versus altitude—the wind velocity assumes a value of zero (Jacobson, 2005). Typical aerodynamic lengths for a variety of different land surfaces are available (e.g., Wallace and Hobbs, 2006). Blocken et al. (2007) have derived a relationship between sand-grain roughness height and aerodynamic length:

$$k_{s,ABL} = \frac{9.793\, y_0}{C_s} \qquad (12)$$

$k_{s,ABL}$ equivalent sand-grain roughness height in the atmospheric boundary layer (m).

y_0= aerodynamic roughness length (m).

C_s roughness constant (default value is 0.5 in Fluent).

3.3 Meshing

Meshing is the process of dividing the model domain into discrete locations (Figure 3.2). During CFD analysis, the fundamental equations are discretized and solved over each mesh element in the model domain. A quality mesh is an essential first step in obtaining a quality CFD analysis. It is important to refine the mesh in areas with large flow gradients. With respect to an open pit mine, these areas include the pit bottom and pollutant sources. A refined mesh is required to capture the large velocity, heat flux, and concentration gradients in these particular areas. The mesh resolution is always a compromise between accuracy and computational reality. At the very least,

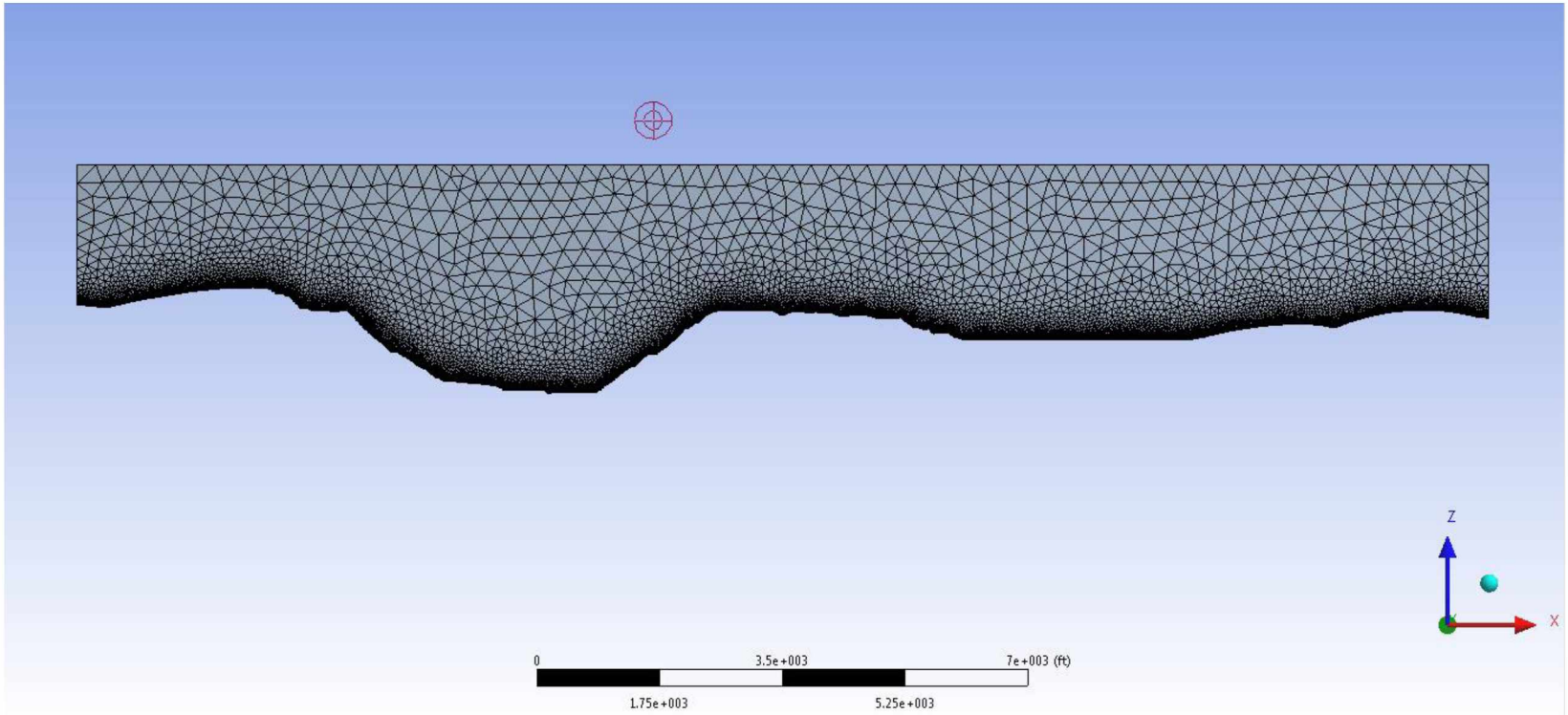

Figure 3.2: Mesh for a 2-D Profile of an Open Pit Mine in ANSYS Fluent

the modeler should ensure that the resulting solution is mesh independent. A mesh independent solution does not change appreciably with a decrease in the size of the mesh (ANSYS, 2009c).

A variety of different meshing styles are available to the Fluent user. For a 2-D geometry, four possible styles are available: 1) Quadrilateral dominant, 2) All triangles, 3) Uniform quad/tri, and 4) Uniform quad. Examples of quadrilateral and triangular mesh elements are shown in Figure 3.3 and Figure 3.4, respectively. In addition to *quantity* (i.e., number of elements), the *quality* of the mesh is important. The choice of meshing style will influence the quality of the resulting mesh for different geometries. A poor quality mesh can result in numerical diffusion in the model (ANSYS, 2009c). Poor quality elements in high gradient areas, such as the pit bottom, can be particularly damaging.

To gauge the quality of the mesh, Fluent provides seven different mesh quality metrics to the user (ANSYS, 2009c). Two of these metrics—aspect ratio and skewness—are particularly critical. The aspect ratio is the ratio of the longest side to the shortest side of the mesh element. Ideally, this ratio should be equal to one (Figure 3.5). Skewness is a measure of the angular deviation from an optimal mesh element. Skewness ranges from zero to one, with a perfect mesh element having a skewness of zero (Figure 3.6). Skewness is calculated as (ANSYS, 2009c):

$$Skewness = max\left[\frac{\theta_{max}-\theta_e}{180-\theta_e}, \frac{\theta_e-\theta_{min}}{\theta_e}\right] \qquad (8)$$

θ_{max} maximum face angle

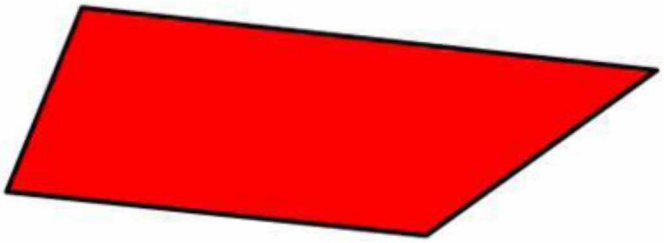

Figure 3.3: 2-D Quadrilateral Element in ANSYS Fluent

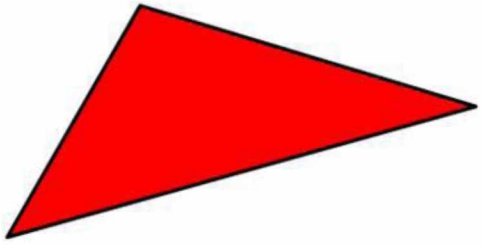

Figure 3.4: 2-D Triangular Element in ANSYS Fluent

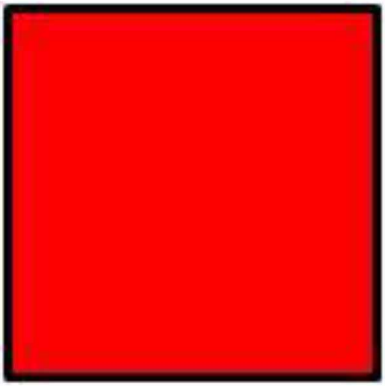

Figure 3.5: 2-D Quadrilateral Element (Aspect Ratio = 1)

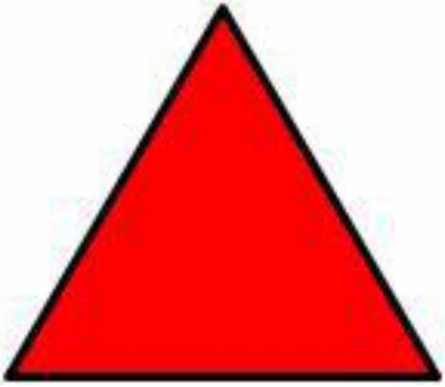

Figure 3.6: 2-D Triangular Element (Skewness = 0)

θ_e equiangular face angle (60° for triangles and 90° for quadrilaterals).

θ_{min} minimum face angle.

Selection of an appropriate mesh is a trial and error process. It appears that a triangular element is well suited for meshing a two-dimensional profile of an open-pit mine (Figure 3.2). With respect to the highly irregular shape of an open pit mine, a triangular mesh seems to yield improved mesh quality metrics when compared to an equivalent quadrilateral mesh. Refinement is important near the bottom of the model domain due to the high gradients at the pit bottom. A mesh size of 1.5 m at the pit bottom seems to capture the important flow features while still allowing simulations to be completed in a reasonable amount of time. Moving away from the bottom of the pit, the edge length of each mesh element is allowed to grow by 20% with each successive layer of elements. This value is recommended by the manufacturer for good simulation results (ANSYS, 2009c).

3.4 Discretization

ANSYS Fluent uses the finite volume method of solving partial differential equations. In the finite volume method, the conservation laws are integrated over each of the control volumes (i.e., the mesh elements) in the model domain. This integration takes the general form of (White, 2006):

$$\frac{dB}{dt} = \frac{d}{dt}\int_{CV}\frac{dB}{dm}\rho dv + \int_{CS}\frac{dB}{dm}\rho \boldsymbol{V}\cdot d\boldsymbol{A} \qquad (9)$$

B any transport property (mass, momentum, energy, etc.).

t time.

m mass.

ρ density.

v volume.

$\boldsymbol{V}$ velocity.

$\boldsymbol{A}$ area vector.

$\int_{CV}$ integral over the control volume.

$\int_{CS}$ integral over the control surface.

The right hand side of Eq. (9) contains both a time dependent ($\frac{d}{dt}\int_{CV}\frac{dB}{dm}\rho dv$) and a convective ($\int_{CS}\frac{dB}{dm}\rho \boldsymbol{V}\cdot d\boldsymbol{A}$) term. The finite volume method is ideal for complex geometries like an open pit mine because, unlike finite difference methods, the finite volume method easily accommodates an irregular grid.

Using this control volume approach, a linear equation can be developed for each element in the mesh. The transport property (B) for each mesh element can be expressed as a linear equation involving all of the neighboring mesh elements. This discretization results in a sparse matrix of coefficients. In Fluent, this system of linear equations is solved using a combination of the Gauss-Seidel and Algebraic Multigrid (AMG) techniques (ANSYS, 2009a). The Gauss-Seidel method is an iterative technique that can be executed without consuming large amounts of memory, making this method ideal for large scale problems. The AMG method is used in conjunction with the Gauss-Seidel method to accelerate the convergence of the solver. The Gauss-Seidel method is

efficient at removing local errors in the domain, while the AMG method is performed at coarser mesh sizes and is used to resolve the global errors in the model (ANSYS, 2009a).

In Fluent, all transport properties are computed at the center of the mesh elements. However, for the convective term in Eq. (9), the transport property at the face of each element must also be estimated. In order to determine the transport property at each element face some form of spatial discretization from the center to the face of each mesh element must be performed. Fluent provides nine different options to accomplish this discretization. Two of these methods perform well for a wide variety of problems: 1) the first-order upwind scheme, and, 2) the second-order upwind scheme.

In the first-order upwind scheme, the value of the transport property at each face is simply assumed to be identical to the transport property at the center of each element. The first-order upwind scheme provides satisfactory results for most modeling cases. If more accuracy is desired, the second-order upwind scheme can be used. In the second-order upwind scheme, the face value can be expressed by the following equation:

$$B_f = B + \nabla \mathrm{B} \cdot \boldsymbol{r} \qquad (10)$$

B_f transport property at the element face.

B any transport property (mass, momentum, energy, etc.).

$\nabla \mathrm{B}$ gradient of the transport property in the upstream element.

$\boldsymbol{r}$ a vector from the centroid of the upstream element to the element face.

For a transient model, the control volume equation must also be discretized over a finite time step. Fluent uses two basic approaches to discretize the time dependent

term. The first approach, the implicit approach, is unconditionally stable in time. The implicit approach is recommended for most models. In some situations, however, the explicit approach provides more accurate results. The explicit approach is typically used to model shock waves in high Mach number flow situations (ANSYS, 2009a). The explicit approach is conditionally stable, and the time step used cannot exceed the Courant-Friedrich-Lewy Condition for the underlying solver.

The Fluent software offers a number of methods to ensure that convergence has been achieved. The default method is the monitoring of "residuals". Residuals represent the round-off error for each transport property in the simulation. The model residuals will generally decay by six orders of magnitude before convergence is achieved. Fluent also allows the user to specify user defined convergence criteria using a number of different techniques.

3.5 Turbulence Modeling

Modeling turbulence is critical to problems in open pit mine ventilation. The natural wind flow in open pit mines is often recirculatory (Baklanov, 2000). The geometry of an open pit mine naturally generates large amounts of mechanical turbulence. Turbulence is important from a modeling perspective because turbulence affects the values of mass diffusion coefficients, convective heat transfer coefficients, and many other parameters.

A mesh resolution ranging from a few meters to a few hundred meters is necessary to resolve the larger scale turbulent eddies in the atmospheric boundary layer

(*Jacobson*, 2005). The size of the smallest turbulent eddies in the atmosphere are given by the Kolmogorov length scale:

$$\eta_k = \left(\frac{\nu}{\varepsilon}\right)^{1/4} \qquad (11)$$

η_k Kolmogorov length scale.

ν kinematic viscosity of air.

ε dissipation rate of turbulent kinetic energy.

For typical conditions in the atmosphere, the Kolmogorov length scale is approximately 2 mm. Consequently, turbulence must be parameterized for any grid cell with dimensions larger than this value.

A large amount of research has been carried out using turbulence models, in order to predict the effects of turbulence. These models have been statistically developed to account for the effects of turbulence without having to resort to a very fine mesh. The kappa-epsilon (κ-ε) family of turbulence models has found widespread acceptance for many different types of engineering simulations (ANSYS, 2009a). These models perform well resolving the dominant flow features in most situations and are relatively low cost computationally. Three different κ-ε turbulence models are included in the Fluent software package. These include the standard, renormalization group (RNG), and realizable κ-ε models. In each of these models, two transport equations are solved to obtain the turbulent kinetic energy (κ) and the turbulent dissipation rate (ε).

The realizable κ-ε model, in particular, has found widespread application in ventilation problems (e.g., Purusotham and Bandopadhyay, 2010; Kantipudi et al., 2009;

Stephens and Calizaya, 2010). This model performs better than the standard κ-ε model for flows involving rotation and recirculation (ANSYS, 2009b). Compared to the standard κ-ε model, the realizable model features a different formulation for turbulent viscosity and a modified transport equation for the turbulent dissipation rate. The realizable κ-ε model corrects a mathematical flaw in the other two κ-ε models. Under high strain conditions the predicted normal stress in the fluid becomes negative in the standard and RNG models. This behavior is physically impossible since a negative normal stress would place the fluid into tension. The realizable κ-ε model eliminates this physical inconsistency.

This research adopted the Reynolds Averaged Navier-Stokes (RANS) equations with the realizable κ-ε model to predict the airflow in the pit. RANS methods are a good compromise between accuracy and computational efficiency. These methods describe the unsteady eddies that form the turbulence by their mean effect on the flow.

This method follows classical procedures used in CFD simulation: geometry definition, meshing of the domain, definition of the problem physics, solution, and, finally, post processing of the results (Figure 3.7).

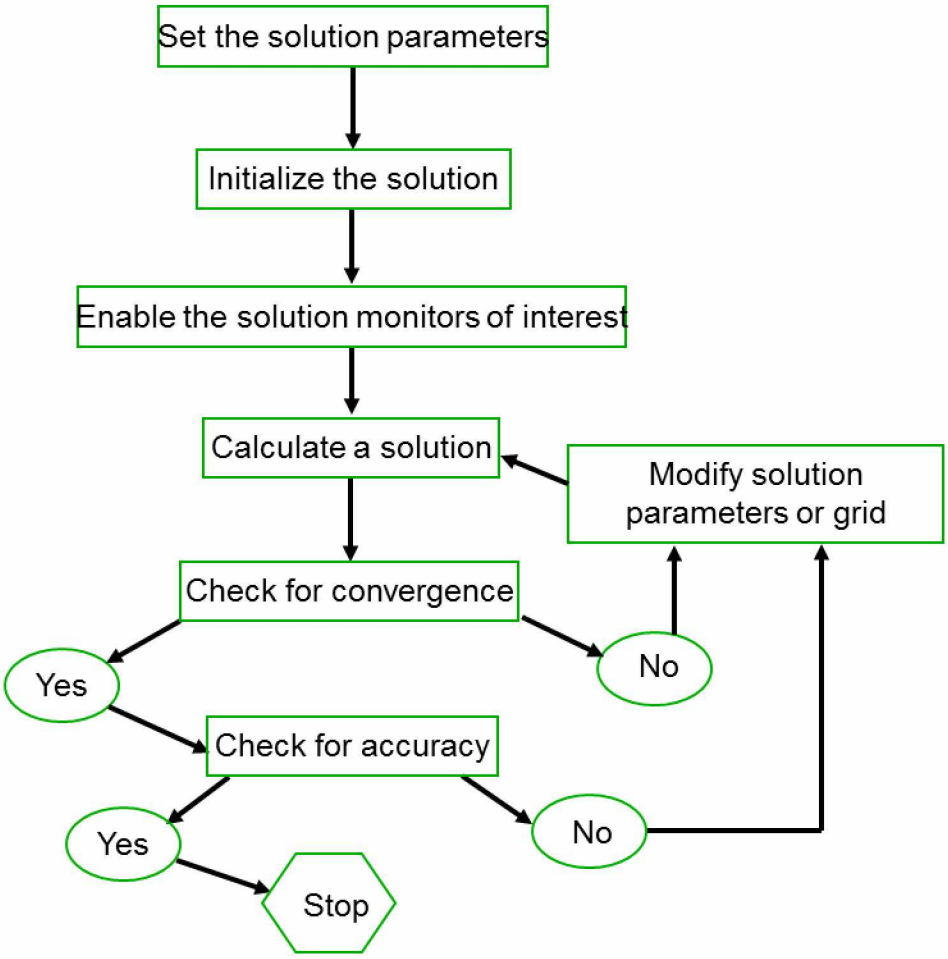

Figure 3.7: Solution Process for a CFD Simulation

3.6 Geometry and Mesh Creation

An open pit mine which—has a closed structure on all sides—is different from other geometries. Its topography is very rugged and uneven. The open pit mine studied here is approximately 1,980 m (6,500 ft) long in the E-W direction, 1,220 m (4,000 ft) wide (N-S) and 274 m (900 ft) deep. The pit slope tends to be flatter on top (35°), while the bottom pit slope is approximately 40°. The pit geometry, as of March 2009, is shown in Figure 3.8.

Figure 3.8: Geometry of the Open Pit Mine Used in the Study

The open pit model geometry started as a series of three meter contour intervals. These contours consisted of 3D Polylines in AutoCAD DWG file format. From these AutoCAD files, two dimensional profiles of the pit were created using the Maptek Vulcan

suite of mine design software. The contour files were imported into Vulcan and "draped" with a three dimensional surface. Profiles were then created along this surface in 30 m (100 ft) intervals perpendicular to the north-south axis of the pit. The profile that depicted the most "extreme" values (i.e., longest and deepest portion of the pit) was selected for the 2D geometry modeling of the 2005 and 2010 pits.

After the profiles had been created in Vulcan they were imported into Design Modeler. Design Modeler is the geometry modeling package bundled with the ANSYS Fluent Software. In Design Modeler, each profile was "filled" with a fluid volume representing the atmosphere inside the pit. Each profile is ready for meshing after this step has been accomplished.

After a fluid volume representing the region to be modeled has been created, the file is ready to be imported into the ANSYS meshing application. A quality mesh is an essential first step in obtaining a quality CFD analysis. It was important to refine the mesh around critical areas. These areas include the inlet, outlet, pit bottom, boundary layer, and pollutant sources. A refined mesh is required to capture the large velocity, heat flux, and concentration gradients in these particular areas. A coarser mesh is acceptable in the interior of the model.

Meshing a large, highly irregular geometry, such as an open pit mine, is a challenge. The sharp edges and irregular boundaries of the model domain can result in poor quality mesh elements. These mesh elements can create numerical diffusion in the program, introducing errors into the solution that can result in instability of the model. Due to

the large size of the domain, a large number of mesh elements are required. As a general rule of thumb, more mesh elements result in a more precise solution. In CFD modeling, there is always a compromise between the precision of the solution and computational realities. The overall goal is to achieve mesh independence. A mesh independent solution will not change appreciably with an increase in the number of mesh elements.

3.7 Wind Flow in Open Pit Mines

Using the model geometry, extensive CFD modeling of wind flow patterns in the selected open pit mine was studied. Numerical experiments about the effect of depth, wind velocity, and pit slope angle on the recirculation within the open pits were conducted. Examples of the airflow patterns in the selected pit are shown in Figure 3.9 through Figure 3.11. It can be seen that as soon as the airflow enters the pit, the air velocity of the flow decreases significantly, such that it soon reverses owing to the resistance due to mechanical forcing of the surfaces within the pit. In general, the flow regime within the model domain transitions from an apparent laminar region at the top of the pit to turbulent flow at the bottom of the pit. The depth has a significant effect on the airflow pattern within the open pit. In case of relatively shallow pit (Figure 3.9) airflow expands gradually without any gap in the mine. There is very little compression of flow line on the outlet area due to action of flow inertia. In the case of a deeper pit (Figure 3.10), the fluid vortex has a shape of flattened ellipse whose height and width differ significantly. For the same inlet air velocity and the same slope angle the

mechanical forcing and the turbulence increases with depth, resulting in or strengthening the reversal of airflow and recirculation. The size of the turbulent eddies vary as a function of velocity, pit depth, and slope angle. The recirculatory patterns observed in the selected open pit closely matched the recirculatory patterns observed by other researchers. Figure 3.9-Figure 3.12 show the effect of the velocity changes on the air recirculation.

Figure 3.9-Figure 3.12 show that under the same conditions the larger the inflow velocity, the stronger is the mechanical turbulence, and the larger is the size of the eddies. Mechanical turbulence increases with depth, which causes and strengthens the reverse airflow and recirculation (Figure 3.14). The airflow then ascends over the leeward side of the pit and joins the oncoming airflow in the upper layer. This generates a closed circulation and eddies in the pit. This is a typical characteristic feature of the stationary ABL of an open pit mine. In order to see clearly the effects of the geometry of the pit, airflow patterns were simulated in the 2010 pit (Figure 3.10-Figure 3.14) show the structure of the stationary ABL in the pit, which is very different in magnitude but has the same re-circulatory trends. The above mentioned effects were observed under neutral atmospheric conditions since no heat was added. Therefore, thermal buoyancy was not a factor in the recirculatory process.

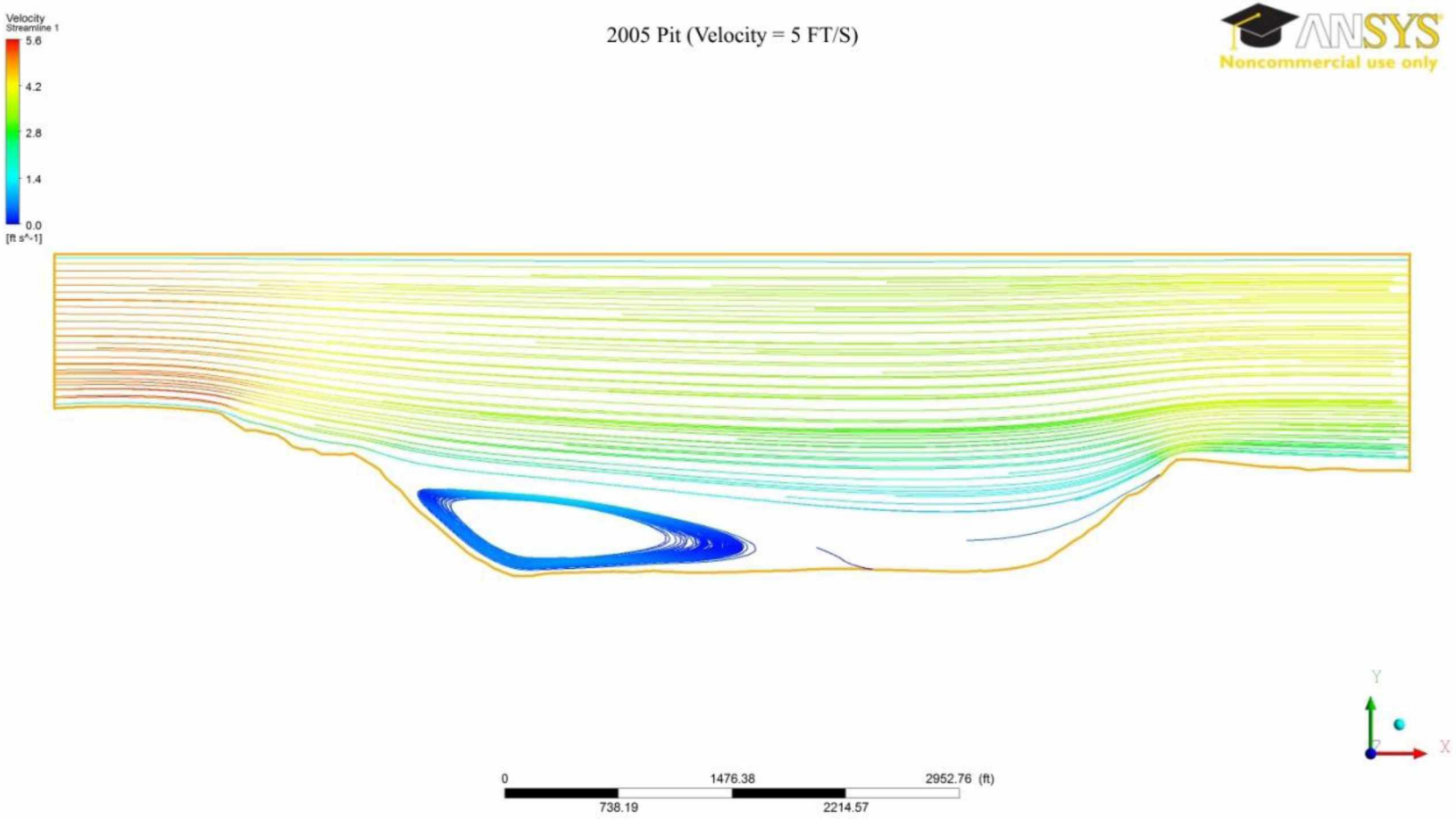

Figure 3.9: Velocity Profiles Showing Recirculation Zones in 2005 Pit (Velocity 5 ft/sec)

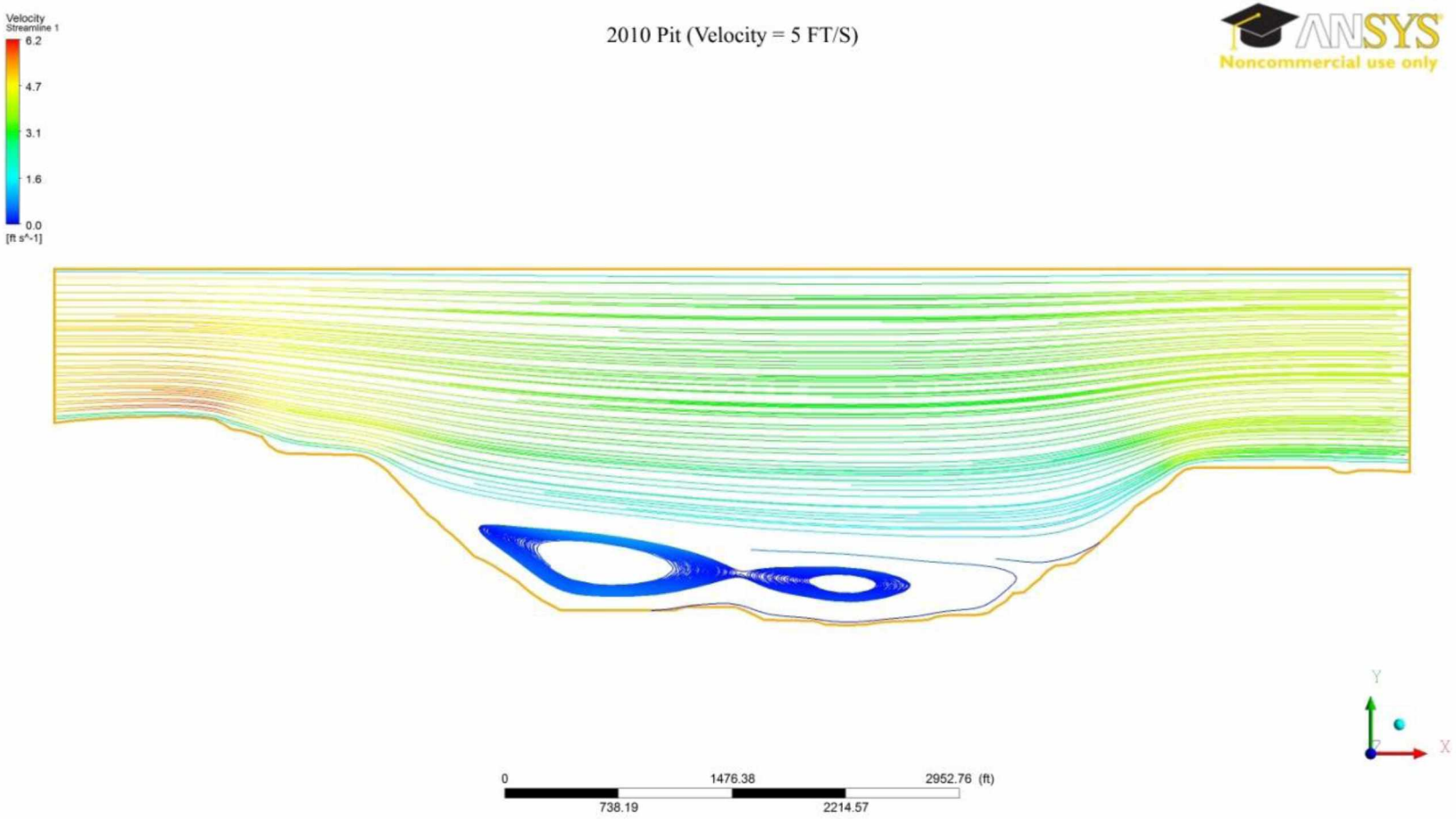

Figure 3.10: Velocity Profiles Showing Recirculation Zones in 2010 Pit (Velocity 5 ft/sec)

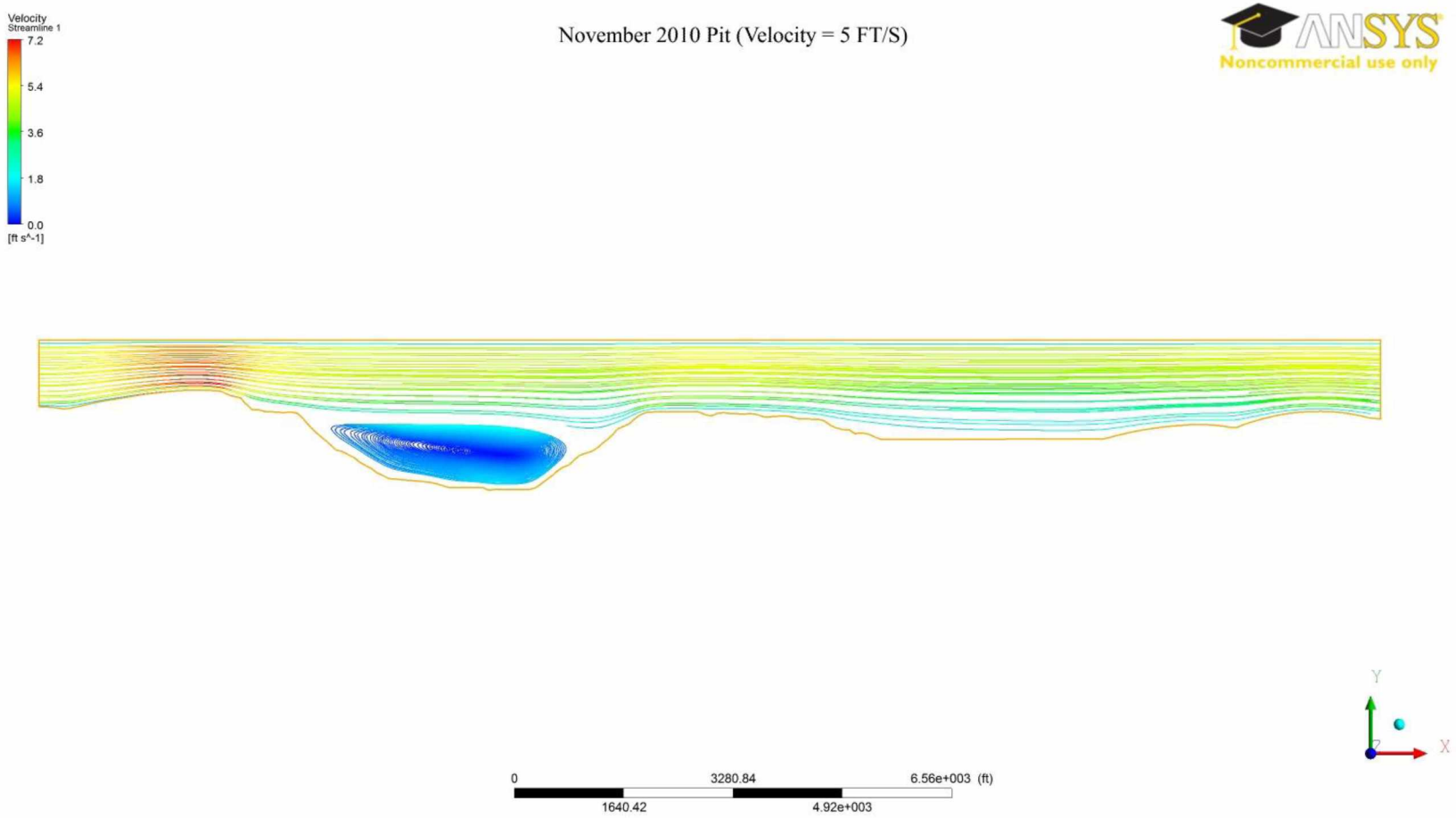

Figure 3.11: Velocity Profiles Showing Recirculation Zones in 2010 Extended Pit (Velocity 5 ft/sec)

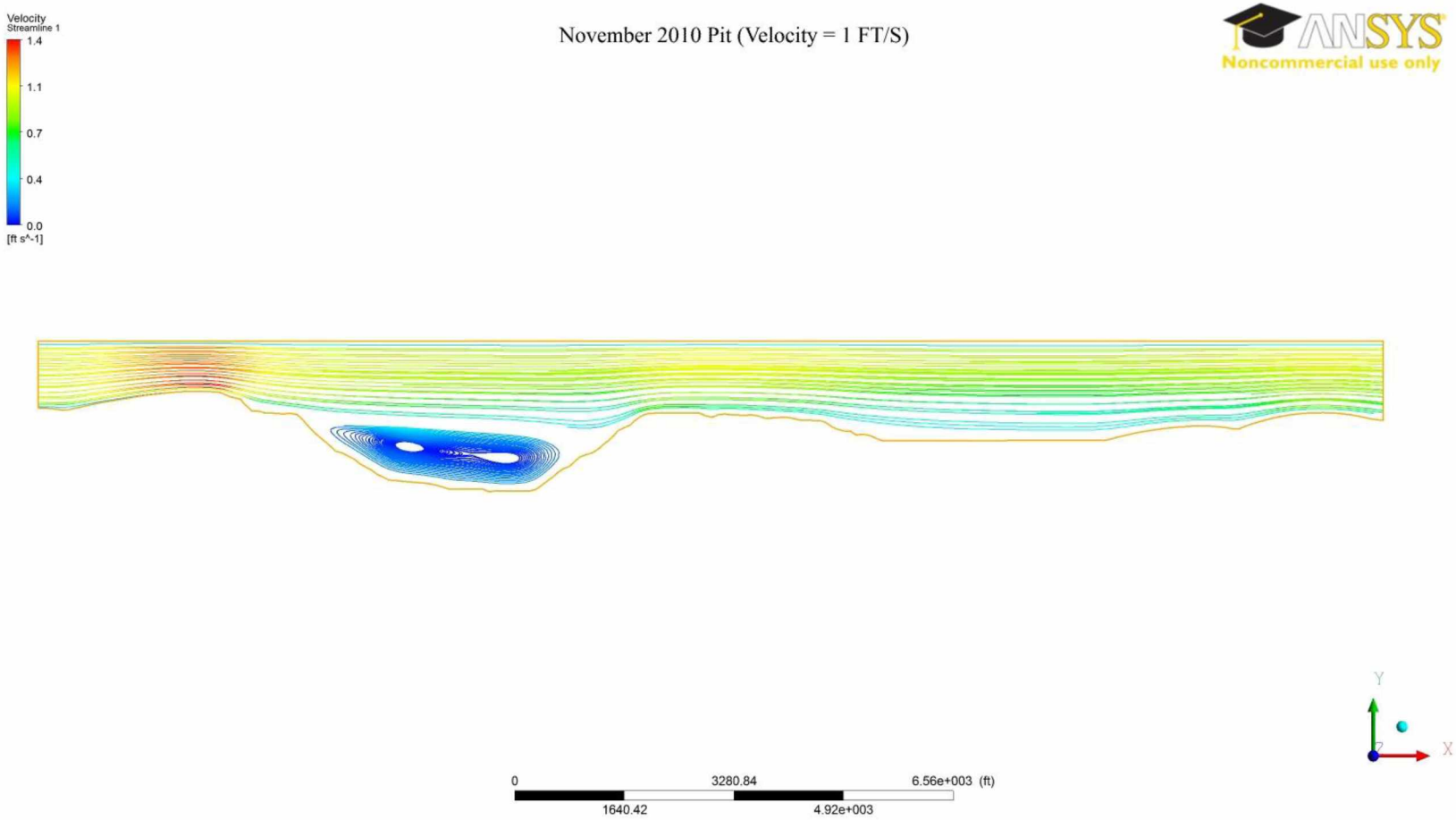

Figure 3.12: Velocity Profiles Showing Recirculation Zones in 2010 Extended Pit (Velocity 1 ft/sec)

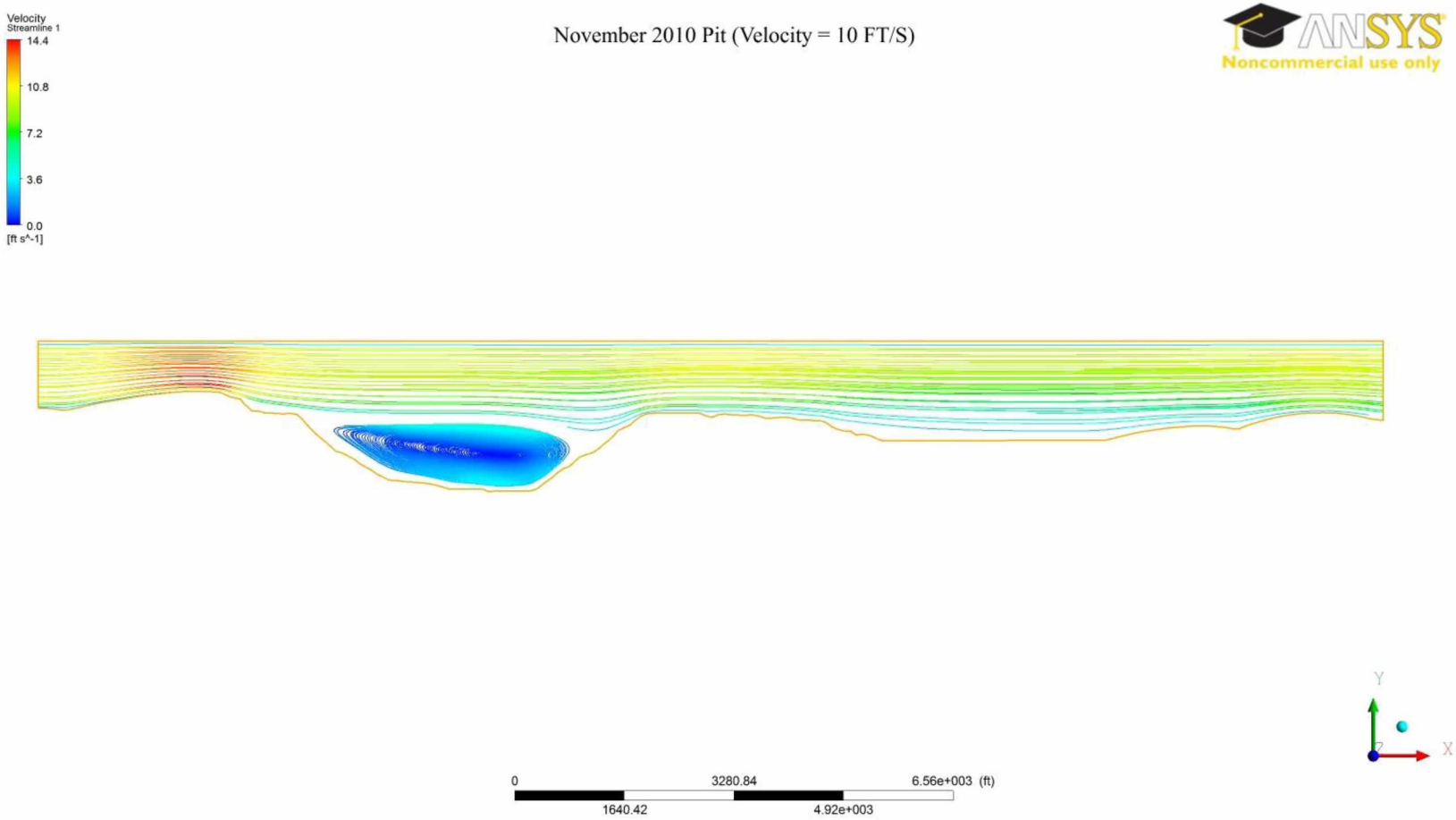

Figure 3.13: Velocity Profiles Showing Recirculation Zones in 2010 Extended Pit (Velocity 10 ft/sec)

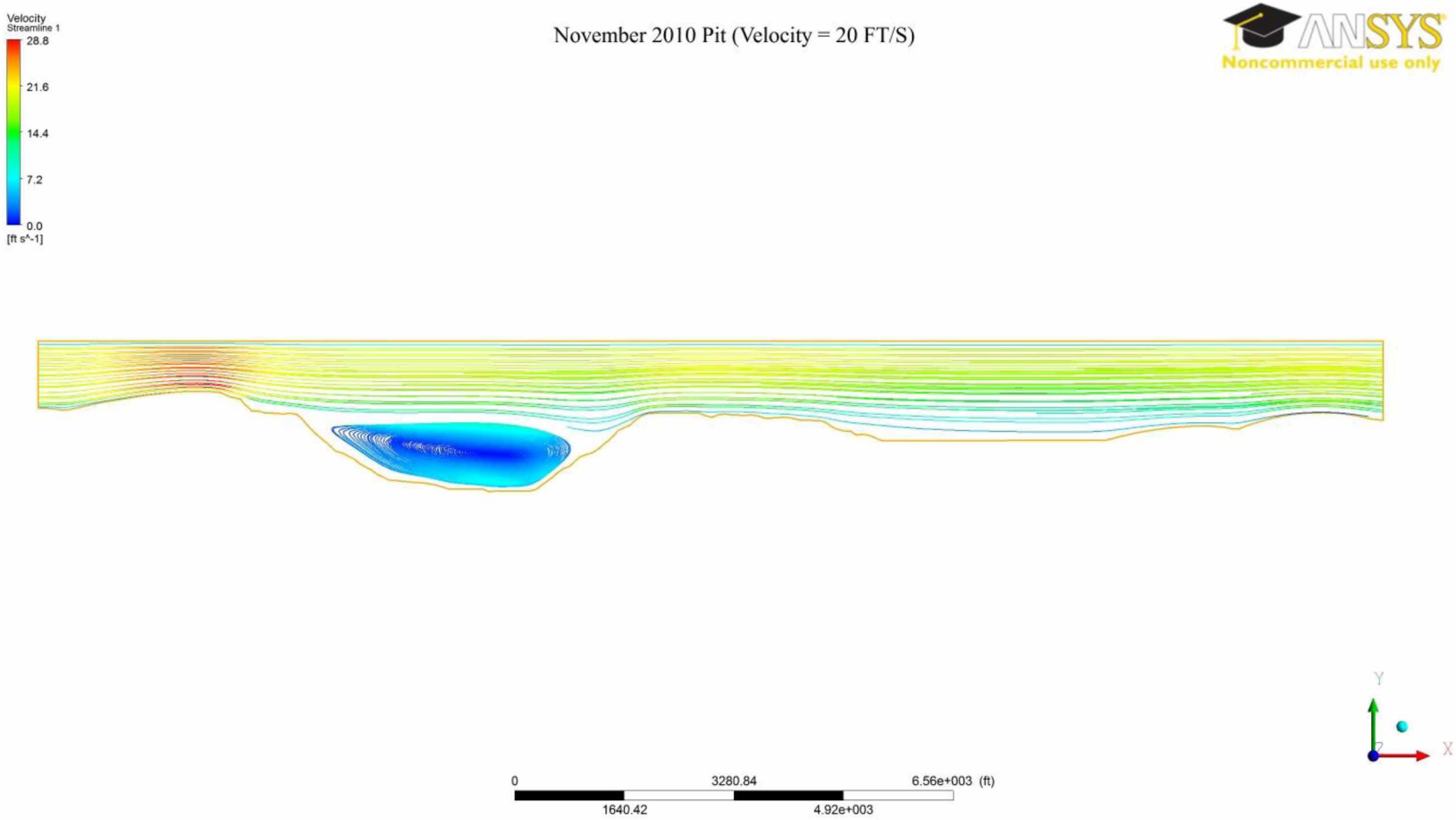

Figure 3.14: Velocity Profiles Showing Recirculation Zones in 2010 Extended Pit (Velocity 20 ft/sec)

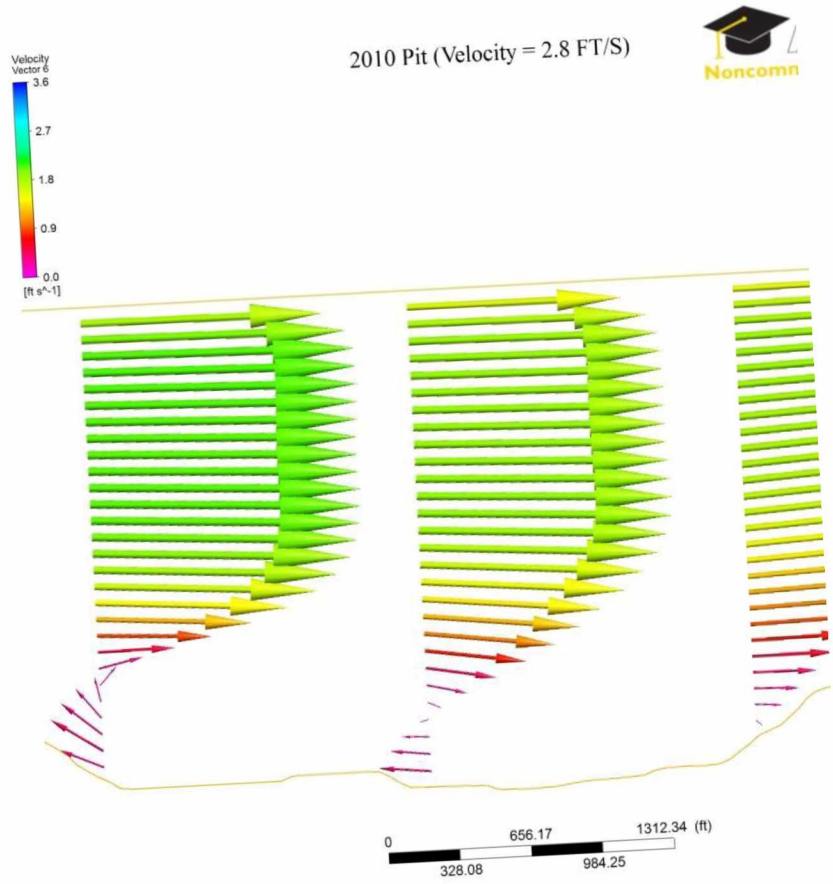

Figure 3.15: Reverse Airflow in the 2010 Pit

The effect of pit slope angles on the wind flow within open pit mines has been presented in the literature (Collingwood et al., 2012). Six different idealized pits were modeled. The first case considered was a rectangular pit with a 46 m (150 ft) bottom width. The overall pit slope was 90°. Five different pit depths were modeled for this particular configuration. The depth of these pits ranged from a minimum of 15 m (50 ft) to a maximum of 76 m (250 ft). A multitude of different wind velocities were modeled. For each of the variables considered, recirculation within the pit proved to be significant. In some instances, multiple recirculation zones are evident in the pit (Figure 3.16). For the pit shown in the figure, the length-to-depth ratio (length across the top of the pit divided by the depth of the pit) is equal to 1.0. As a general rule, it seems that—for a given velocity—recirculation in the pit intensifies as the length-to-depth ratio decreases.

The next case considered was a trapezoidal pit with a 46 m (150 ft) bottom width. This time, the overall pit slope was set to 60°. Four different pit depths were modeled for this particular pit geometry. The depth of these pits ranged from a minimum of 76 m (250 ft) to a maximum of 305 m (1000 ft). As before, a multitude of different wind velocities were modeled. Recirculation was again present in each pit. As with the rectangular pits, multiple recirculation zones are present in some instances (Figure 3.17). As can be seen from the figure, the magnitude of the wind velocity in the pit is relatively low in this particular instance. For the pit shown in the figure, the length-to-depth ratio is approximately equal to 1.5.

A trapezoidal pit with 45° overall slopes was also modeled. As before, four different pit depths were modeled for this particular pit configuration, ranging from a minimum depth of 76 m (250 ft) to a maximum of 305 m (1000 ft). The wind flow patterns in the trapezoidal pit with 45° overall slopes are quite similar to the recirculatory patterns in the pit with 60° slopes. In each simulation, the multiple recirculation zones do not seem to appear until the wind velocity and the length-to-depth ratio of the pit reach certain threshold values (Figure 3.18). For the pit shown in the figure, the length-to-depth ratio is equal to 2.6.

The final idealized geometry modeled was a trapezoidal pit with 30° side slopes. The minimum length-to-depth ratio for the idealized geometry with 30° slopes is approximately equal to 3.6. These simulations exhibited some unique characteristics. None of the multiple recirculation zones observed in the other models are present in the model with 30° overall slopes (Figure 3.19). Nevertheless, all of these idealized models still had prominent recirculation zones in the pit.

The final task was to model the wind flow in the actual pit geometry and compare it to the idealized pit models. Although recirculation can still be observed in the pit bottom, the magnitude of recirculation in the pit bottom is reduced in comparison to the idealized pit models (Figure 3.20). In the actual geometry, the airflow within the pit appears to have segregated into regions of laminar and turbulent airflow. This observation is consistent with the concept of the expansion angle introduced by other researchers. Moreover, this result seems to be supported by real world observations.

In Figure 1.2 it is seen that the top portion of the pit—dominated by laminar flow—is well ventilated. The bottom portion of the pit—the region in which recirculation dominates—is filled with a high concentration of pollutants. This visual evidence is supported by contaminant concentration data collected at the selected mine site during inversions. This data shows a significant decrease in contaminant concentrations above the inversion. Similar results were also observed by other researchers (Meroney and Grainger, 1992).

The wind penetrates further into the pit in the actual model than in the idealized models. The same effect was observed in similar numerical studies conducted by Tandon and Bhaskar (1998). In wind tunnel studies, it has been observed that the penetration of flow into the pit depends heavily on the Froude number of the pit (Meroney and Grainger, 1992). Clearly, wind velocity and the geometry of the pit play a very significant role in determining the nature of the local recirculation patterns within the pit.

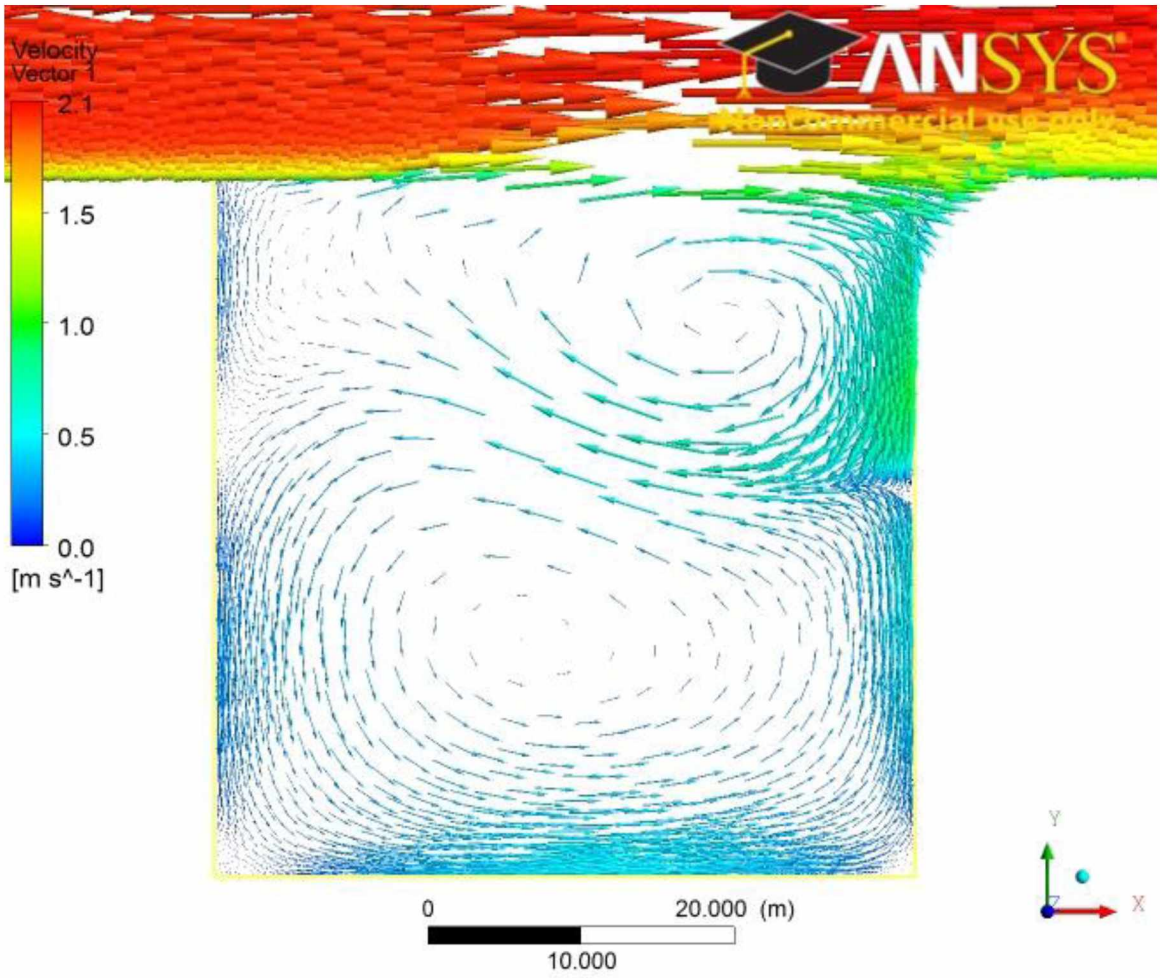

Figure 3.16: Velocity Vectors for a 46 m X 46 m Pit (Initial Wind Velocity = 2 m/s)

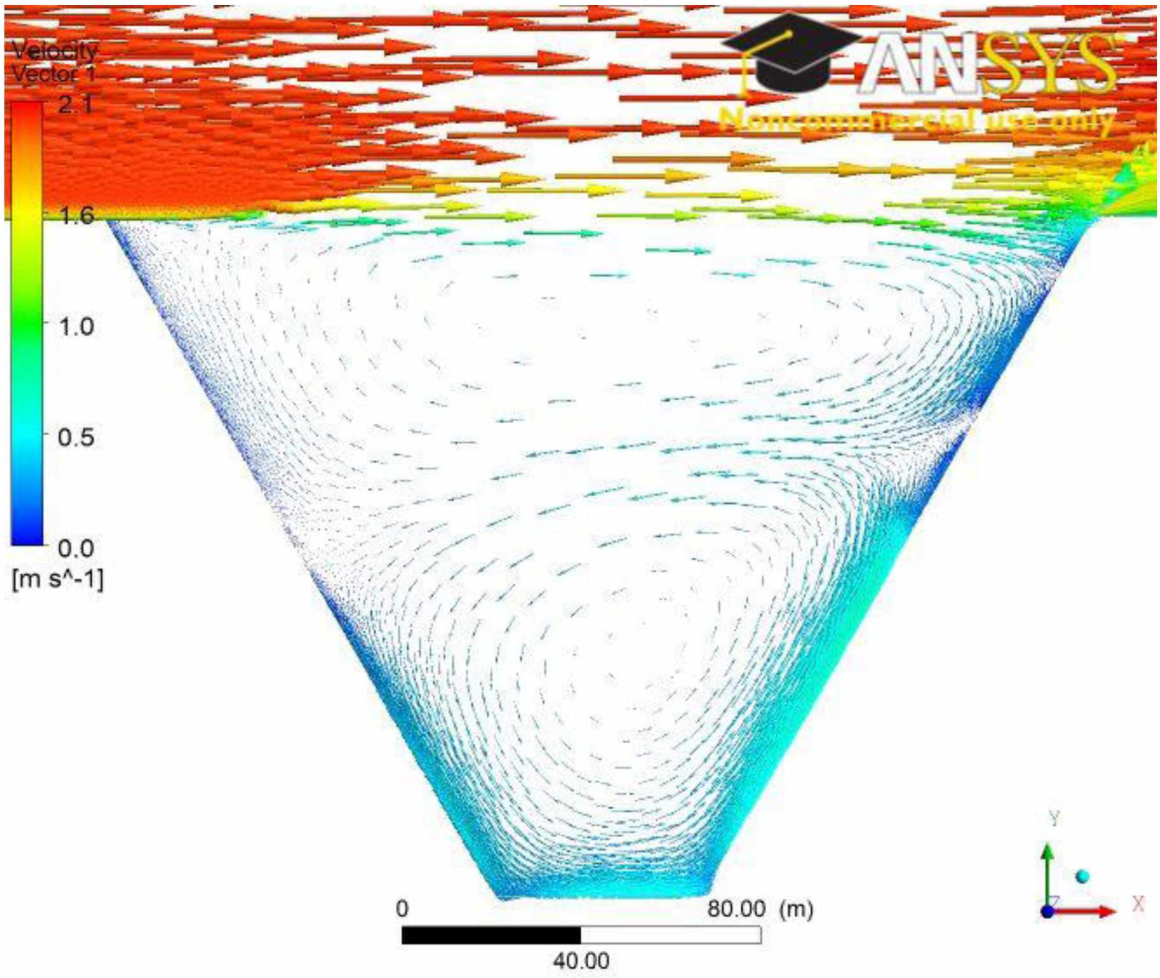

Figure 3.17: Velocity Vectors for a 60° Trapezoidal Pit 152m in Depth (Initial Wind Velocity = 2 m/s)

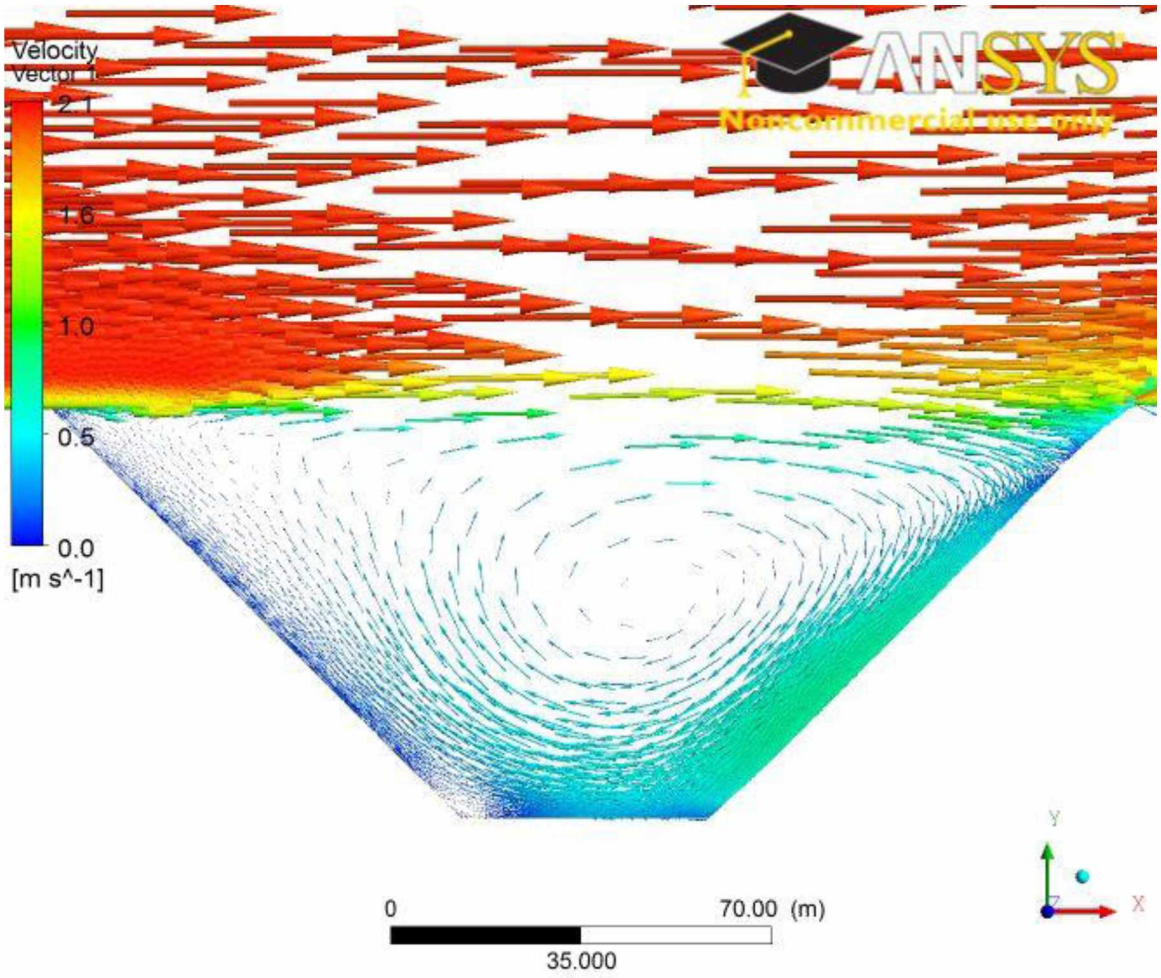

Figure 3.18: Velocity Vectors for a 45° Trapezoidal Pit 76m in Depth (Initial Wind Velocity = 2 m/s)

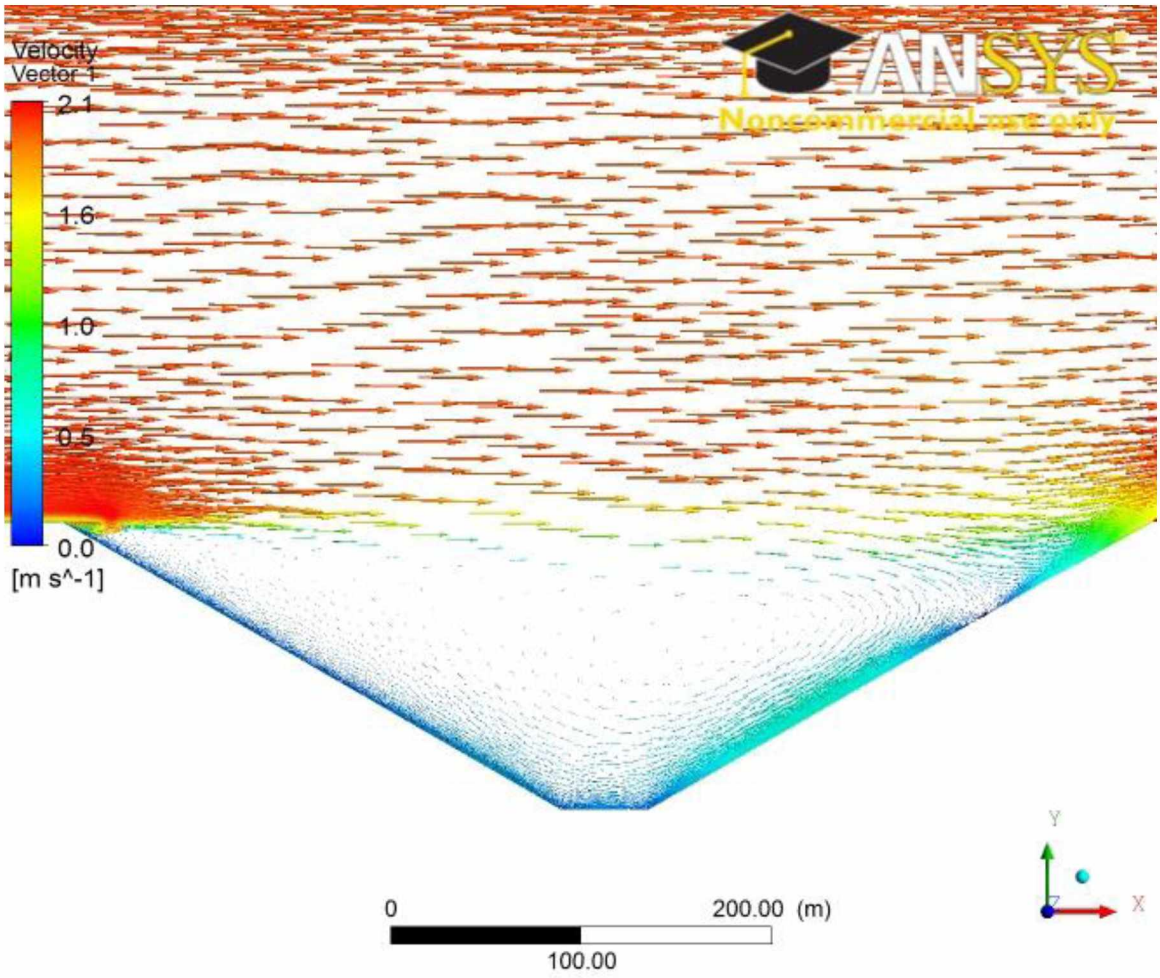

Figure 3.19: Velocity Vectors for a 30° Trapezoidal Pit 152m in Depth (Initial Wind Velocity = 2 m/s)

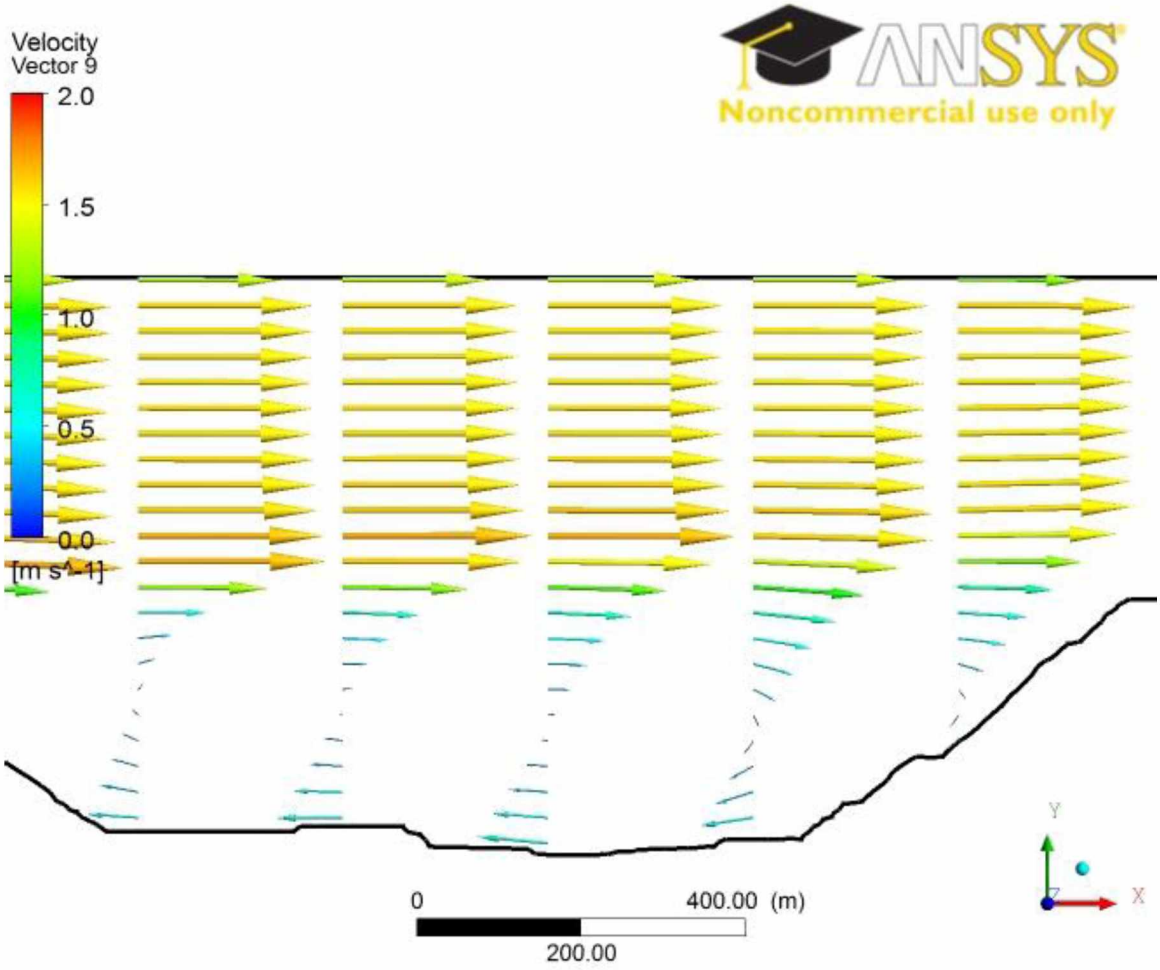

Figure 3.20: Velocity Vectors for Actual Pit Geometry (Initial Wind Velocity = 2 m/s)

3.8 Development of an Atmospheric Inversion

Initial simulations of airflow and pollution transport were performed under neutral atmospheric conditions. In a neutral atmosphere, all turbulence generation is mechanical; in other words, thermal turbulence is not present (Stull, 2003). Modeling heat flux at the pit boundaries is necessary to simulate an atmospheric inversion. Initially, the model failed to converge when heat flux was added at the pit boundary. This failure was likely due to the presence of small, skewed mesh elements near the pit bottom boundary. These elements, in conjunction with the high gradients near the pit bottom, are a source of instability in the model. A modified meshing and modeling approach has allowed for model convergence under non-neutral atmospheric conditions. One of the most significant changes made to the modeling approach was to locate the outflow boundary region further away from the study area to minimize boundary effects.

A coarser mesh has greatly aided the model convergence and has reduced the time required to run the models under non-adiabatic conditions. The resolution of the mesh is satisfactory enough to capture the larger scale mechanical and thermal turbulent eddies in the open pit.

The variation in air density within the pit is needed in order to model buoyancy driven flow. A fully compressible CFD model (which uses the ideal gas law to determine density) is complex, and convergence problems are very common. An alternative to the fully compressible approach is to use the incompressible ideal gas law (Eq. 7) to

determine the air density. The alternative approach modifies the ideal gas law by assuming a constant operating pressure. The density is then calculated solely as a function of temperature. Model convergence is much more easily achieved when the incompressible ideal gas law is used as opposed to a fully compressible model. It has been observed in the selected mine that the temperature gradient between the top and the bottom of the pit is small enough that this approach provides sufficient accuracy without convergence issues.

There are two basic choices for the outlet boundary in our models (i.e., the area where the airflow exits the model): a pressure outlet boundary and an outflow boundary. The pressure outlet type requires knowledge of several of the flow properties at the outlet. These include pressure and backflow properties (temperature, turbulence parameters, etc.) For airflow and contaminant transport in a 2-D model domain, an outflow boundary allows for better convergence. An outflow boundary is valid for fully developed flows. Fluent extrapolates the flow characteristics at the boundary from the interior of the model. The extended pit topography (Figure 3.11) and the outflow boundary have greatly improved the model convergence. As a general rule, it is best to move the boundaries as far away as possible from the region of interest when running atmospheric models. Errors at the boundaries can propagate into the interior of the model domain over time (Warner et al., 1997).

Since an atmospheric inversion is not a steady state phenomenon, modeling of the transient state (i.e., time dependent) is required to model the inversion. Two different

approaches can be used for time stepping in the transient model. In the first approach, a constant time step is used throughout the model run. In the second approach, adaptive time stepping, the optimal time step size for convergence and computational efficiency is automatically selected.

The adaptive time stepping approach works much better for 2-D models of the open pit. Using the adaptive approach, a small time step is used for the initial iterations where the flow is still very unsteady. In the interest of efficiency, Fluent can subsequently increase the time step size after the initial iterations have been performed. For most of the models, a time step of around 0.5 second is sufficient to achieve convergence during the initial calculations. Depending on the convergence characteristics, Fluent will generally increase the average time step to around 30 second as the model progresses.

Figure 3.21 through **Error! Reference source not found.** illustrate the simulated growth of a temperature inversion in an open pit mine. In this particular case, a negative surface energy balance of 20 W/m^2 was used to simulate the inversion. This value is typical value for nighttime winter inversions in the area of the selected mine (Wendler and Jayaweera, 1972). The resulting temperature stratification approximates the measured data acquired at the selected mine site.

Simulations were performed using the 2005 and 2010 pit geometries to determine the effect geometry has on the temperature stratification within open pit mines. Temperature and air density were plotted along a vertical cross section of the 2005 and

2010 pits (Figure 3.26). Figure 3.27 and Figure 3.28 illustrate the growth of the inversion in the 2005 pit during the 18 hour simulation. Figure 3.27 shows the change in temperature with altitude, and Figure 3.28 shows the change in air density with altitude. The figures show that the strength of the temperature inversion increases over the course of the simulation, with the air progressively getting colder and denser. The top of the inversion cap is located at an approximate elevation of 660 m. Figure 3.29 and Figure 3.30 show the simulated temperature and air density, respectively, for the 2010 pit along the same vertical cross section. It can be seen that the strength of the inversion also increases in the 2010 pit as time progresses.

The final temperature (Figure 3.31) and air density (Figure 3.32) profiles for the 2005 and 2010 pits are shown. The inversion cap is located at approximately the same elevation (660 m) in both geometries. The figures show that the depth of the inversion is approximately 120 m greater in the 2010 pit than in the 2005 pit. The final air density at the bottom of the 2010 pit is greater than the air density at the bottom of the 2005 pit (Figure 3.32).

Figure 3.33 illustrates the velocity vectors in the 2010 pit model during an inversion. As shown in Figure 3.33, air movement in the pit has virtually ceased. Under these conditions, contaminants can easily accumulate in the pit if a source is present.

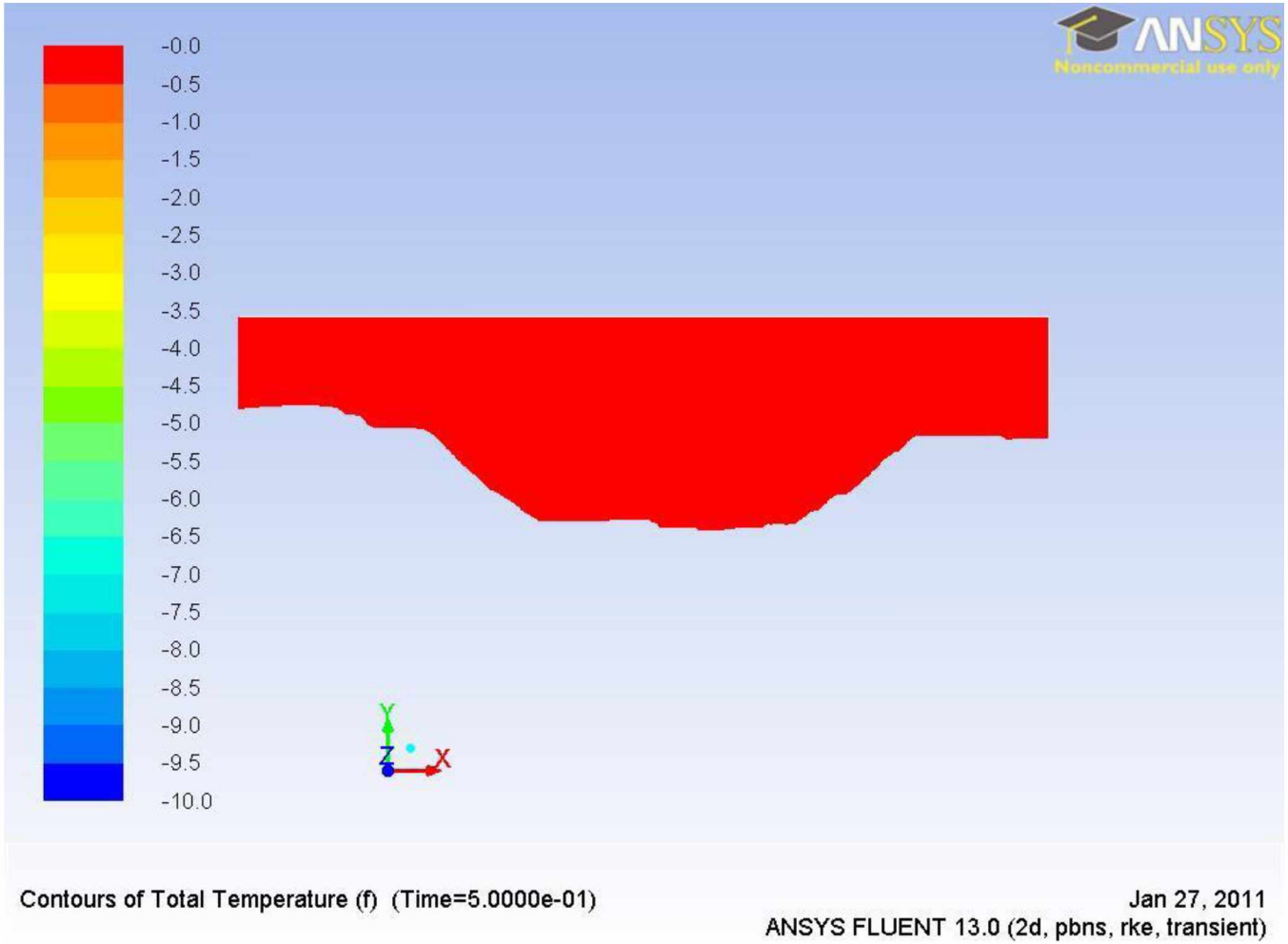

Figure 3.21: Pit Temperature Contours during an Inversion (Time = 0 Hrs.)

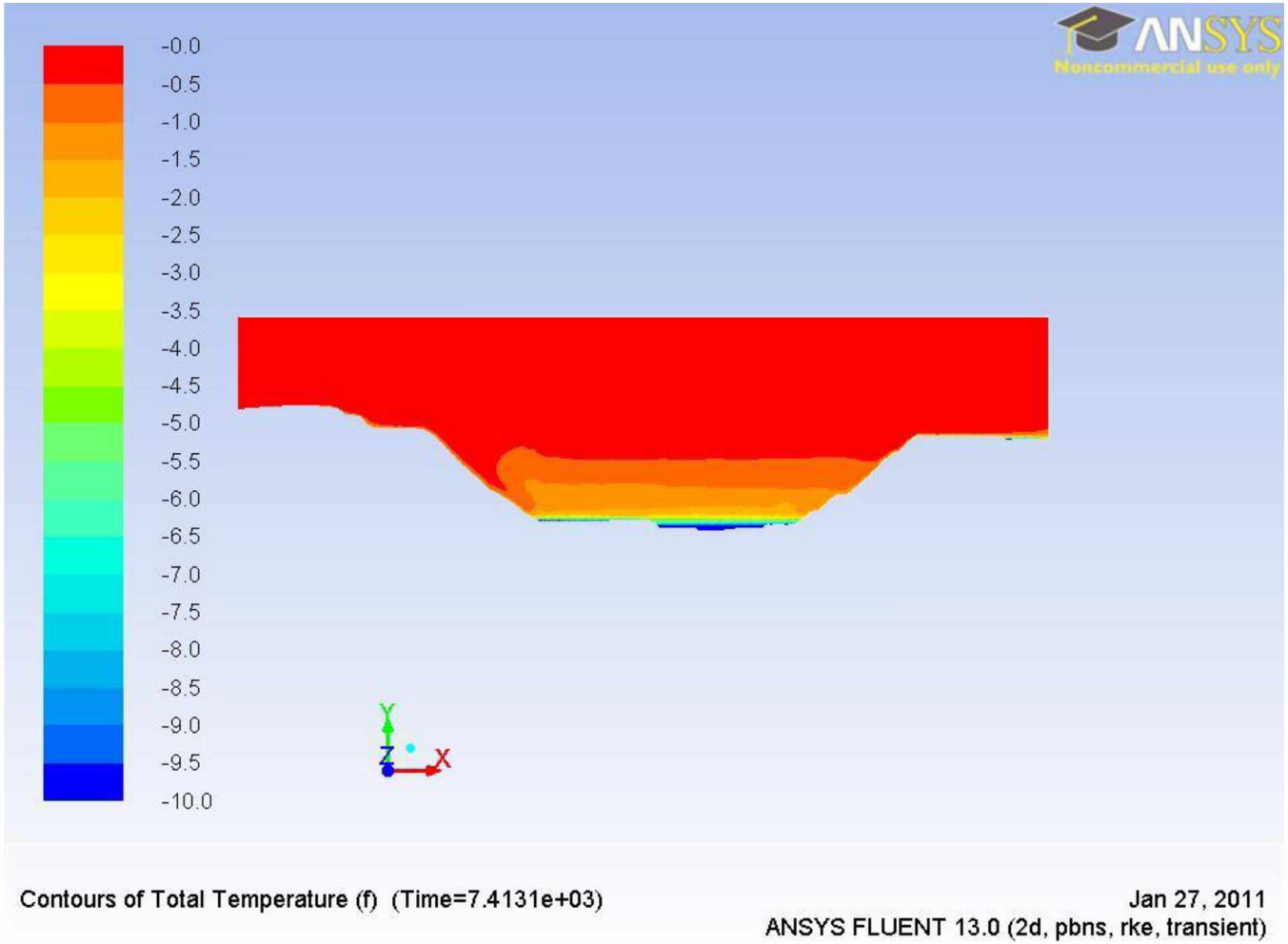

Figure 3.22: Pit Temperature Contours during an Inversion (Time ≈ 2.1 Hrs.)

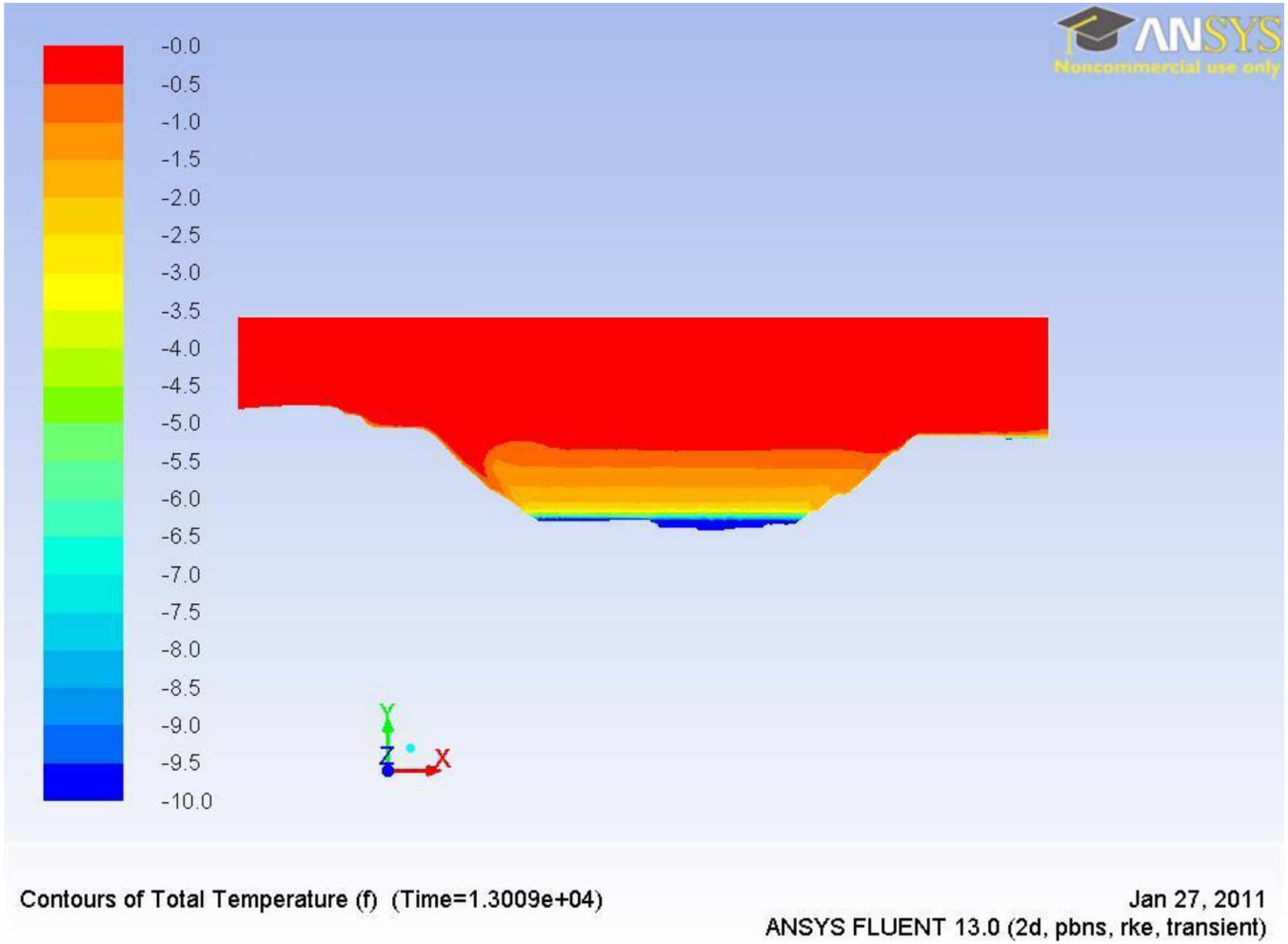

Figure 3.23: Pit Temperature Contours during an Inversion (Time ≈ 3.6 Hrs.)

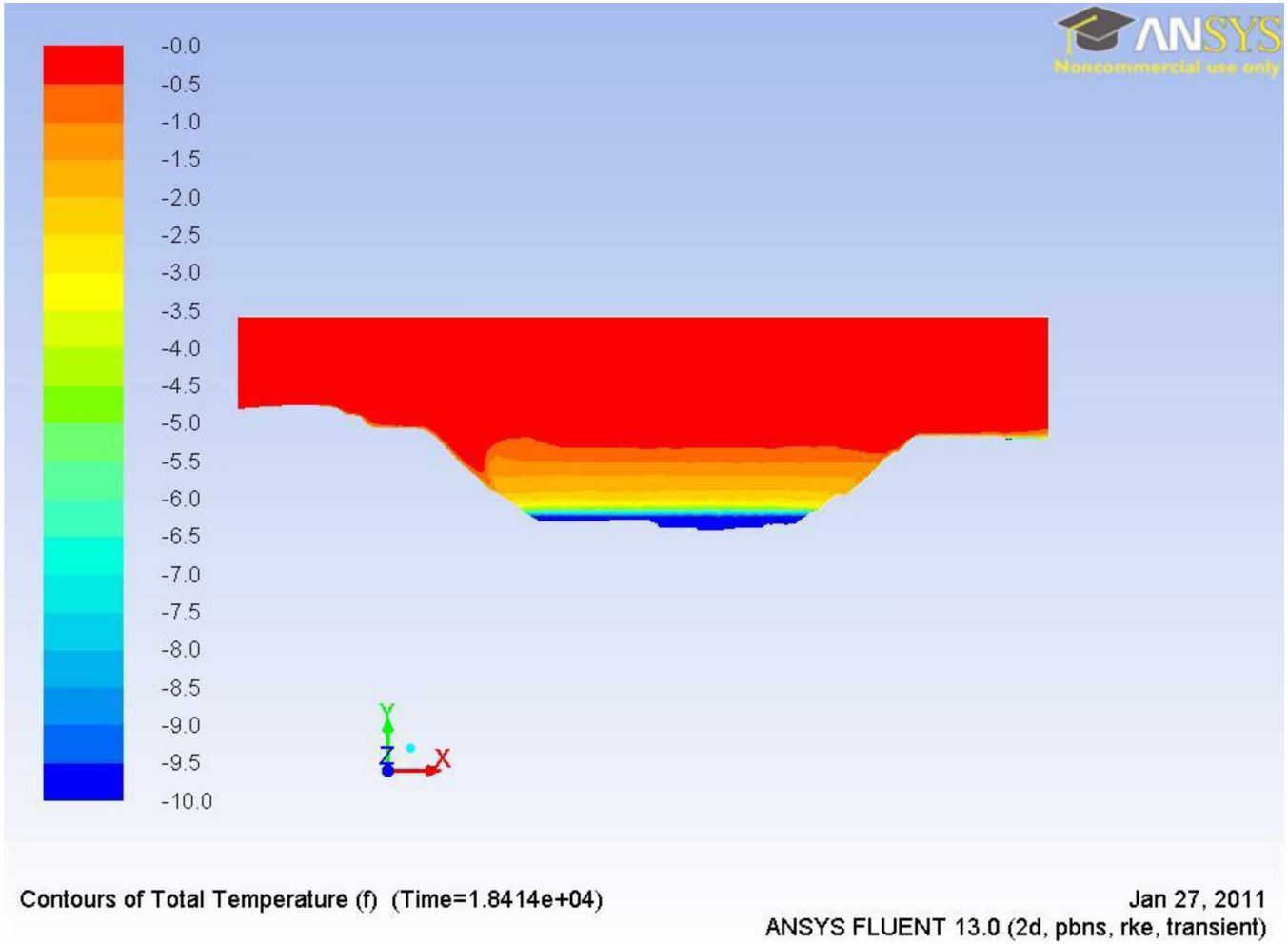

Figure 3.24: Pit Temperature Contours during an Inversion (Time ≈ 5.0 Hrs.)

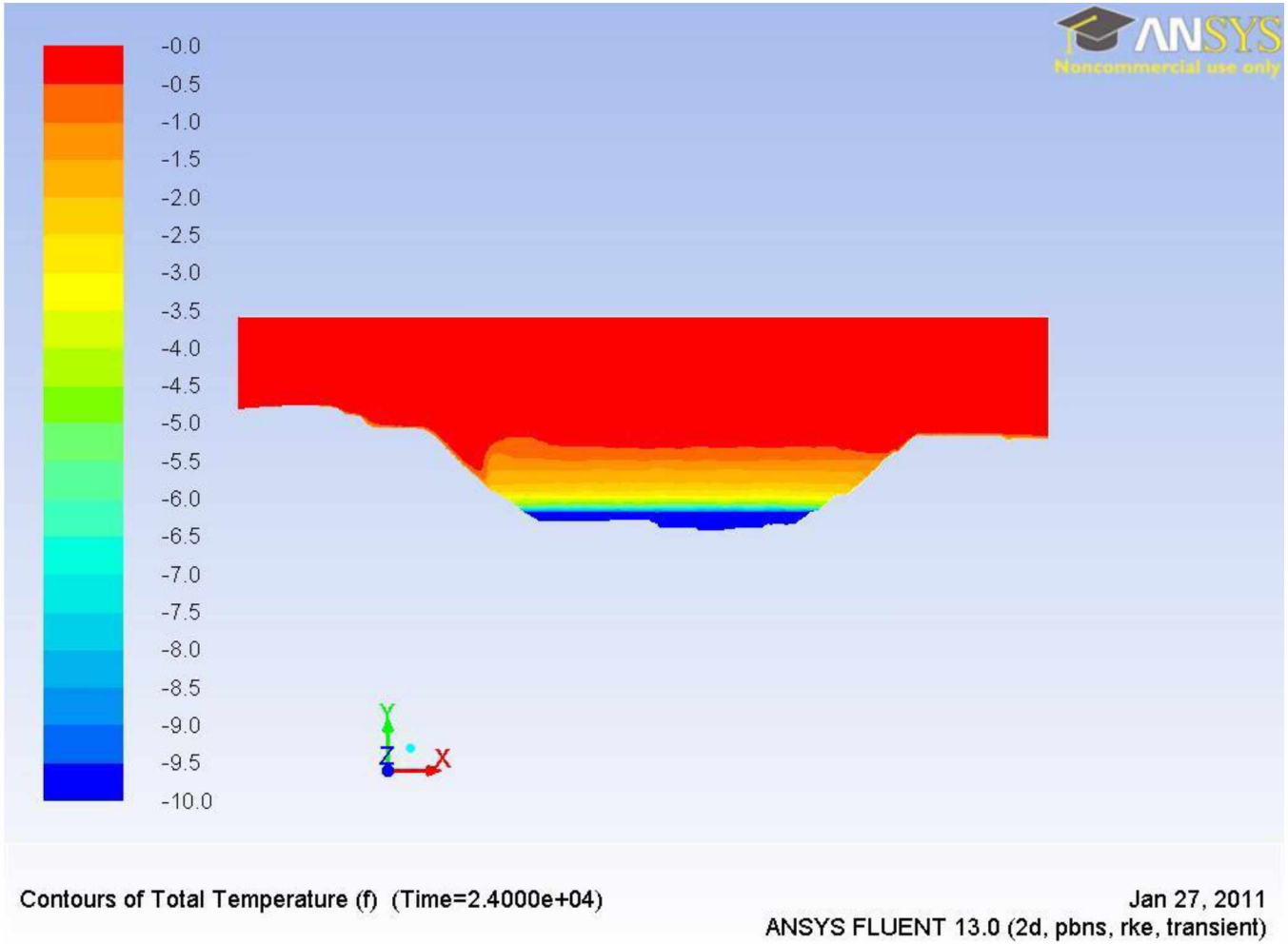

Figure 3.25: Pit Temperature Contours during an Inversion (Time ≈ 6.7 Hrs.)

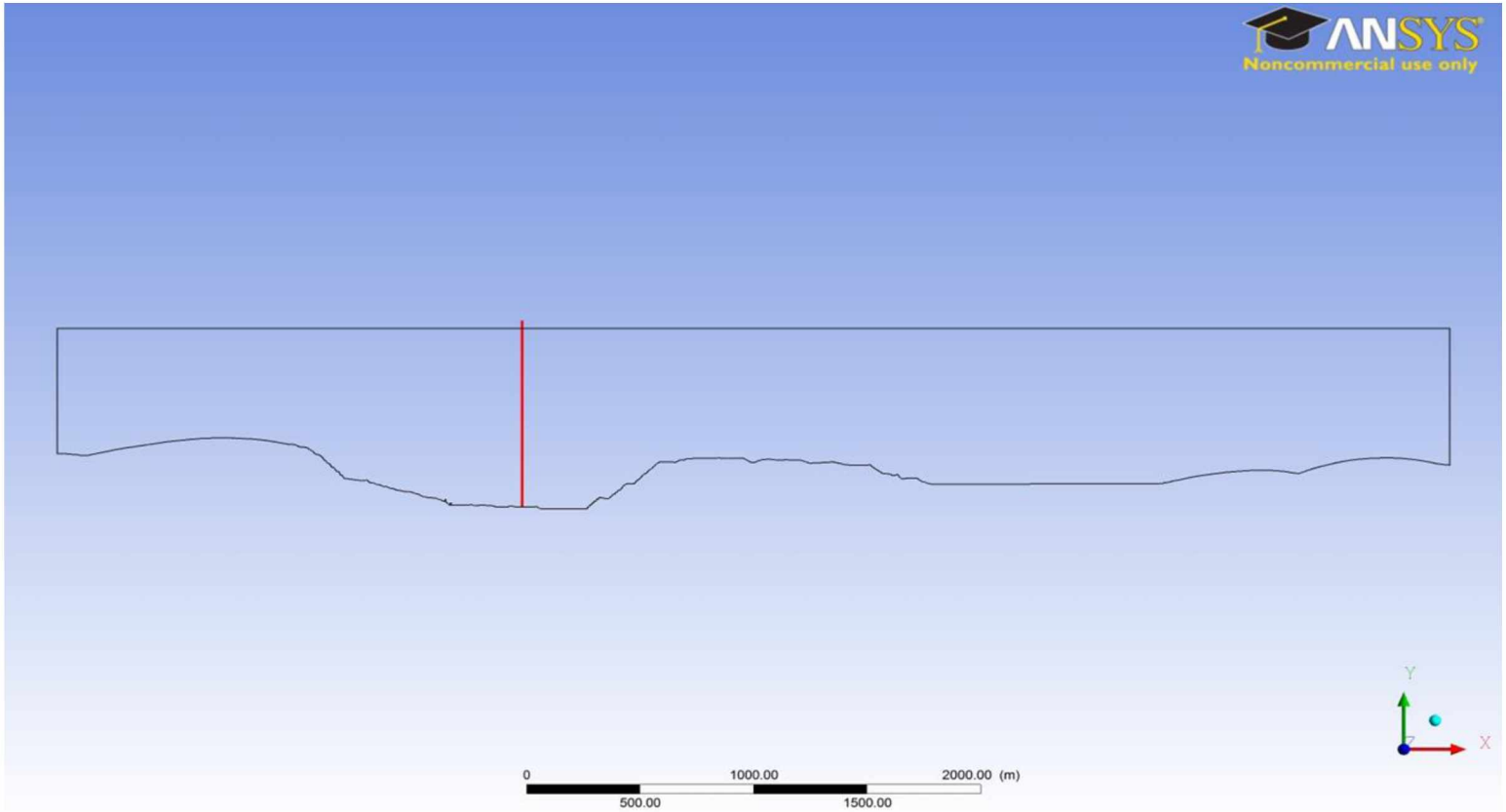

Figure 3.26: Vertical Cross Section along the Open Pit Geometry

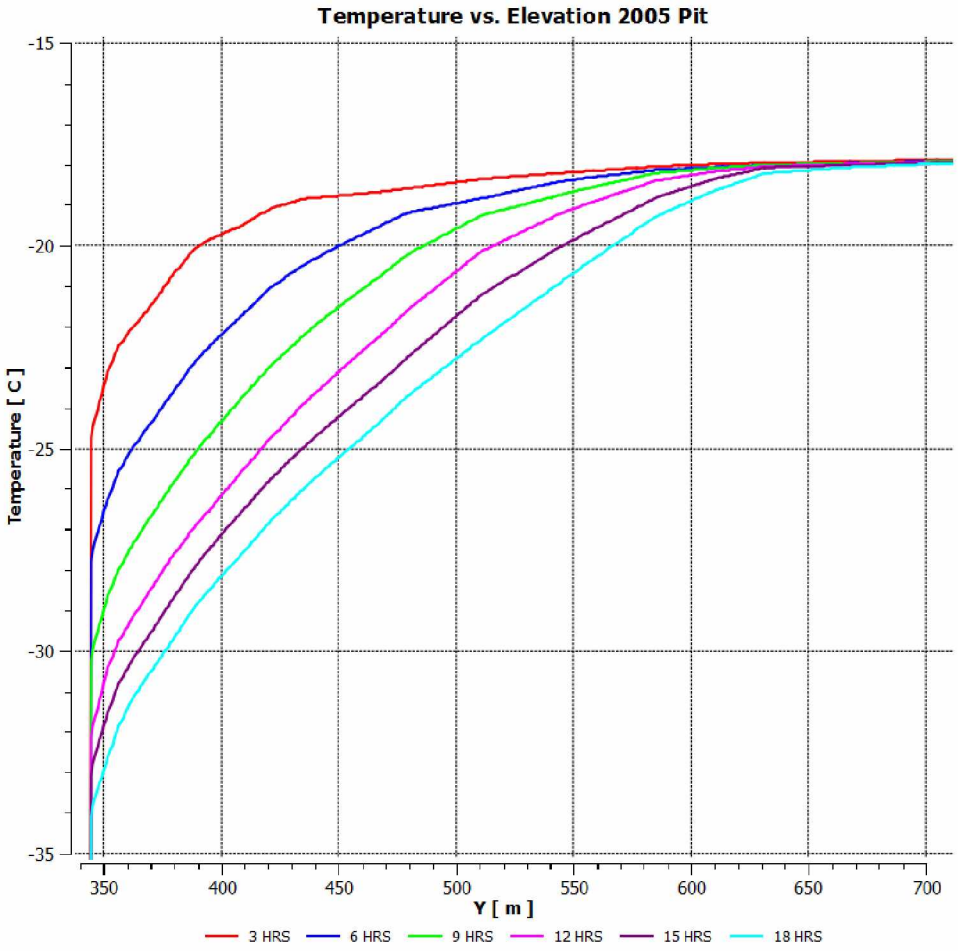

Figure 3.27: Temperature Change in the 2005 Pit (3 Hour Intervals)

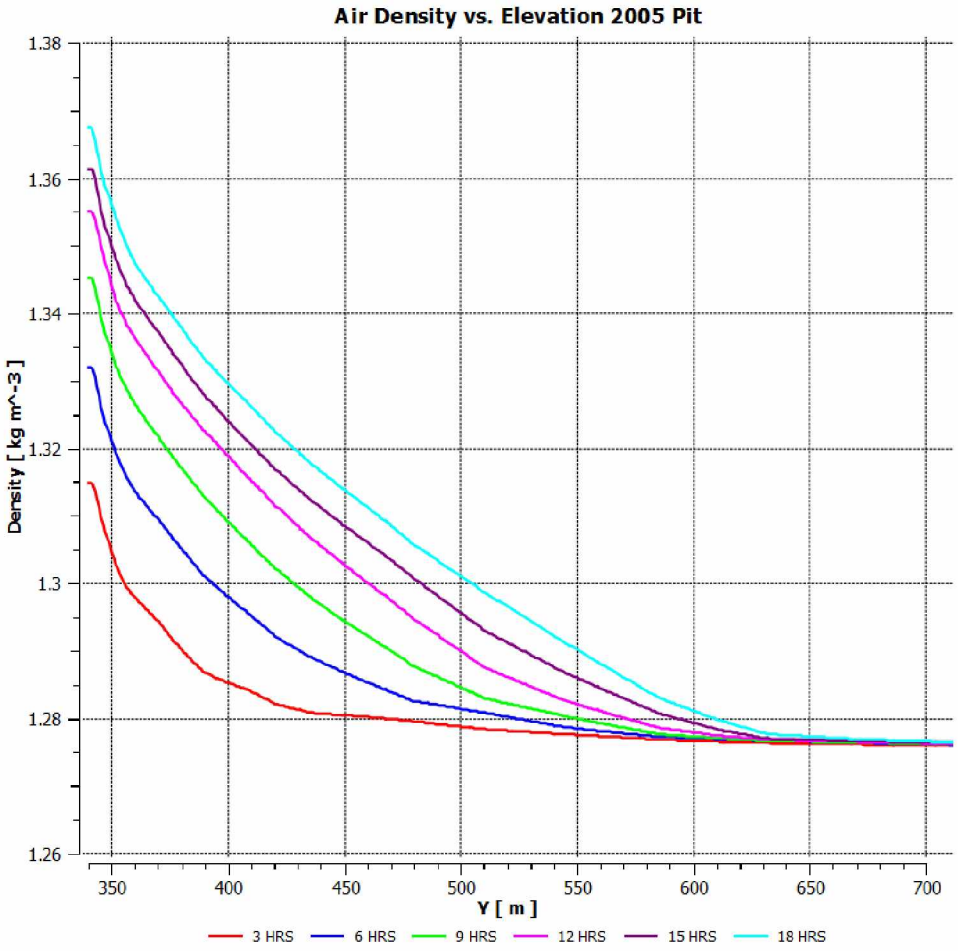

Figure 3.28: Air Density Change in the 2005 Pit (3 Hour Intervals)

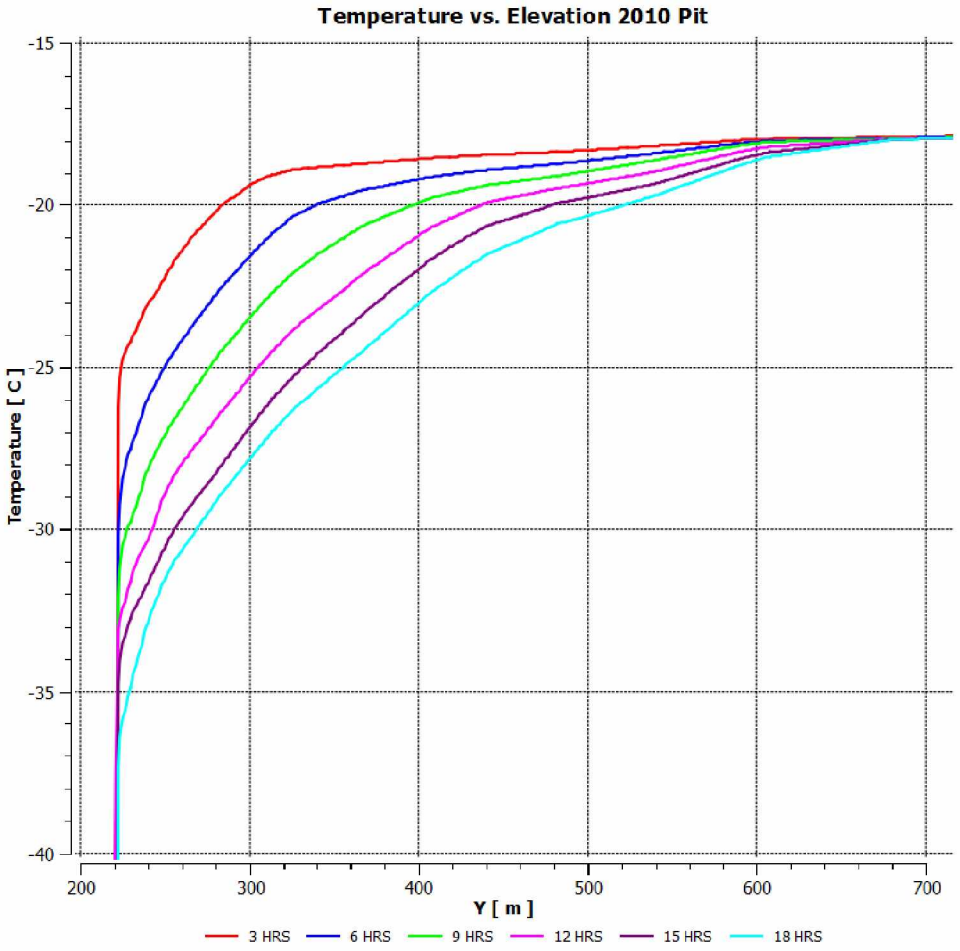

Figure 3.29: Temperature Change in the 2010 Pit (3 Hour Intervals)

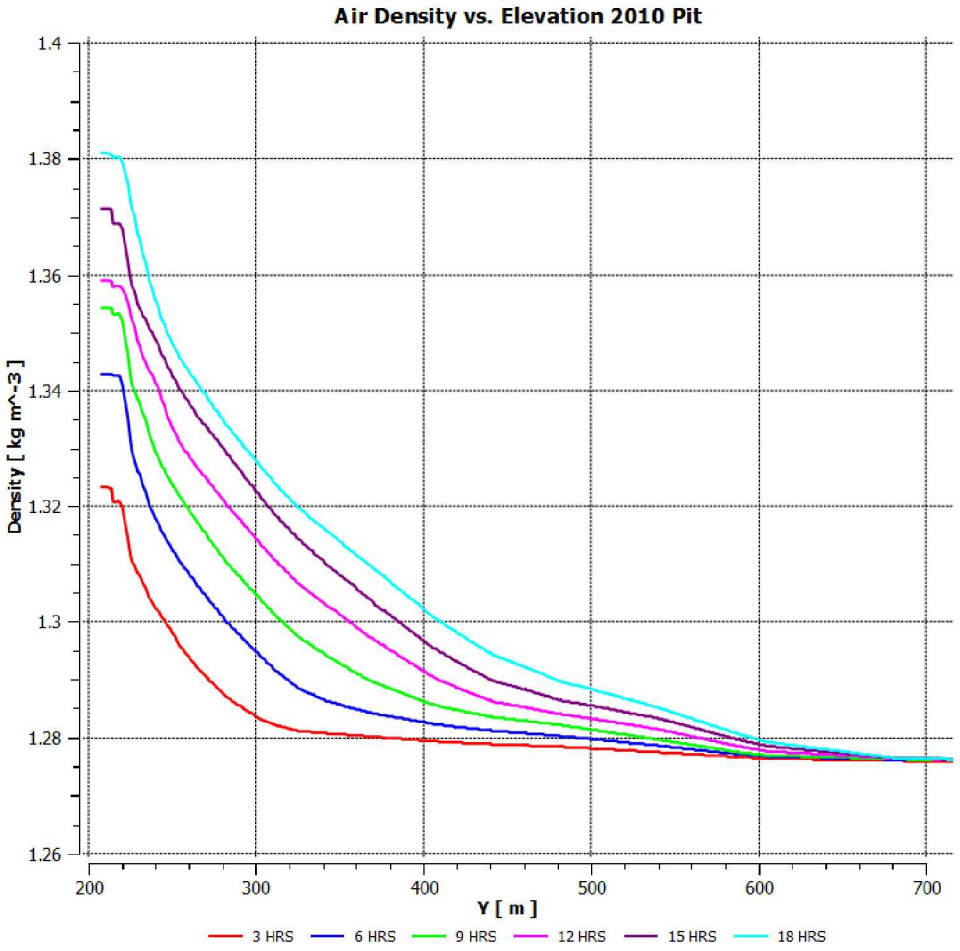

Figure 3.30: Air Density Change in the 2010 Pit (3 Hour Intervals)

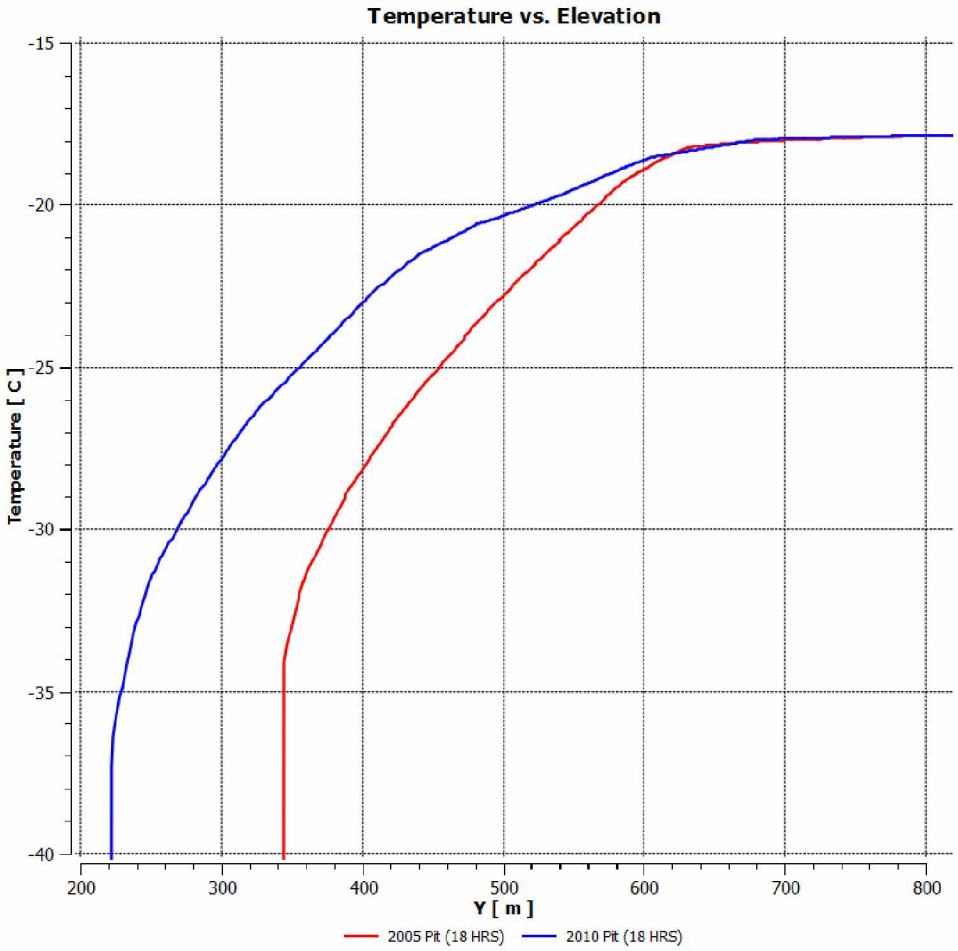

Figure 3.31: Temperature Change in the 2005 and 2010 Pits (18 Hrs)

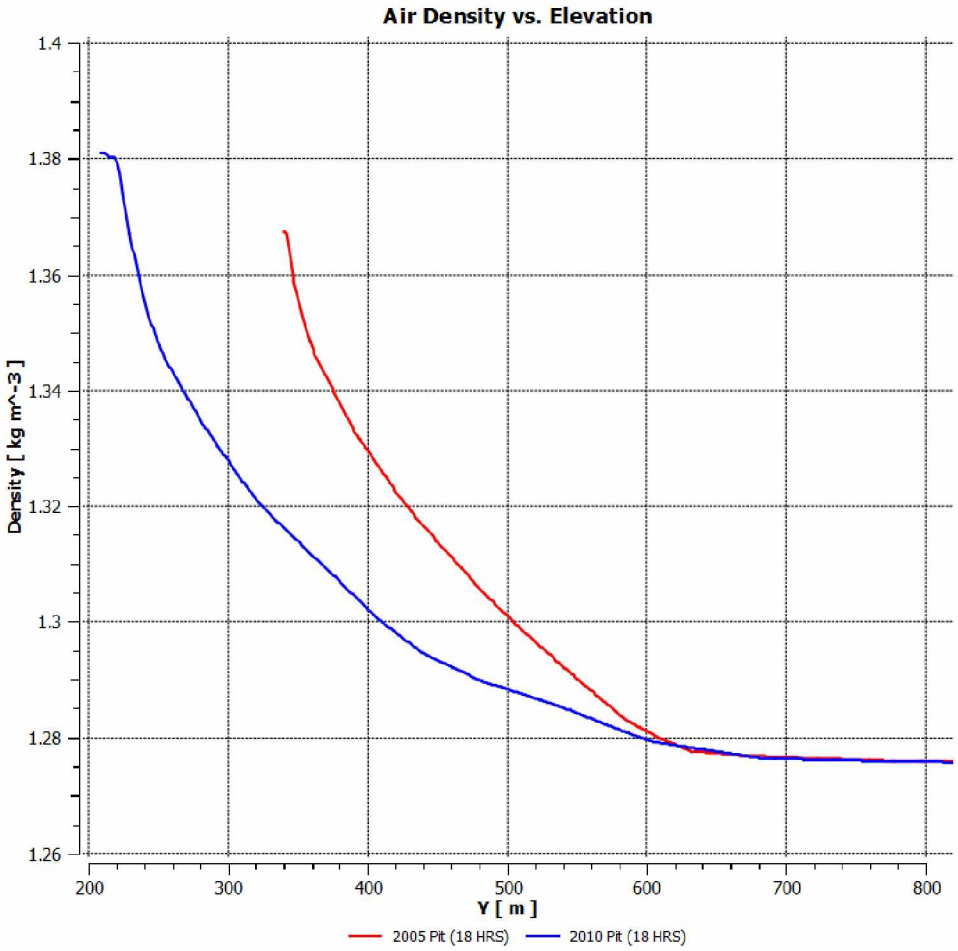

Figure 3.32: Air Density Change in the 2005 and 2010 Pits (18 Hrs)

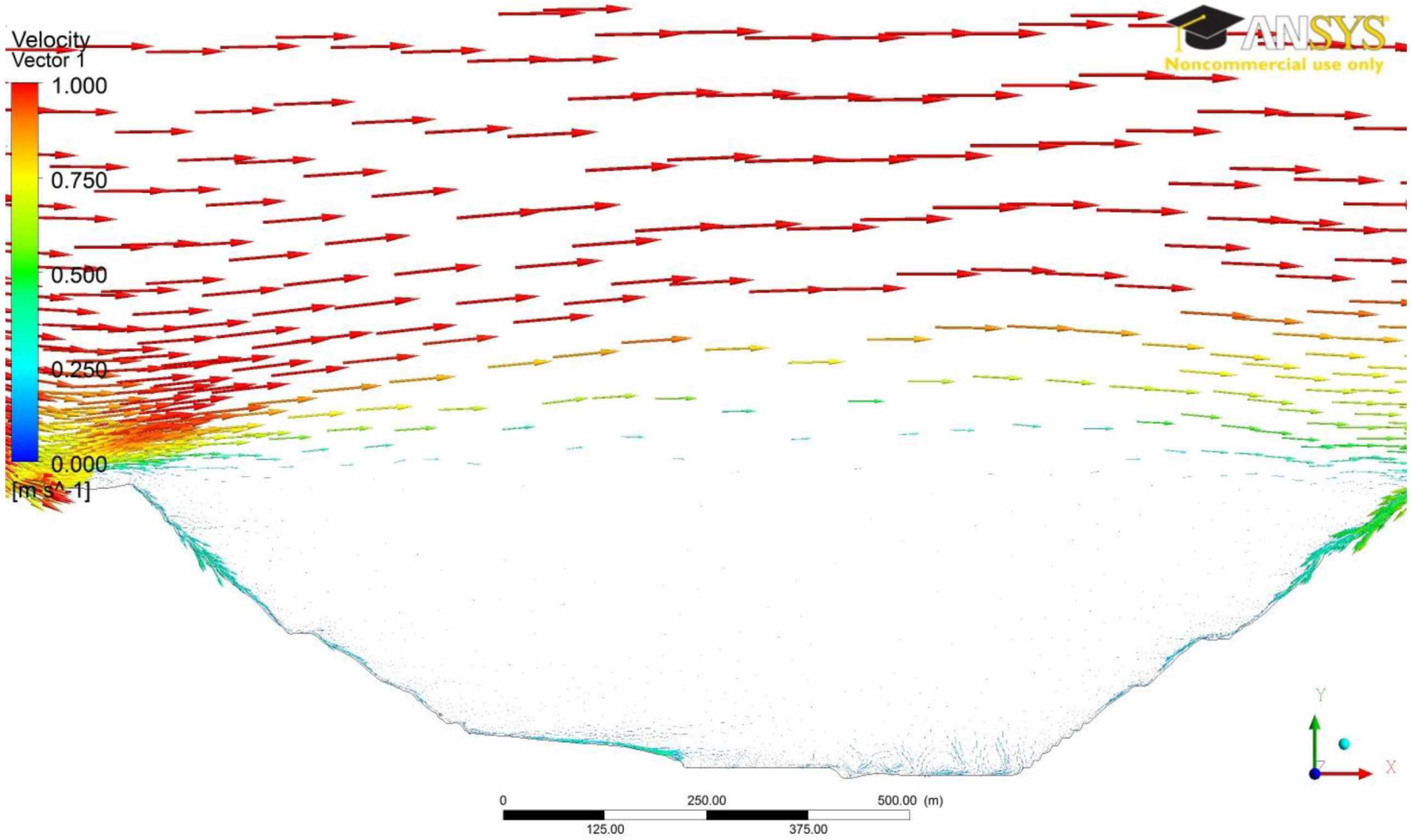

Figure 3.33: Velocity Vectors in the Pit during an Inversion

Chapter 4: Pollutant Transport in an Open Pit Mine Under Arctic Air Inversion

The pollutant transport and dispersion problem under arctic air inversion is complex and any solution approach would require a good understanding of the interaction of the aerodynamic movement of air, air inversion process, meteorology, pollutant sources, radiation heat balances, and application of air movers in open pit mines. The pollutant emission rate is not constant or even continuous. Even if the airflow remains steady state, the pollutant transport and dispersion are usually unsteady. It was observed that local air quality is closely related to the influence of the ABL across complex terrain. This effect was discussed in Chapter 3. The dilution and dispersion of pollutant emissions within the open pit is principally determined by the inlet airflow characterized by the atmospheric boundary layer (ABL). The prediction of local wind flow over complex terrain including hills, valleys and urban canyons provides information that is critical to assess the prediction of pollutant dispersion in the open pit. For the purposes of predicting local wind patterns, it is necessary to use microscale models, which are usually based on the numerical solution of the Reynolds-averaged Navier–Stokes (RANS) equations and a turbulence model in a domain that includes the local terrain. An open-pit mine is radically different from the usually studied valleys formed from fluvial or glacial activity. The open-pit terrain can create internal circulations, which generate a microclimate within the opening.

The actual terrain of an open pit mine located near Fairbanks was selected to define the computational domain. The floor of the open-pit is 190 m (620 ft) in the X-direction

and 785 m (2,575 ft) in the Y-direction. Above the pit bottom, the ground rises in an open trapezoidal trough to the rim of the pit. The average pit slope is 40°. The mine is approximately 1,370 m (4,500 ft) in the X-direction and 1,980 m (6,500 ft) in the Y-direction at the rim. Orientation of the model shows that the longer dimension is in the east-west direction.

CFD models of contaminant transport have been successfully converged. Achieving convergence has required a modification to prior methodology. In the CFD models, the sources and sinks were originally introduced as small geometric objects in the model domain. For example, a 20 ft X 20 ft rectangle could be used to represent the pollution source from a piece of equipment. This approach created meshing and convergence difficulties. Meshing an extremely small object (i.e., a truck) inside of an extremely large domain (i.e., an open pit mine) results in very small, highly skewed mesh elements surrounding the object. These small, highly skewed elements—in conjunction with the high heat and concentration gradients in the surrounding model space—create instability in the model.

To achieve convergence, source and sink terms had to be introduced into the model domain at the level of the individual mesh element. Source terms represent a source of heat or contaminants. Sink terms represent mass flow out of the model domain. To accomplish this in Fluent, individual cells must be marked for adaptation. These cell(s) can then be separated from the interior of the model and placed in their own unique cell zones. A mass source for each species (CO, NO, etc.) can be assigned to the

separated cell(s). For sinks, a mass flow out of the domain can be assigned to each separated cell.

After convergence of the 2-D contaminant transport models was finally achieved, it was discovered that the predicted contaminant concentrations were much higher than the concentrations measured in the field. It became clear that—in the 2-D model— the mass flow of contaminants would need to be scaled to reflect the reduced volume of the 2-D model space relative to the 3-D pit. An analysis of the contaminant concentration data from the mine site revealed that the top of the contaminated air mass could be found at an approximate elevation of 1,210 ft. It was determined that this represents a contaminated air mass with a volume of approximately 1.26 billion ft^3.

Since Fluent is a finite volume solver, even a 2-D CFD model must have a defined thickness. A thickness of 1 foot was used in our 2-D models. At an elevation of 1,210 ft. (the top of the contaminated air mass), the volume of the 3-D pit is 1,100 times larger than the volume of the 2-D model. To achieve similarity between the 2-D model and the 3-D pit, all source and sink terms were scaled by a factor of 1,100. Much better results were obtained after this scaling was performed. Figure 4.1-Figure 4.6 illustrates the spread of CO over an 18 hour period during an inversion. In this particular simulation experiment, the contaminant sources are located on the western side of the pit bottom.

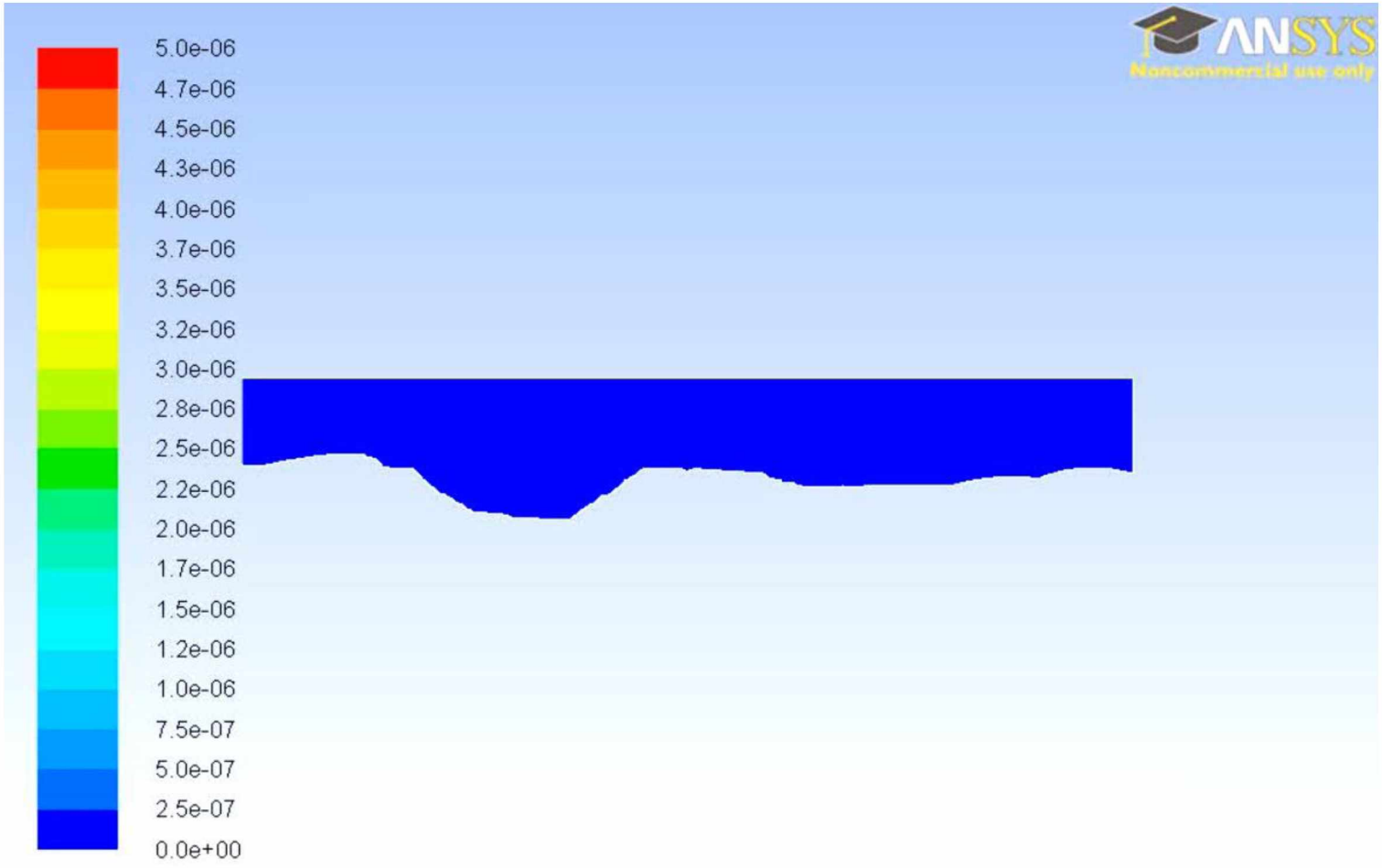

Figure 4.1: CO Concentration Contours during an Inversion (Time ≈ 0 Hrs.)

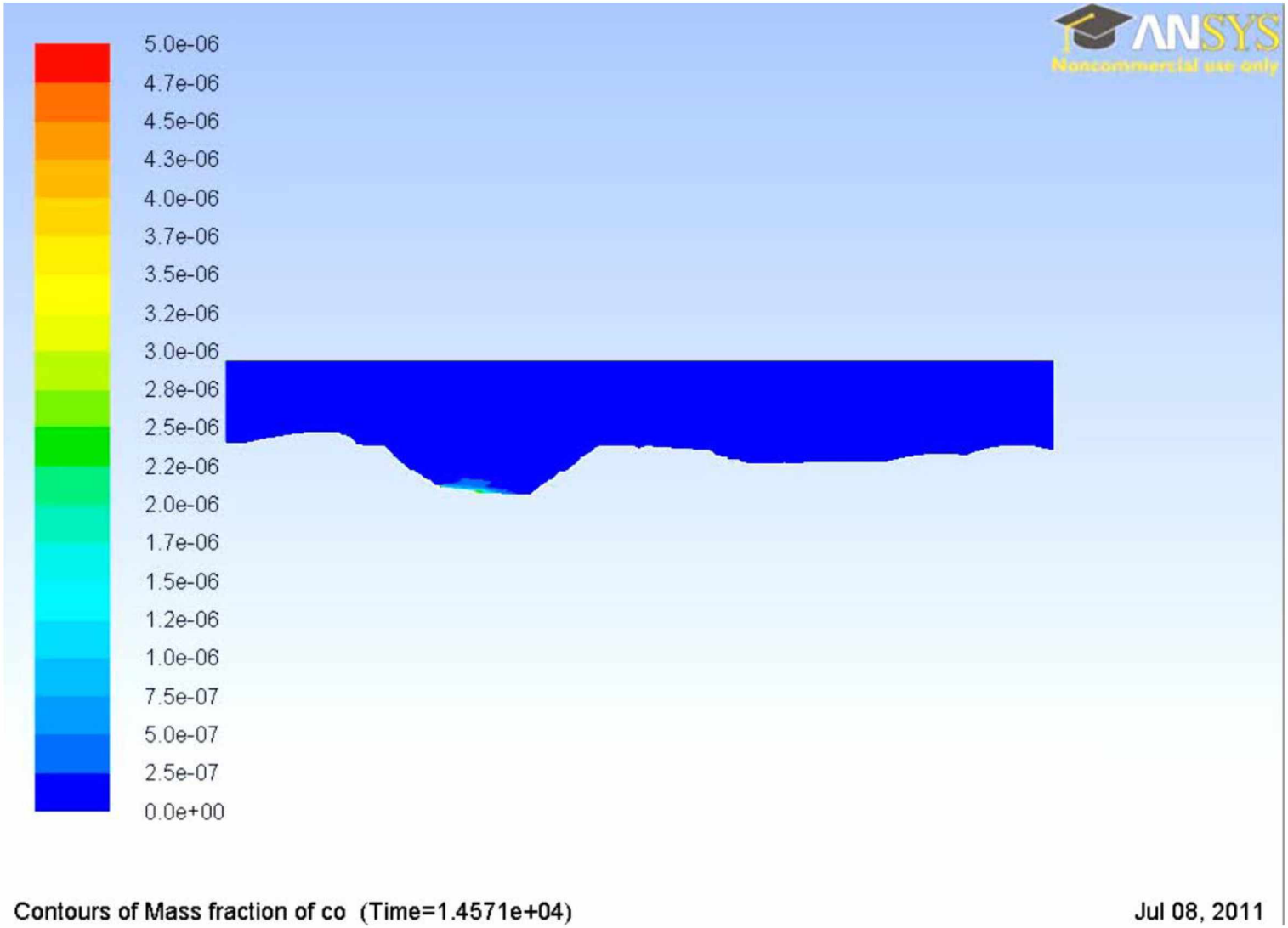

Figure 4.2: CO Concentration Contours during an Inversion (Time ≈ 4.0 Hrs.)

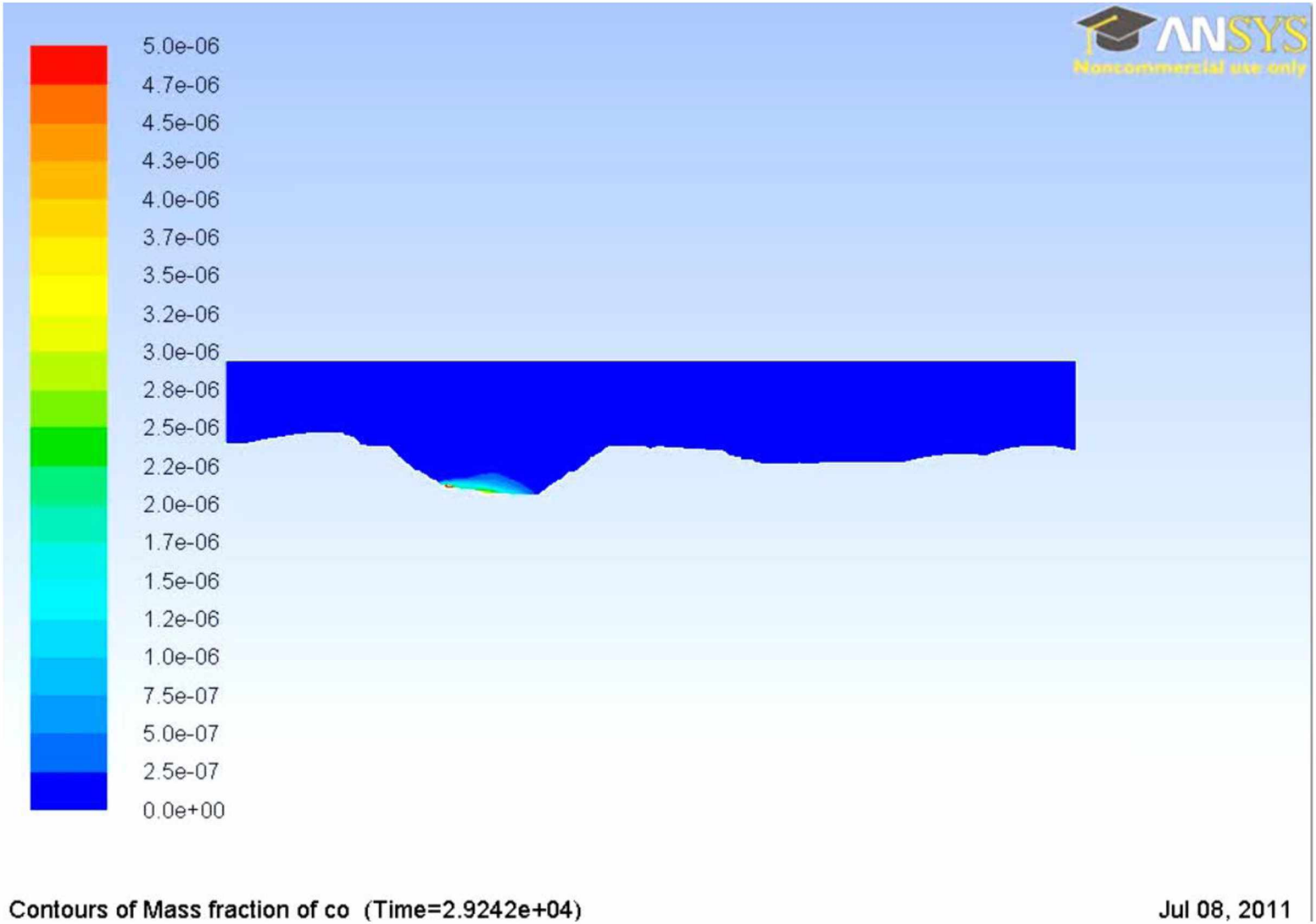

Figure 4.3: CO Concentration Contours during an Inversion (Time ≈ 8.1 Hrs.)

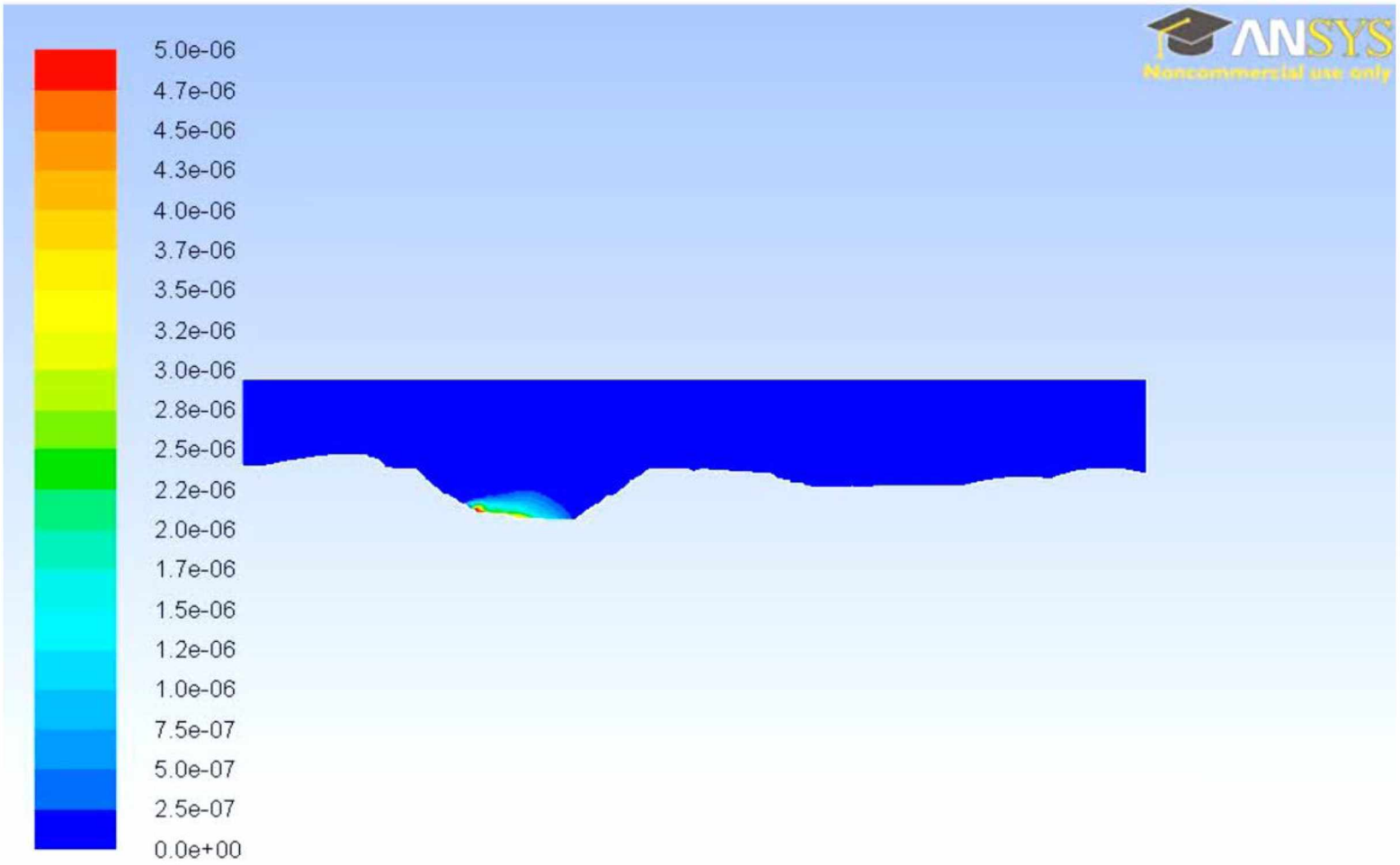

Figure 4.4: CO Concentration Contours during an Inversion (Time ≈ 12.0 Hrs.)

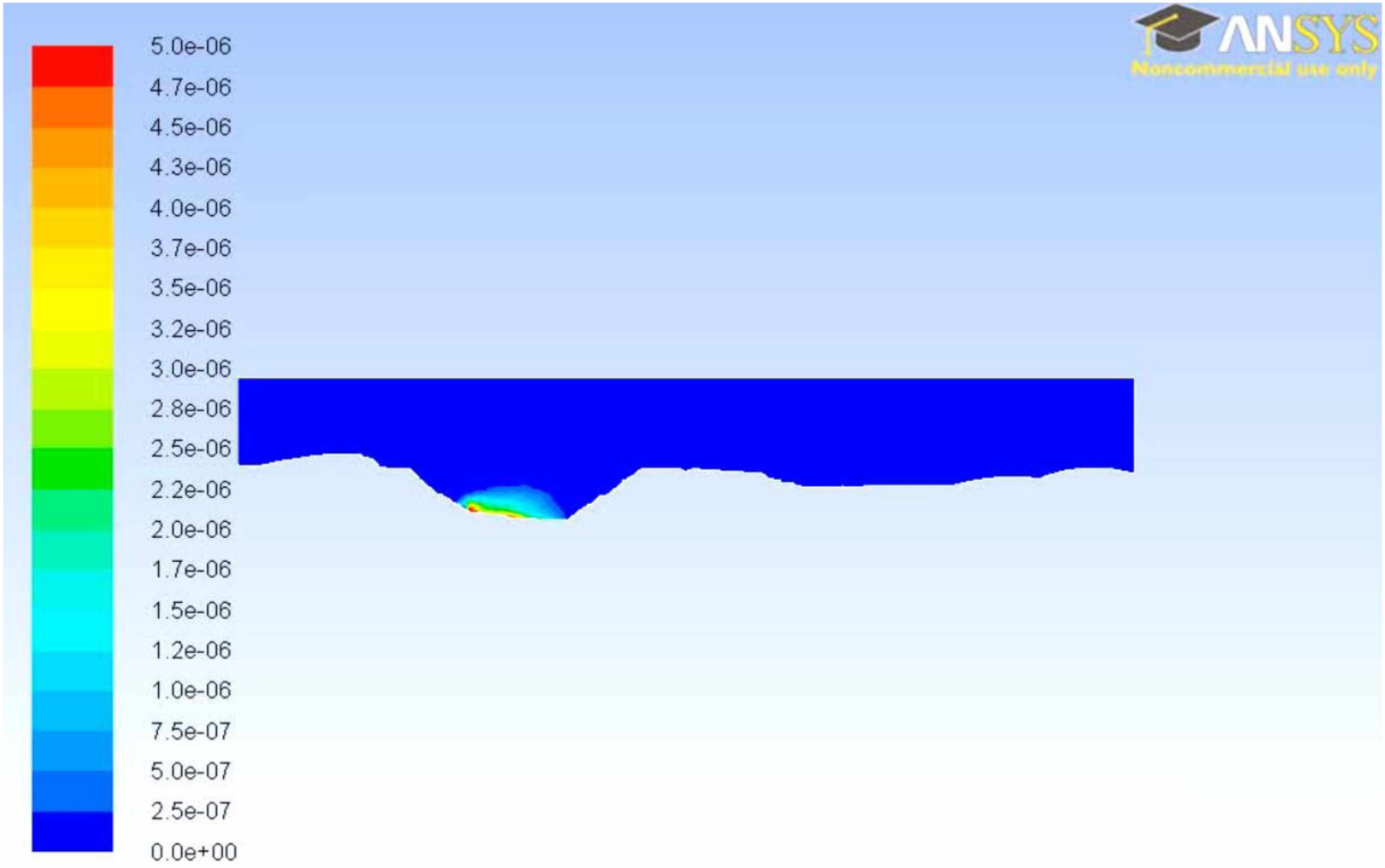

Figure 4.5: CO Concentration Contours during an Inversion (Time ≈ 16.1 Hrs.)

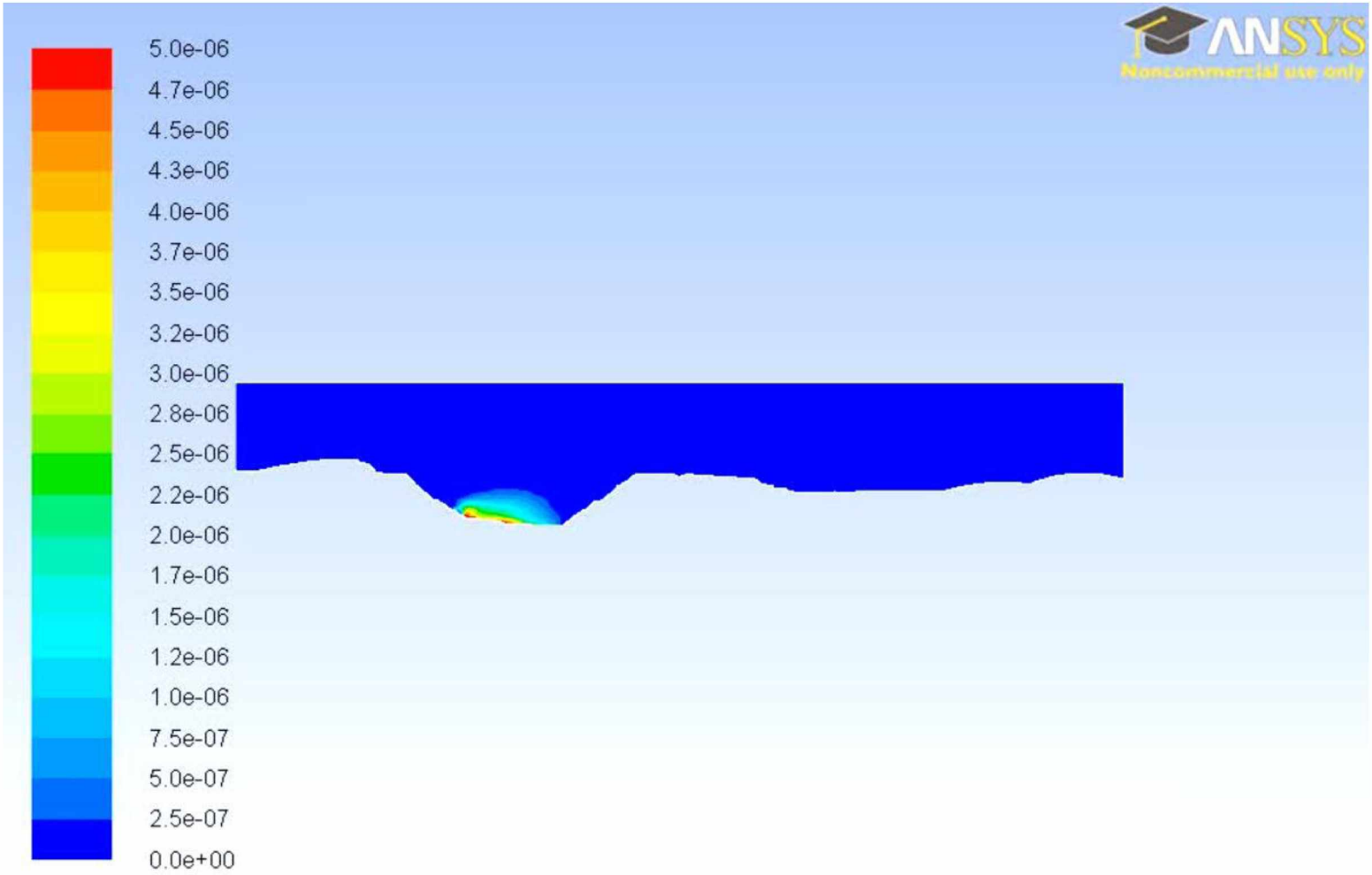

Figure 4.6: CO Concentration Contours during an Inversion (Time ≈ 18.0 Hrs.)

The CFD models were used to simulate CO, NO, NO_2, and NO_X concentrations in the 2005 and 2010 pits under conditions of inversion. Figures showing the build-up of CO (Figure 4.7), NO (Figure 4.8), NO_2 (Figure 4.9), and NO_X (Figure 4.10) in the 2005 pit are provided. Each of these figures shows the contaminant concentrations plotted along the vertical cross section depicted in Figure 3.26. Figures showing the build-up of CO (Figure 4.11), NO (Figure 4.12), NO_2 (Figure 4.13), and NO_X (Figure 4.14) in the 2010 pit are also provided. The results show high concentrations near the ground surface with a sharp drop in concentration within the first 20 m in altitude (e.g., Figure 4.7). Above 20 m, the concentration of contaminants decreases more gradually until the inversion cap is reached. As expected, the concentration of contaminants above the inversion cap (located at approximately 660 m) is negligible.

In the U.S. mining industry, the statutory limits for worker exposure to contaminants are set by the Mine Safety and Health Administration (MSHA). The MSHA threshold limit values (TLVs) for CO and NO_2 are 50 ppm and 5 ppm, respectively. The peak CO concentrations along the vertical cross section are well within this limit (e.g., peak concentration of 8 ppm in Figure 4.7). The peak NO_2 concentrations, however, are quite high (e.g., peak concentration of 3.3 ppm in Figure 4.9). In general, the predicted concentrations of contaminants in the 2005 pit are higher than the concentrations of contaminants in the 2010 pit. This is due to the fact that the same mass flow of contaminants are added to the 2005 and 2010 pits, but the volume of air below the inversion cap is smaller in the 2005 pit than in the 2010 pit.

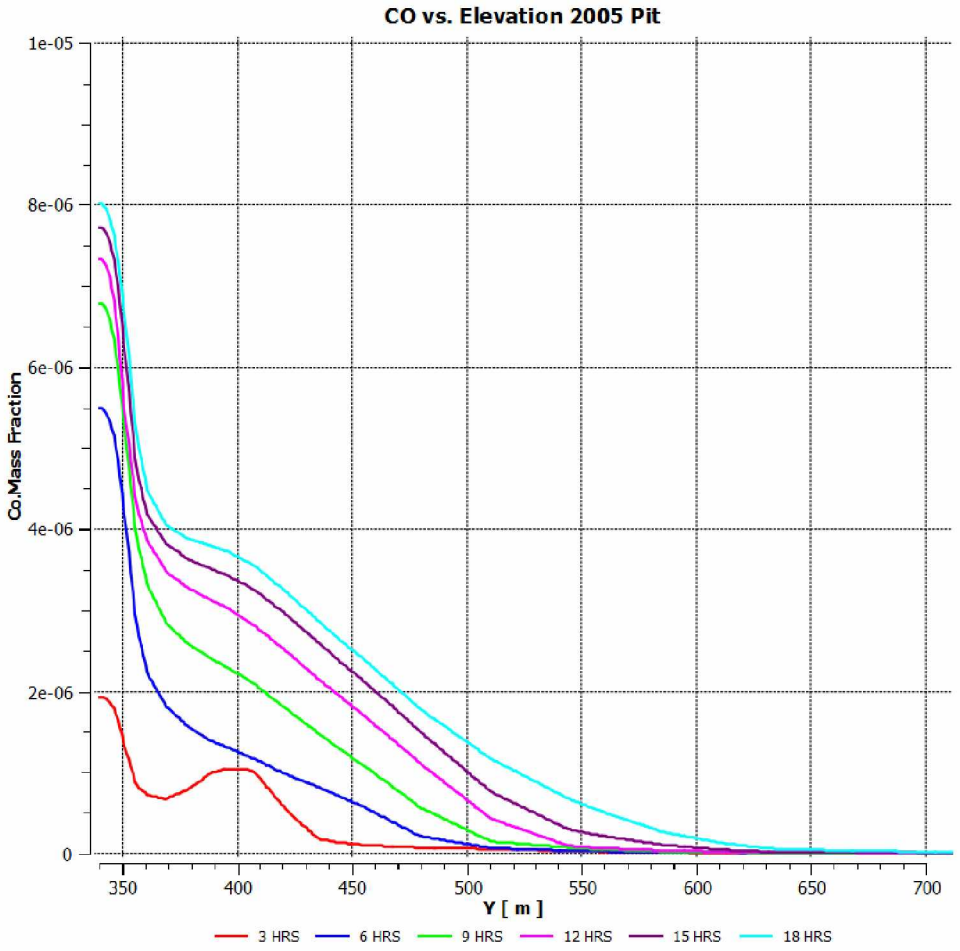

Figure 4.7: CO Concentration in the 2005 Pit (3 Hour Intervals)

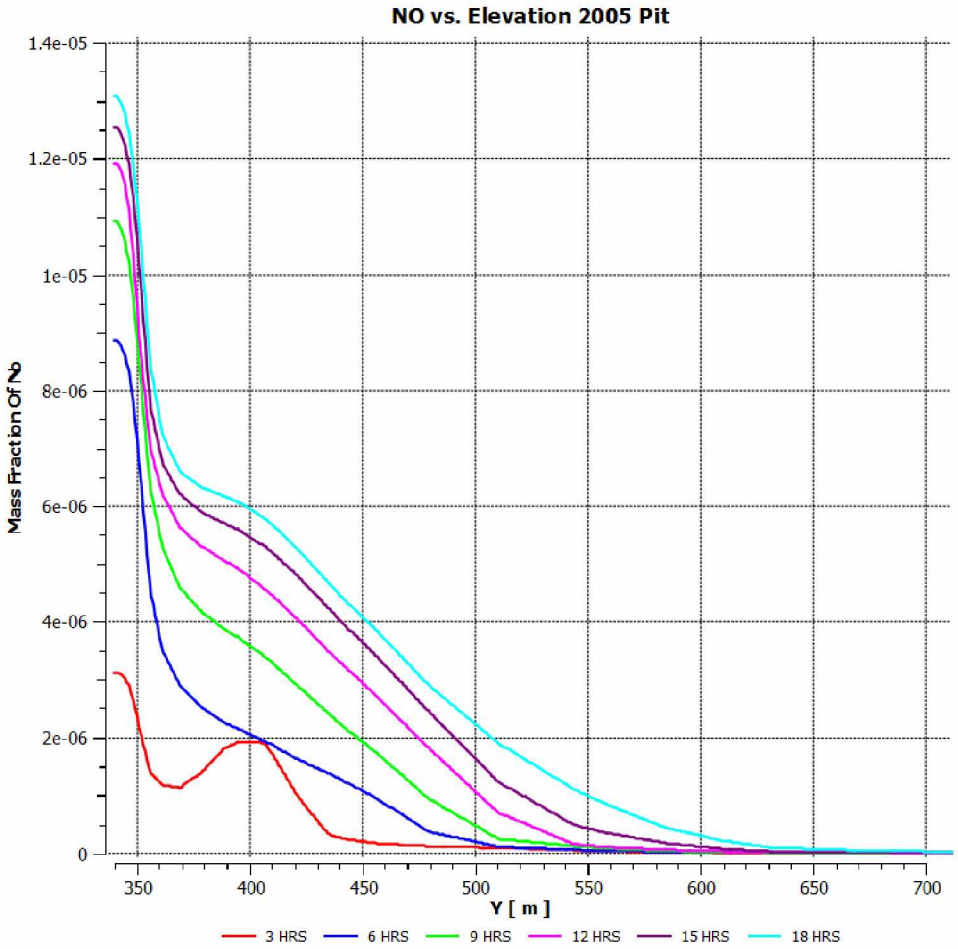

Figure 4.8: NO Concentration in the 2005 Pit (3 Hour Intervals)

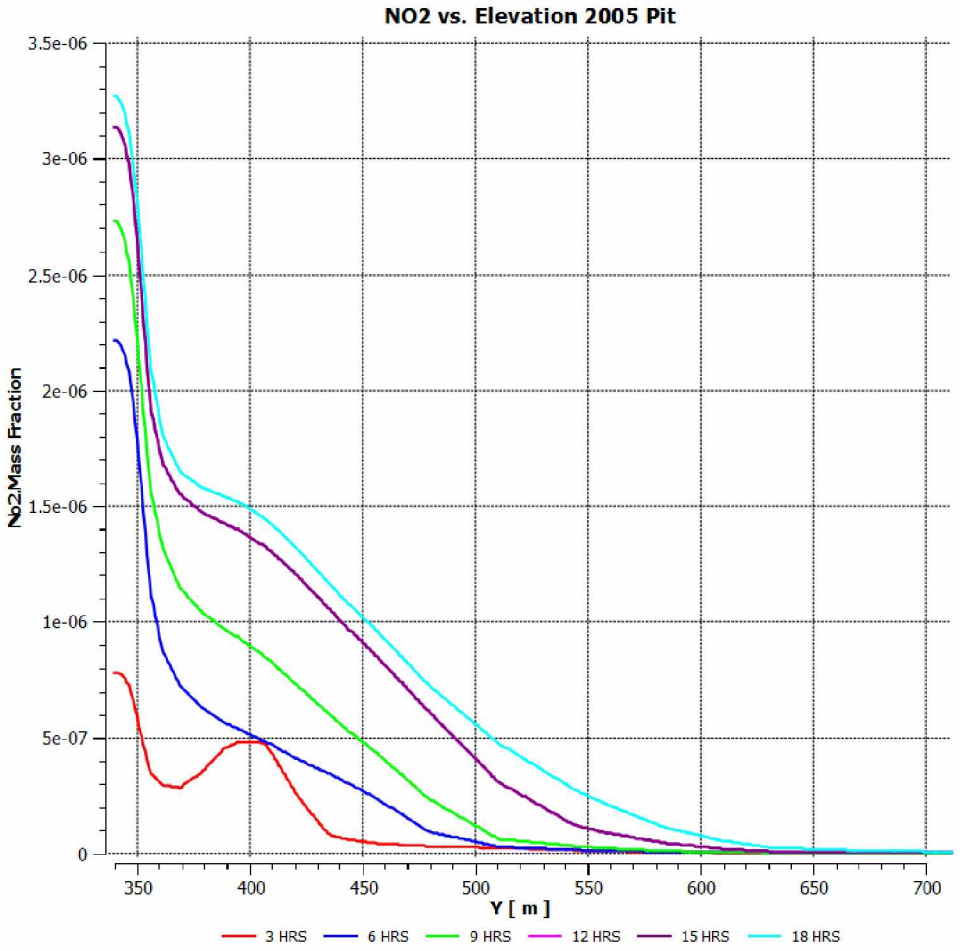

Figure 4.9: NO_2 Concentration in the 2005 Pit (3 Hour Intervals)

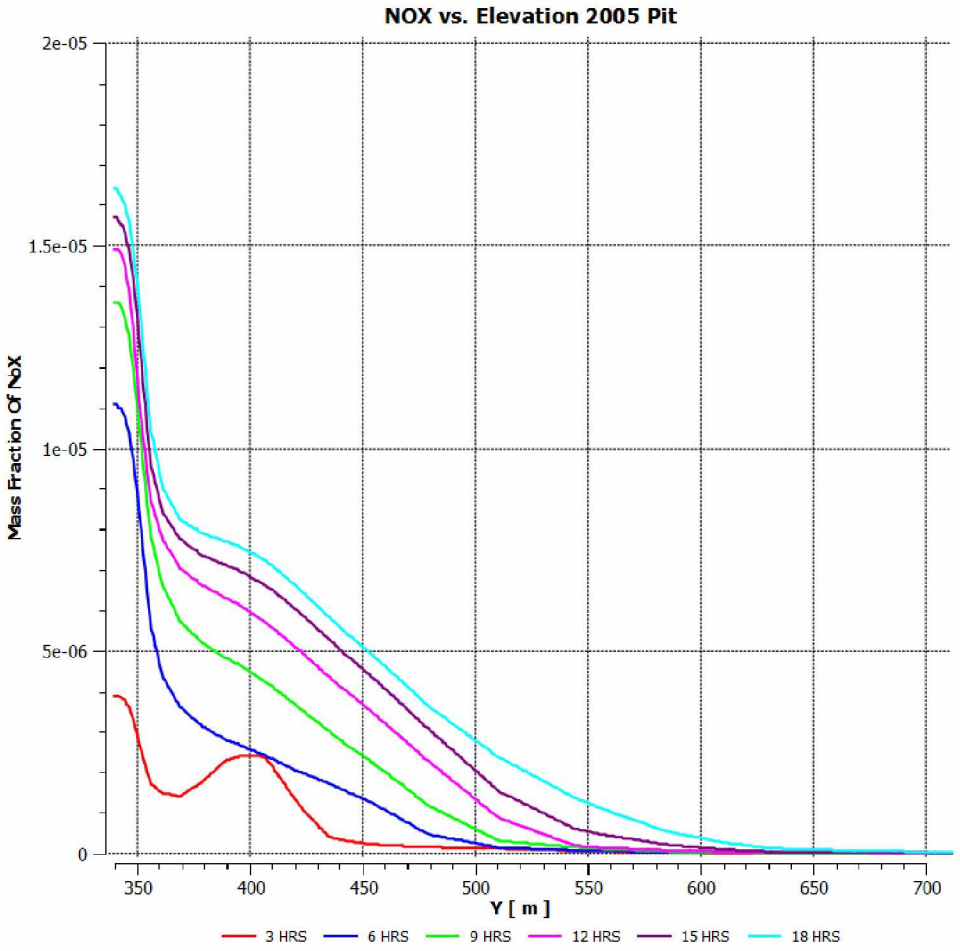

Figure 4.10: NO_x Concentration in the 2005 Pit (3 Hour Intervals)

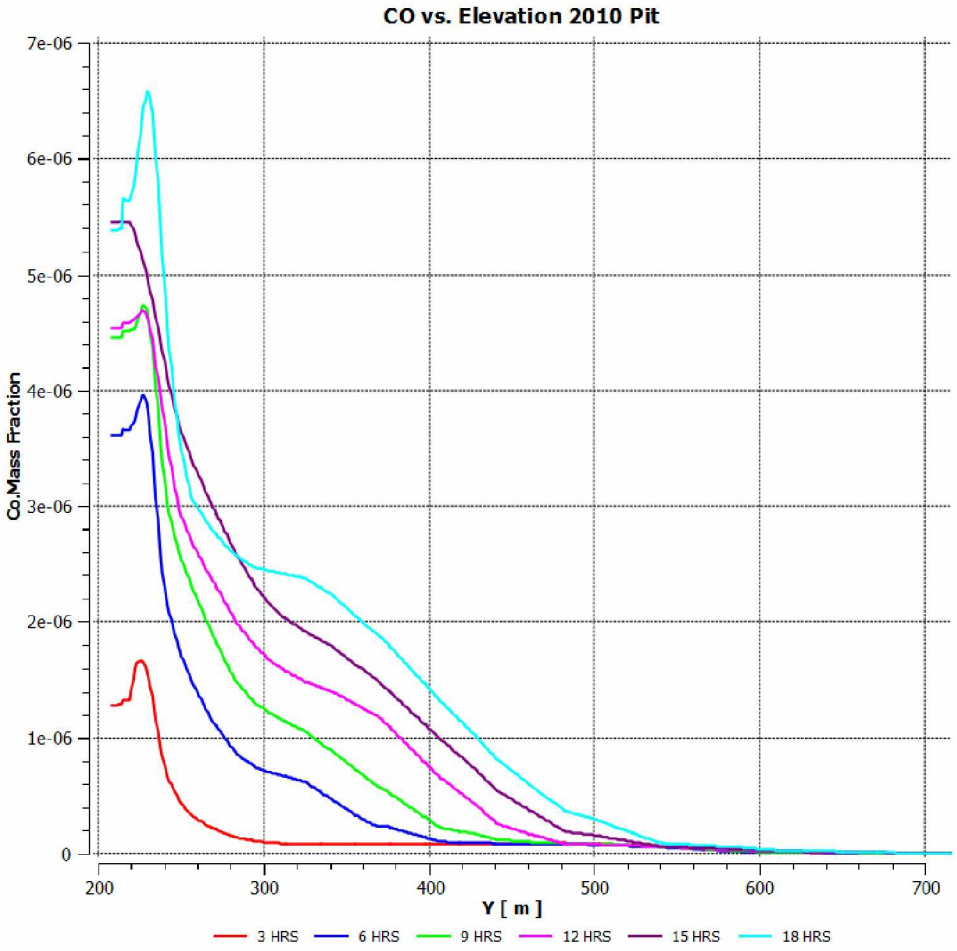

Figure 4.11: CO Concentration in the 2010 Pit (3 Hour Intervals)

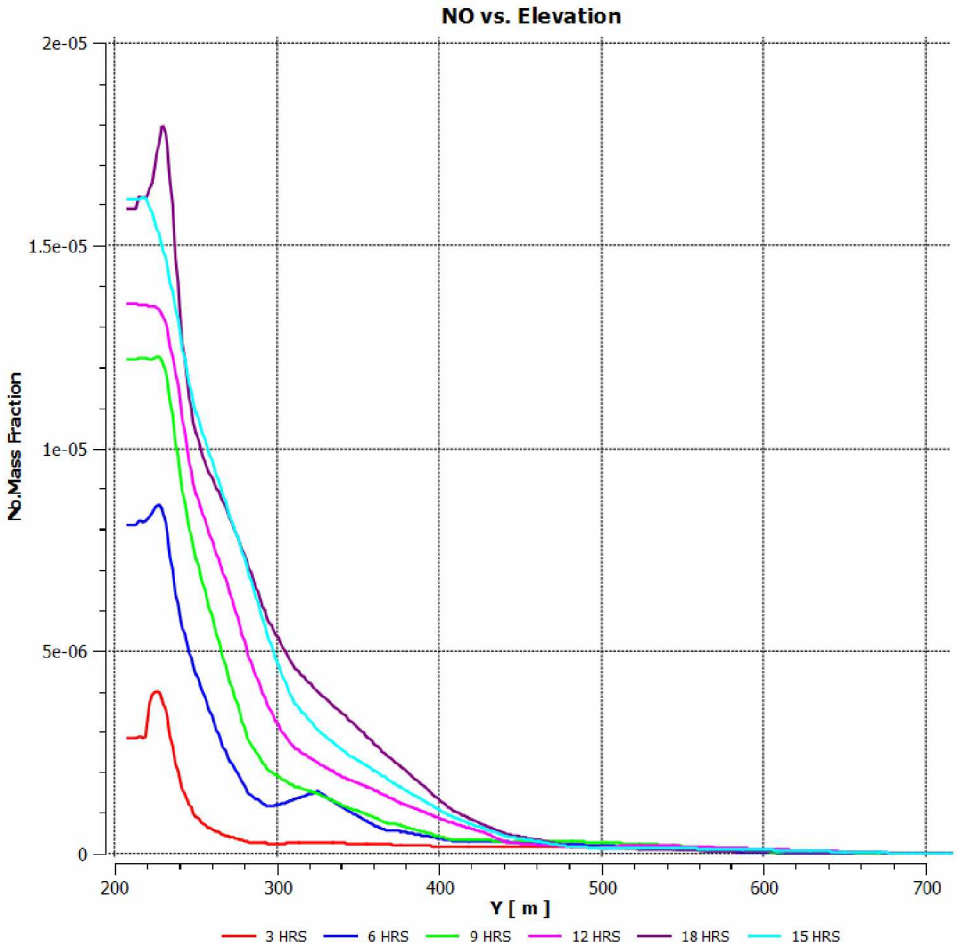

Figure 4.12: NO Concentration in the 2010 Pit (3 Hour Intervals)

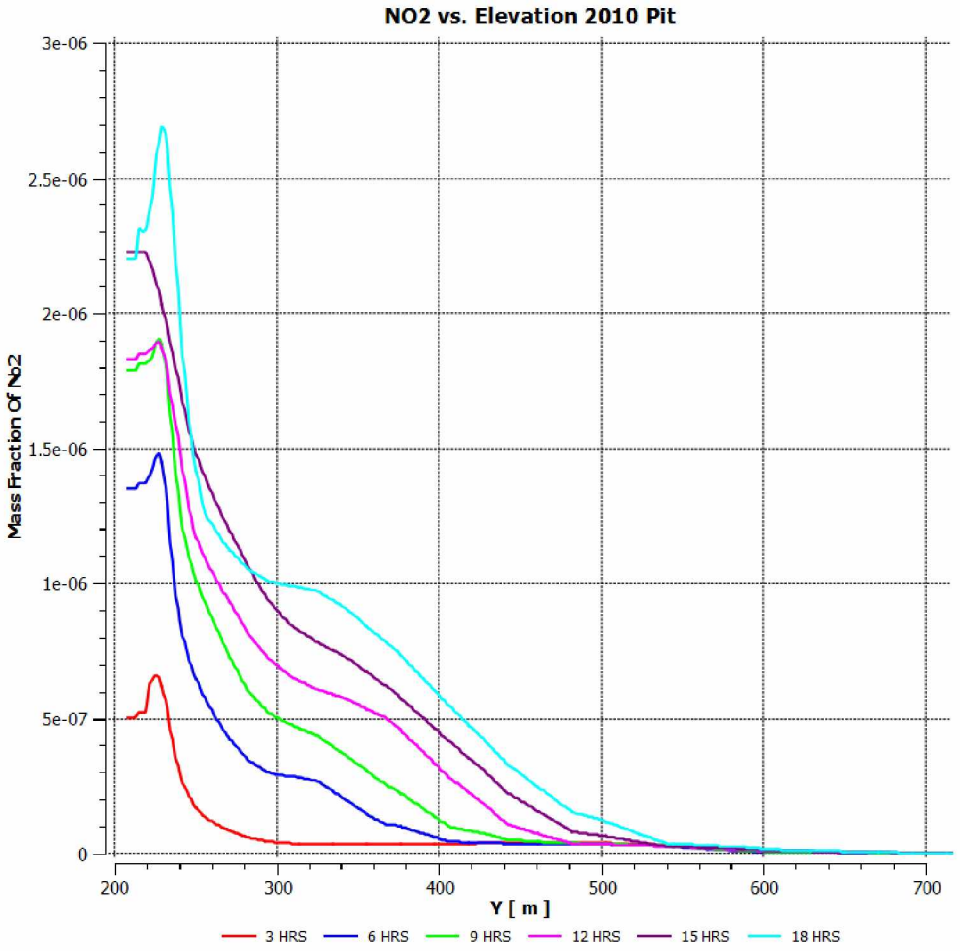

Figure 4.13: NO_2 Concentration in the 2010 Pit (3 Hour Intervals)

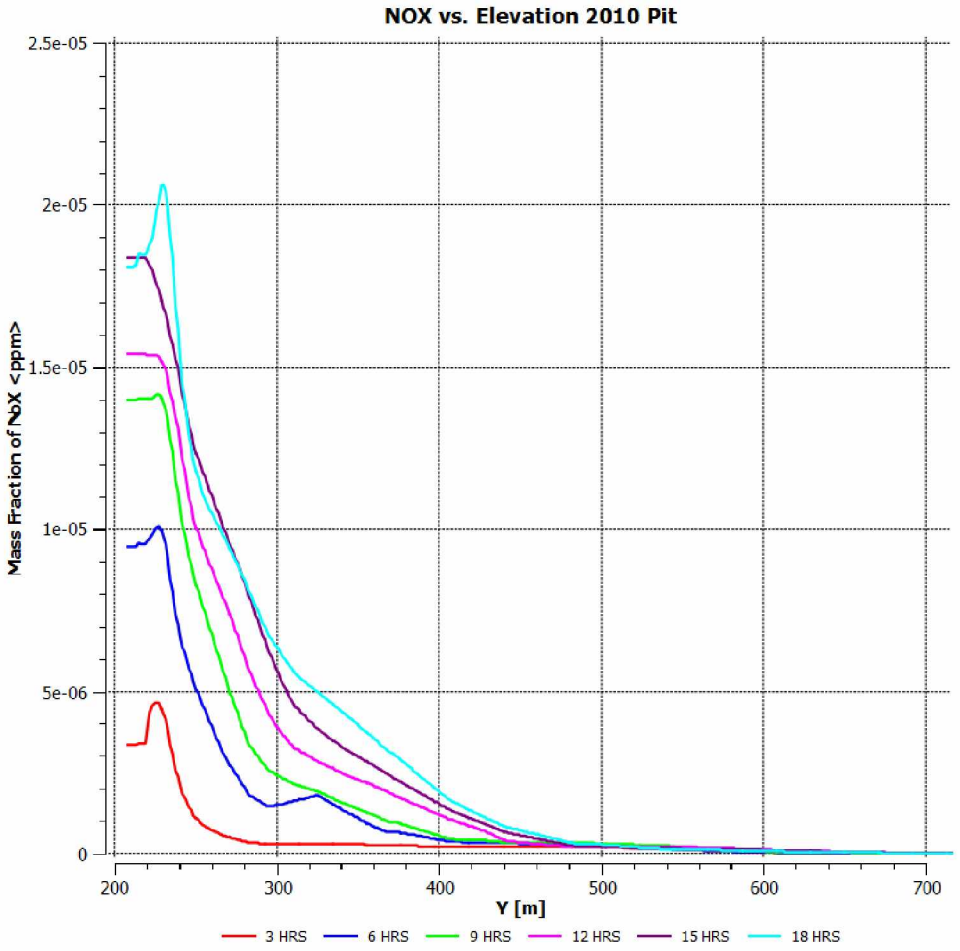

Figure 4.14: NO_x Concentration in the 2010 Pit (3 Hour Intervals)

The contaminant concentrations near the surface are of primary interest for this research, because this is where miners are working. Plots of contaminant concentration along a horizontal cross section near the ground surface (Figure 4.15) were created. The concentrations of CO and NO_2 along this cross section are shown in Figure 4.16 and Figure 4.17, respectively. A large spike in contaminant concentration is visible near the contaminant sources at the west side of the pit. The concentrations decrease from west to east. Although the CO concentrations do not exceed the applicable TLV, the predicted peak NO_2 concentration is more than twice the legal limit in the immediate vicinity of the sources (Figure 4.17). Figure 4.18 and Figure 4.19 compare the CO and NO_2 concentrations for the 2005 and 2010 pit along the horizontal cross section. As previously discussed, the predicted contaminant concentrations are slightly higher for the 2005 pit.

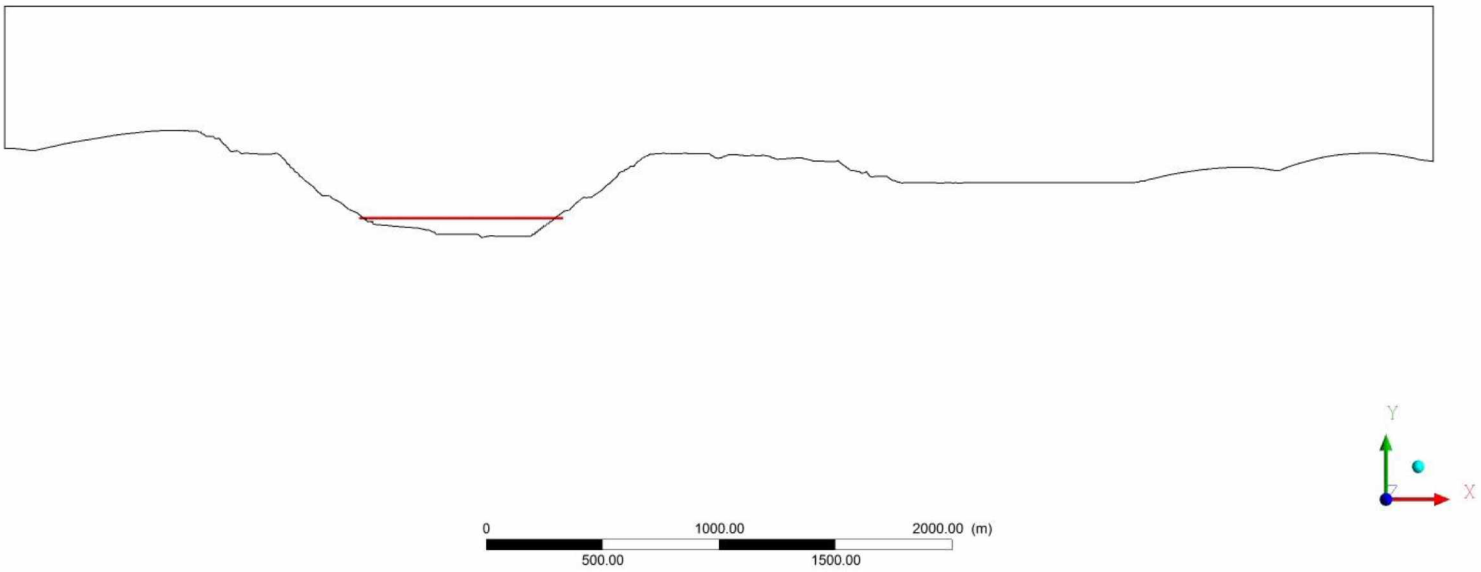

Figure 4.15: Horizontal Cross Section along the Open Pit Geometry

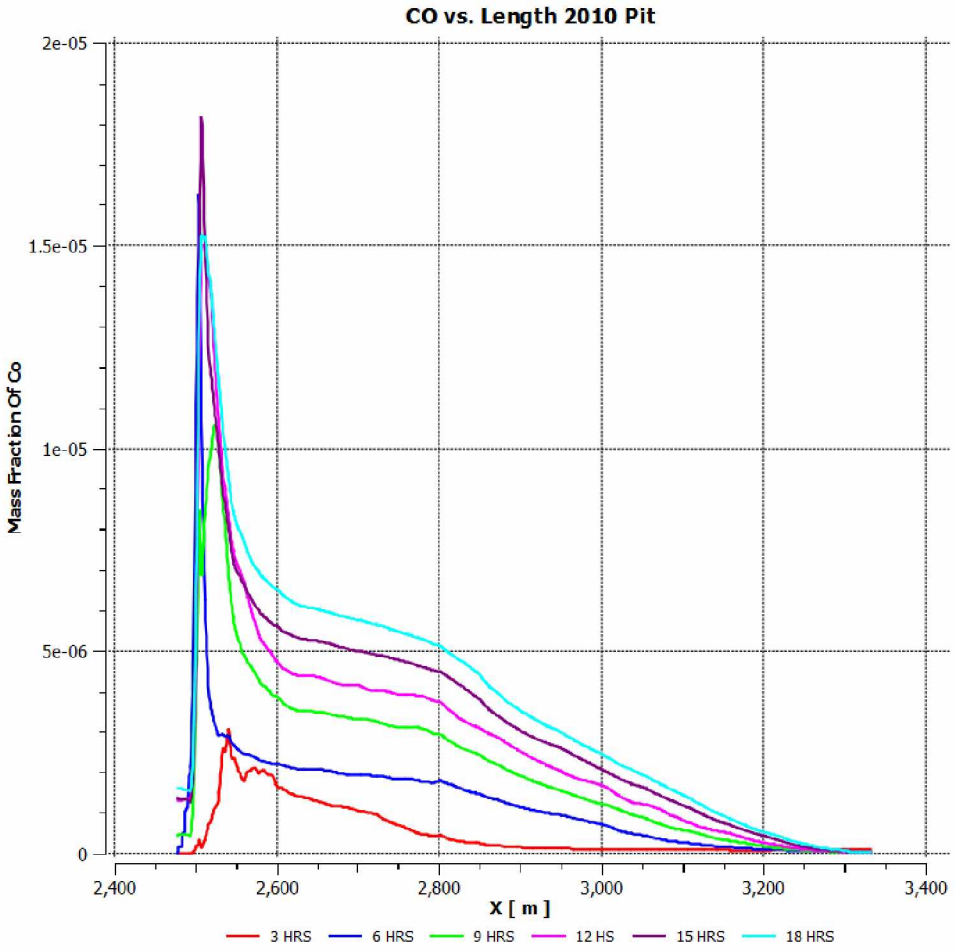

Figure 4.16: CO Concentration in the 2010 Pit (3 Hour Intervals)

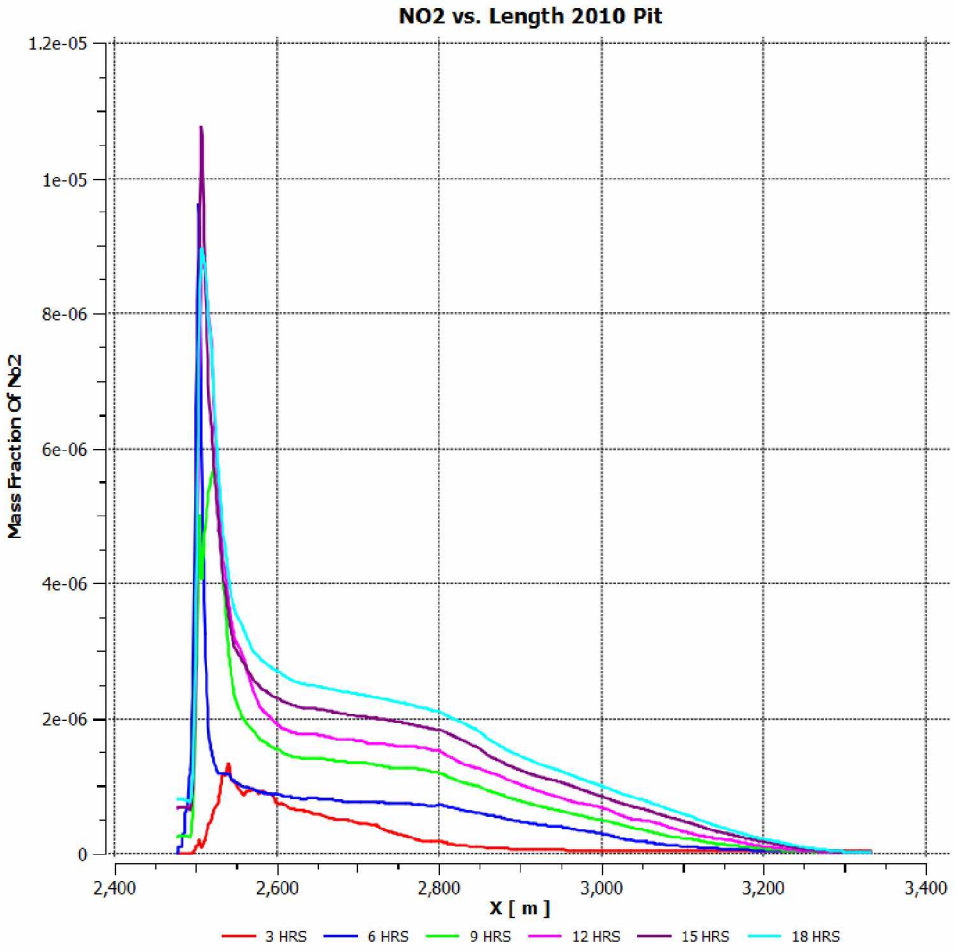

Figure 4.17: NO_2 Concentration in the 2010 Pit (3 Hour Intervals)

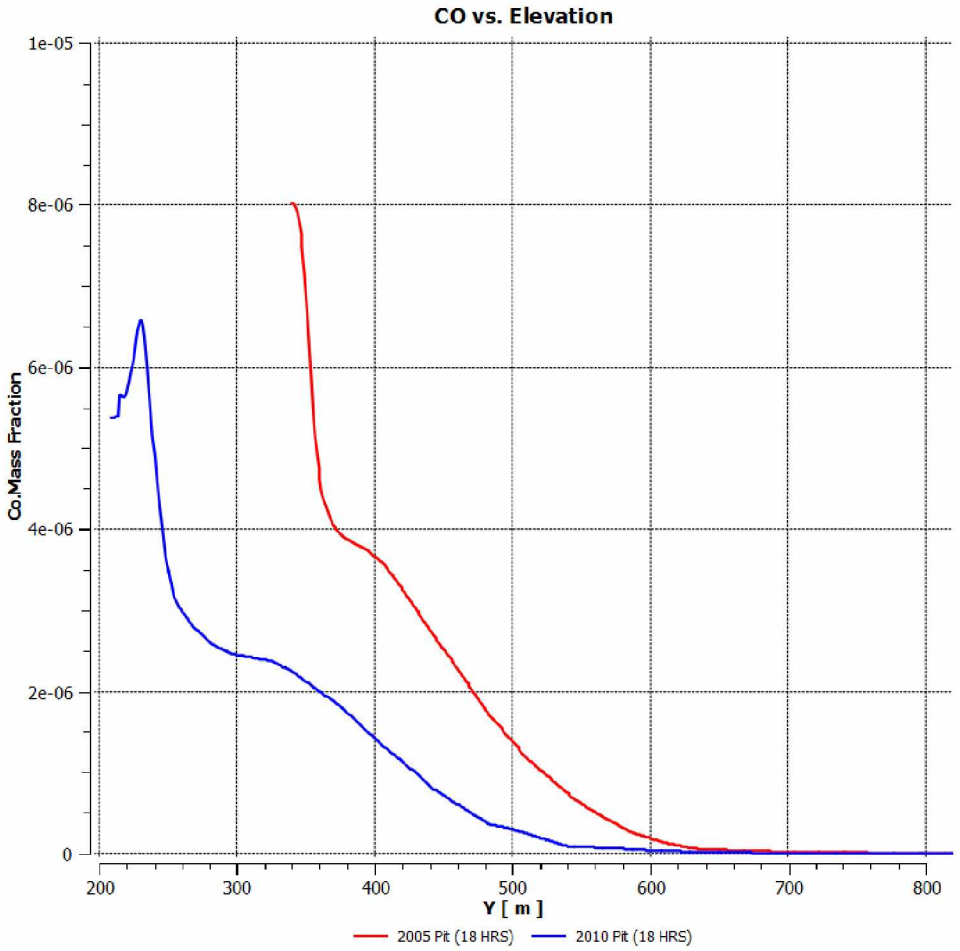

Figure 4.18: CO Concentration in the 2005 and 2010 Pits (18 Hrs)

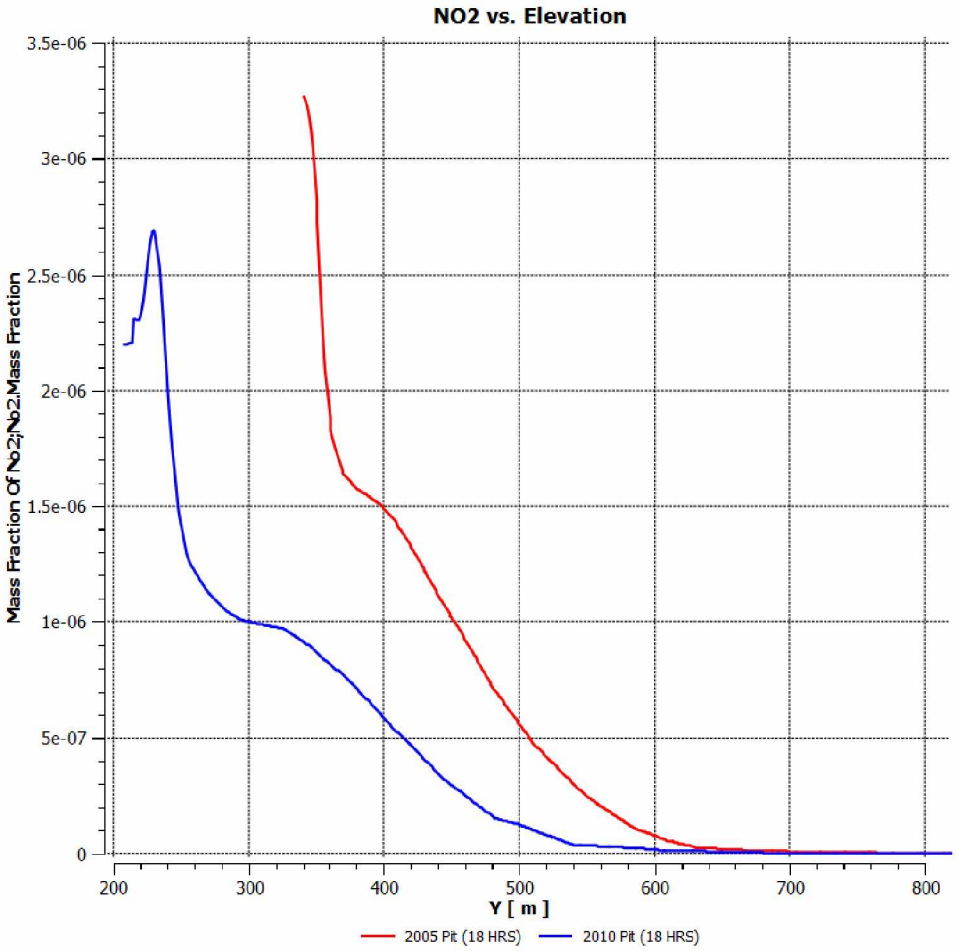

Figure 4.19: CO Concentration in the 2005 and 2010 Pits (18 Hrs)

Chapter 5: Mitigation of Pollutants

In order to mitigate the pollution problem in the selected open pit mine, several remedial measures could be considered. The layer of air closest to the ground requires energy to restart the convective cycle and dissipate the pollutants. This energy can be imparted to the air either kinetically or thermally. A kinetic solution would entail placing a fan in the mine pit or at the top of the pit, thus resulting in dilution ventilation. A truck mounted fan-duct system is ideal for such an operation. Figure 5.1 shows an example of a mobile ventilation fan.

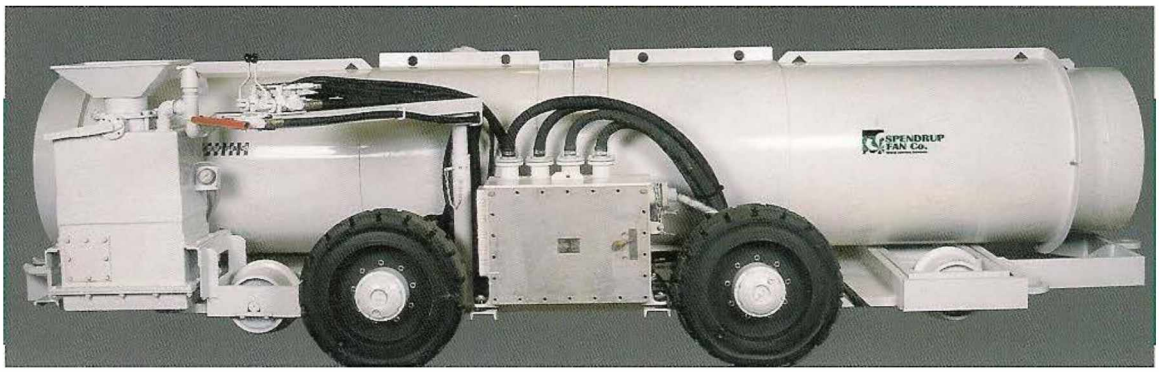

Figure 5.1: Mobile Ventilation Fan (Photo Credit: Spendrup Fan Company)

A thermal solution would entail adding heat to the air, creating a chimney effect. Cascade ventilation is another possible solution. In cascade ventilation, horizontal and vertical fans work in conjunction to clear contaminants from the pit. The horizontal fan supplies air to the working area of the pit, diluting contaminants, and the vertical fan is used to remove the contaminated air from the pit.

A variety of different exhaust fan configurations were modeled to determine if mechanical ventilation could successfully clear the pit of contaminants during an inversion. It was necessary to scale the mass flow of the source and sink terms to achieve similarity between the 2-D model and the 3-D pit. The mass flow of both the source and the sink terms was reduced by a factor of 1,100. Although 2-D models are good for illustrating general trends, 3-D remediation models are still needed to draw meaningful conclusions about the success (or lack thereof) of the various remediation measures. The knowledge gained through trial and error with the 2-D models should help us to simulate remediation in the 3-D models.

CFD models of contaminant transport and remediation measures have been successfully converged. Achieving convergence has required a modification to our methodology. In the CFD models, the sources and sinks were originally introduced as small geometric objects in the model domain. For example, a 20 ft x 20 ft rectangle could be used to represent the pollution from a piece of equipment. This approach created meshing and convergence difficulties. Meshing an extremely small object (i.e., a truck) inside of an extremely large domain (i.e., an open pit mine) results in very small, highly skewed mesh elements surrounding the object. These small, highly skewed elements—in conjunction with the high heat and concentration gradients in the surrounding model space—create instability in the model.

Model convergence requires that source and sink terms be introduced into the model domain at the level of the individual mesh element. Source terms represent a

source of heat or contaminants. A sink term represents mass flow out of the model domain. Although convergence is not an issue, the predicted pollutant concentrations in the pit are much higher than observed. This overprediction is, most likely, because the entire mass flow of pollutants has been injected into the comparatively small 2-D model domain. Various ways to scale the input source terms—appropriate for the reduced size of the 2-D model domain—are presently being investigated.

5.1 Helicopter

One potential remediation measure attempted by the industrial partner involved flying a helicopter immediately above the top of an inversion (Figure 5.2). The expectation was that the rotor on the helicopter would mix warm, uncontaminated air into the inversion and help lift the inversion in the pit. Air samples were taken before and after the flight. The sample values showed only a small decrease in contaminant concentration while the helicopter was close to the sampling point. The concentration went back up when the helicopter moved away from the sample point. The presence of the helicopter created two important causations: 1.) the addition of heat to the air mass, and 2.) downward thrust on the air mass, creating a very small amount of mechanical turbulence. Neither effect, however, proved to be sufficient to lift the inversion.

Figure 5.2: Helicopter Flying Over an Open Pit Mine during an Inversion

5.2 Exhaust Fan—142 m^3/s

The first remediation measure modeled consisted of a single source and sink (i.e., one shovel and a fleet of trucks). In the initial model, the source was located at the west end of the pit, and the sink was located at the east end of the pit. The sink was assigned a volumetric flow rate of approximately 142 m^3/s (300,000 cfm). In other words, the sink can be thought of as an exhaust fan continuously removing 142 m^3/s of air from the pit. The model was run for 18 hours under these conditions. Figure 5.3-Figure 5.8 illustrate the CO concentration in the pit with the 142 m^3/s exhaust fan running continuously. In comparing this simulation to the base case without the fan (Figure 4.1-Figure 4.6), it is apparent that the 142 m^3/s fan has little effect on the CO concentrations

within the pit. The exhaust ventilation fan alone was not effective enough due to its small area of influence. A combination of a mobile free jet source providing a constant mixing of the polluted air and the exhaust fan duct may be sufficient to clear the pit of pollutants.

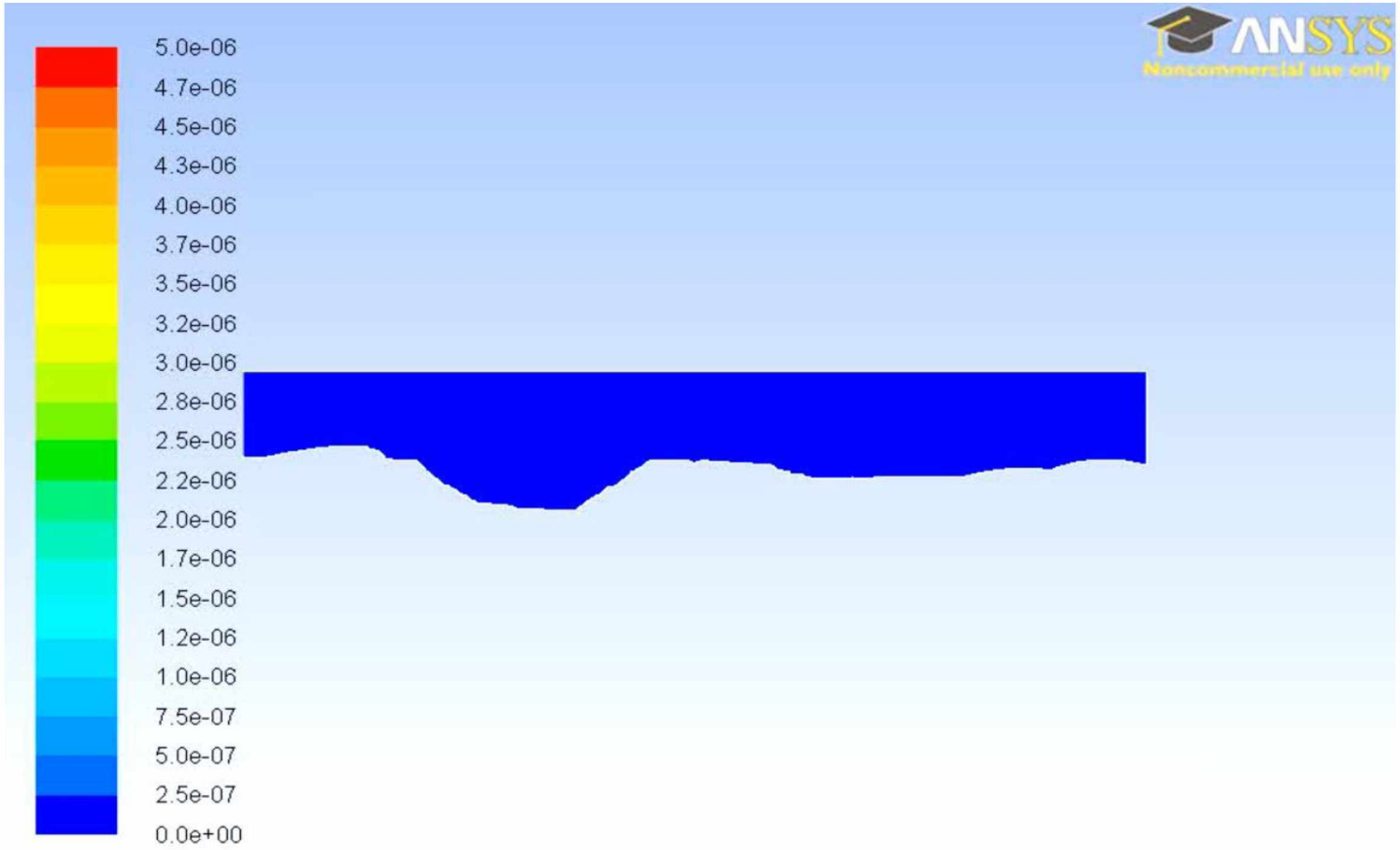

Figure 5.3: CO Concentration Contours with a 142 m^3/s Fan Located Opposite the Source (Time ≈ 0 Hrs.)

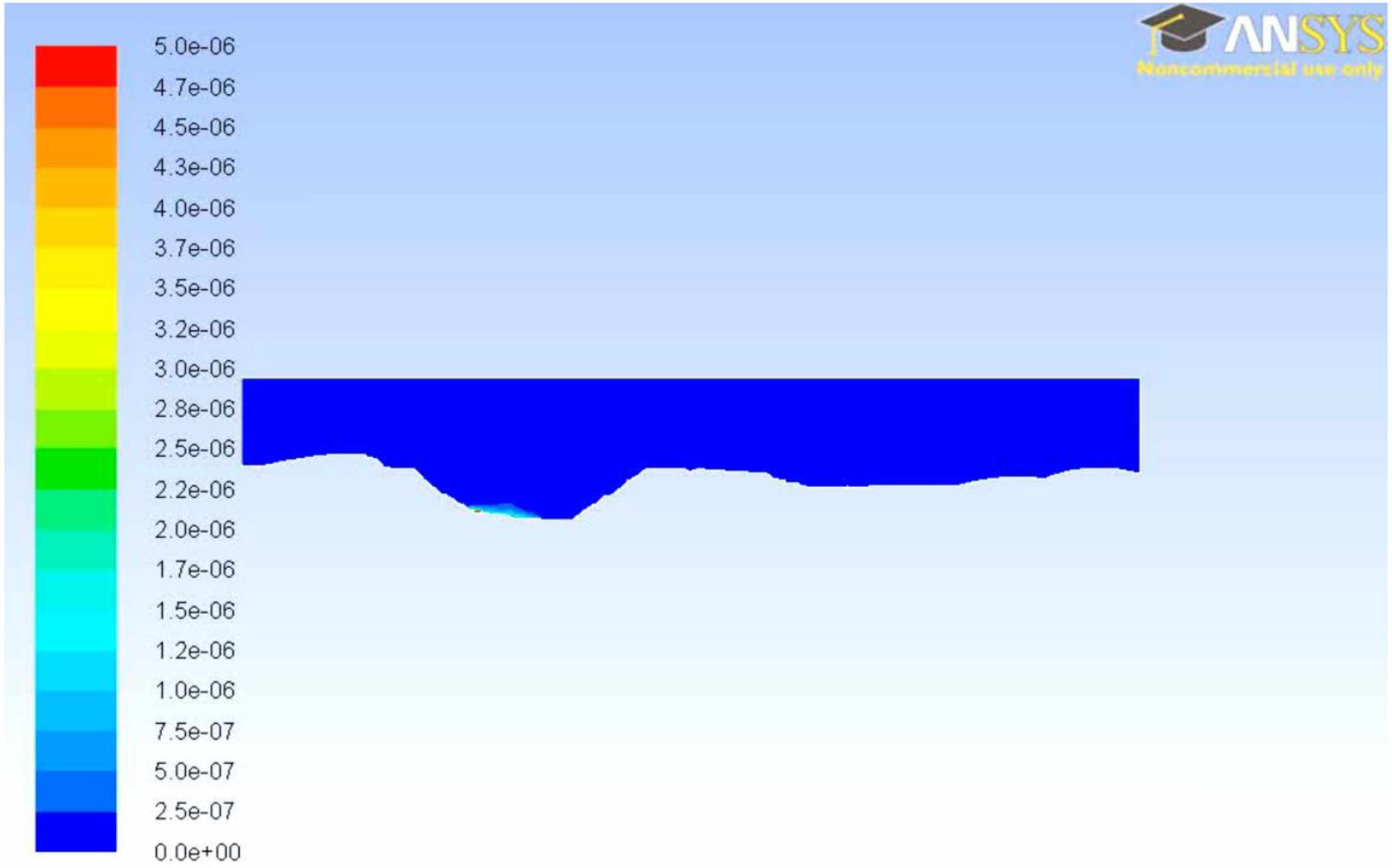

Figure 5.4: CO Concentration Contours with a 142 m^3/s Fan Located Opposite the Source (Time ≈ 4.0 Hrs.)

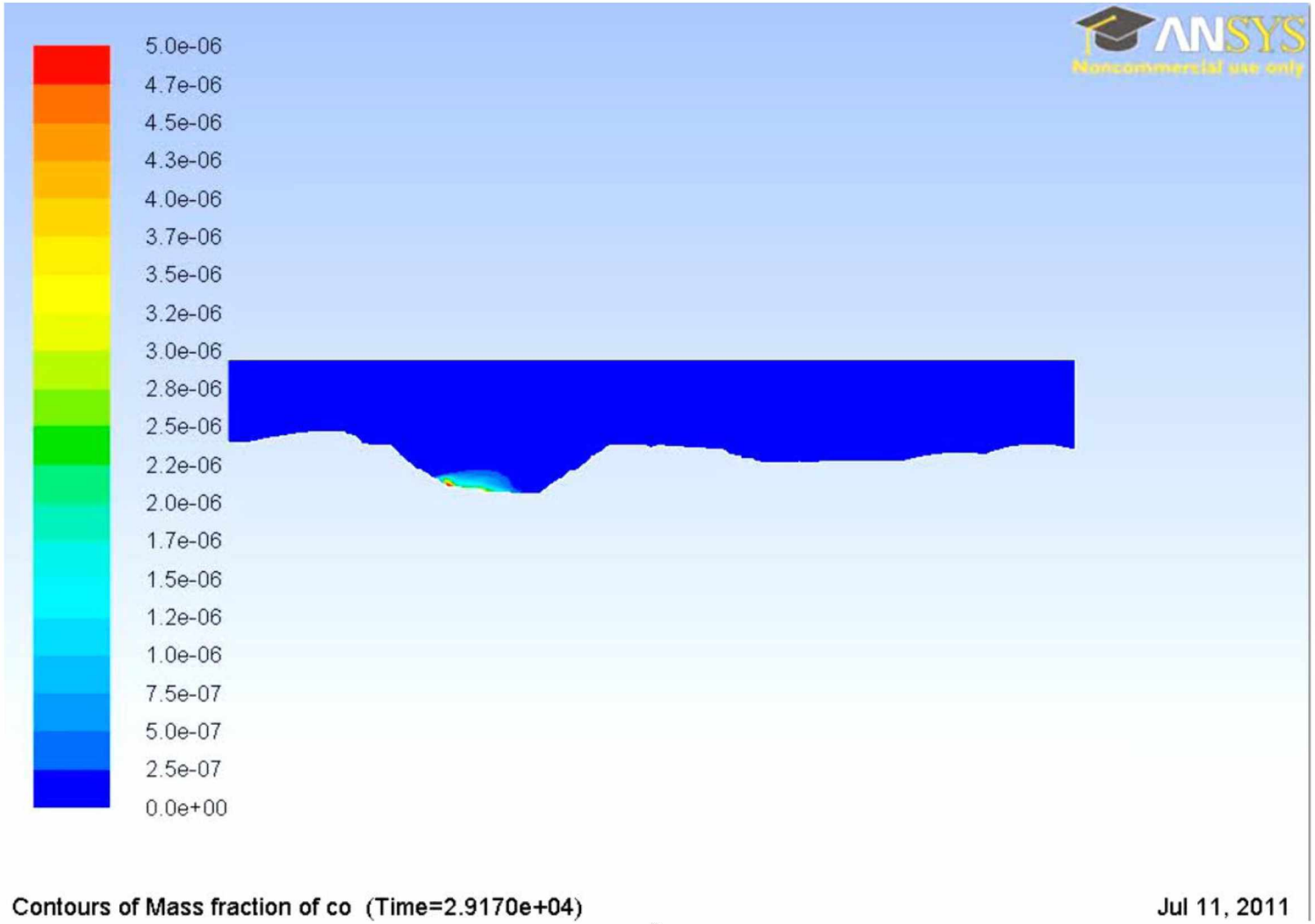

Figure 5.5: CO Concentration Contours with a 142 m^3/s Fan Located Opposite the Source (Time ≈ 8.1 Hrs.)

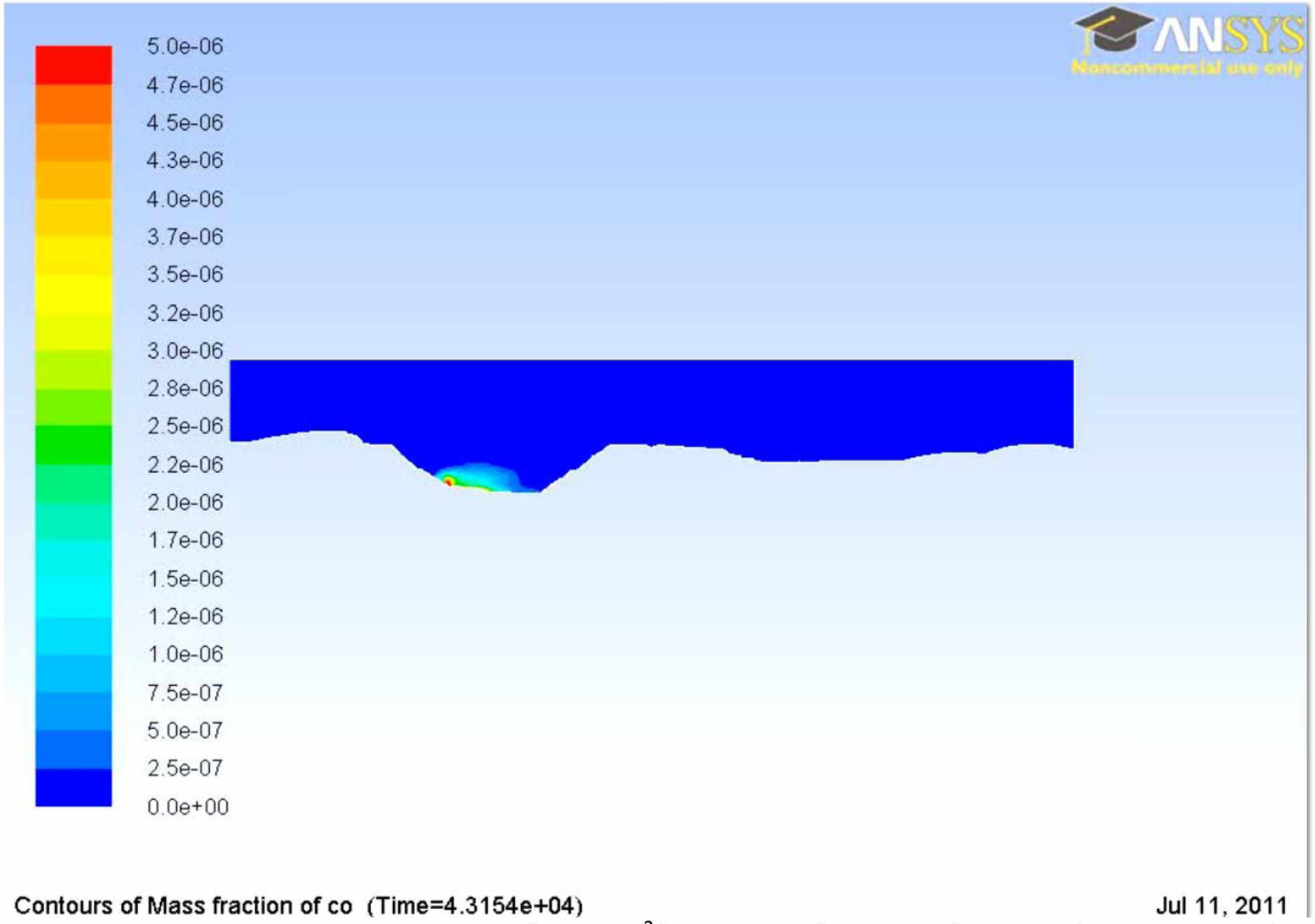

Figure 5.6: CO Concentration Contours with a 142 m^3/s Fan Located Opposite the Source (Time ≈ 12.0 Hrs.)

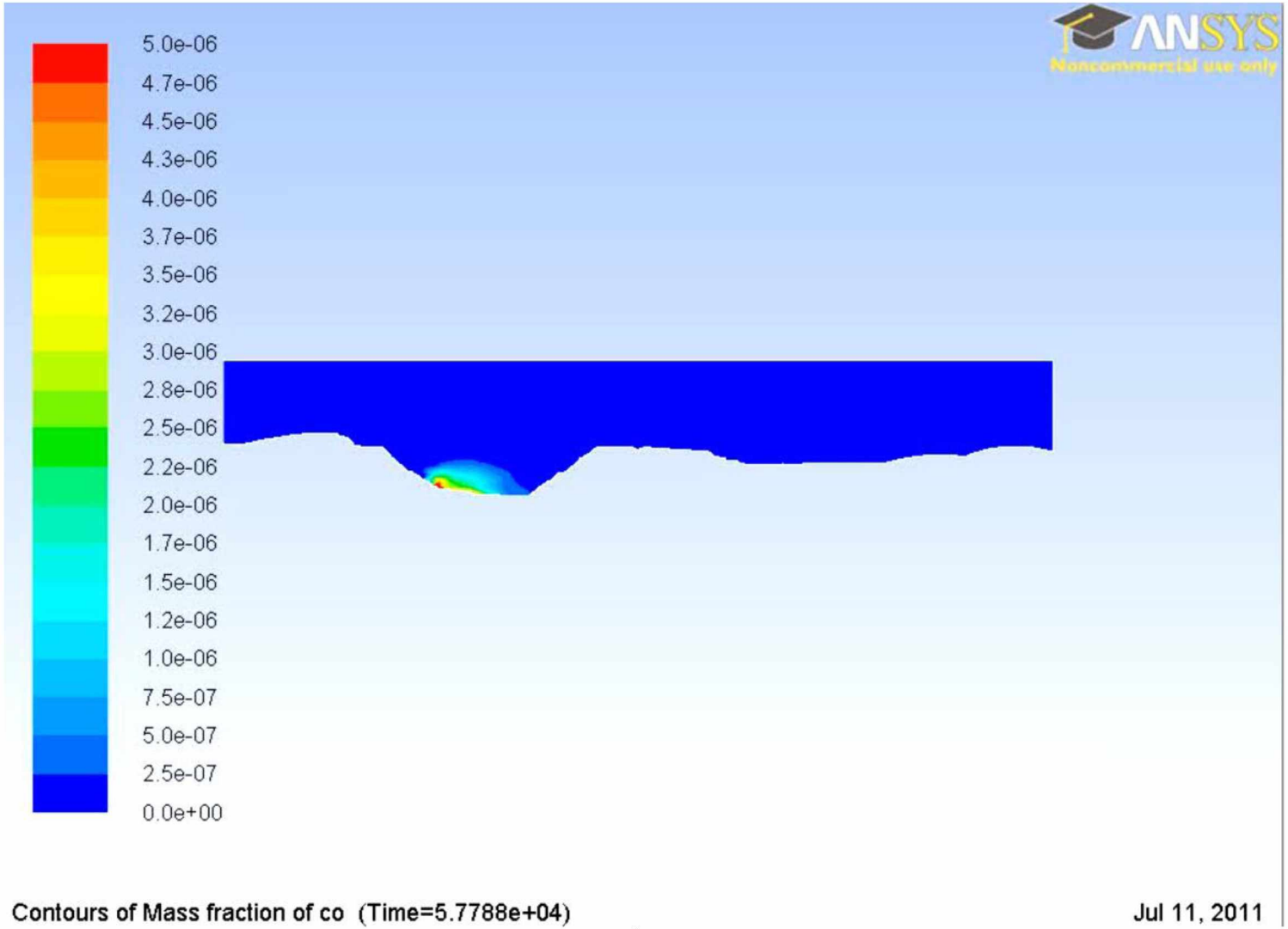

Figure 5.7: CO Concentration Contours with a 142 m^3/s Fan Located Opposite the Source (Time ≈ 16.1 Hrs.)

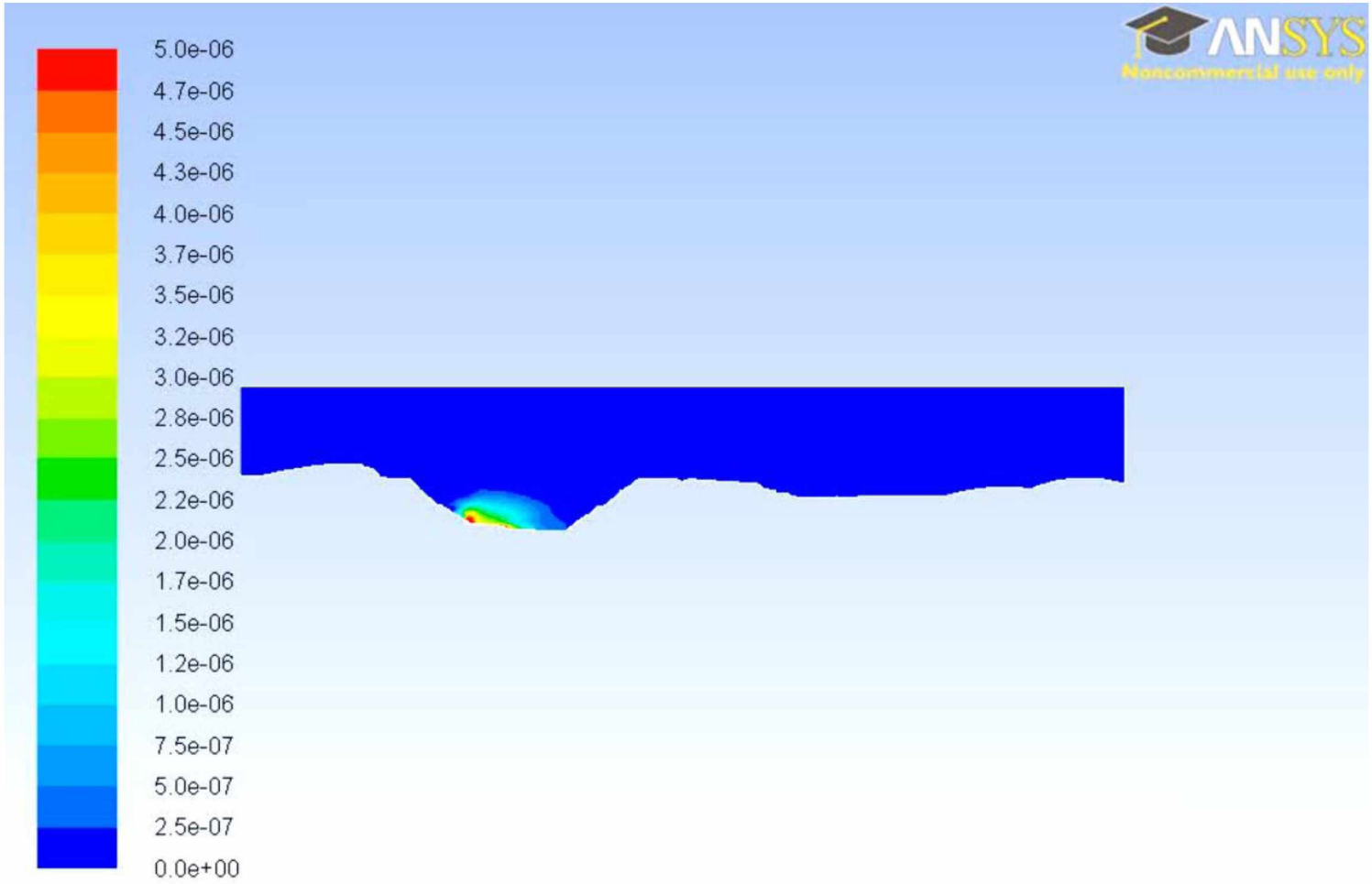

Figure 5.8: CO Concentration Contours with a 142 m^3/s Fan Located Opposite the Source (Time ≈ 18.0 Hrs.)

5.3 Exhaust Fan—556 m^3/s

In the next remediation measure simulation, the source term was increased to approximately 556 m^3/s (1.2 million cfm). As before, the single source was located at the west end of the pit, and the sink was located at the east end of the pit. The resulting CO concentration in the pit is illustrated in Figure 5.9-Figure 5.14. The 556 m^3/s exhaust fan was sufficient to keep the eastern portion of the pit clear of contaminants in this case. As can be seen from the figures, contaminants were still able to build up in the western portion of the pit near the source term

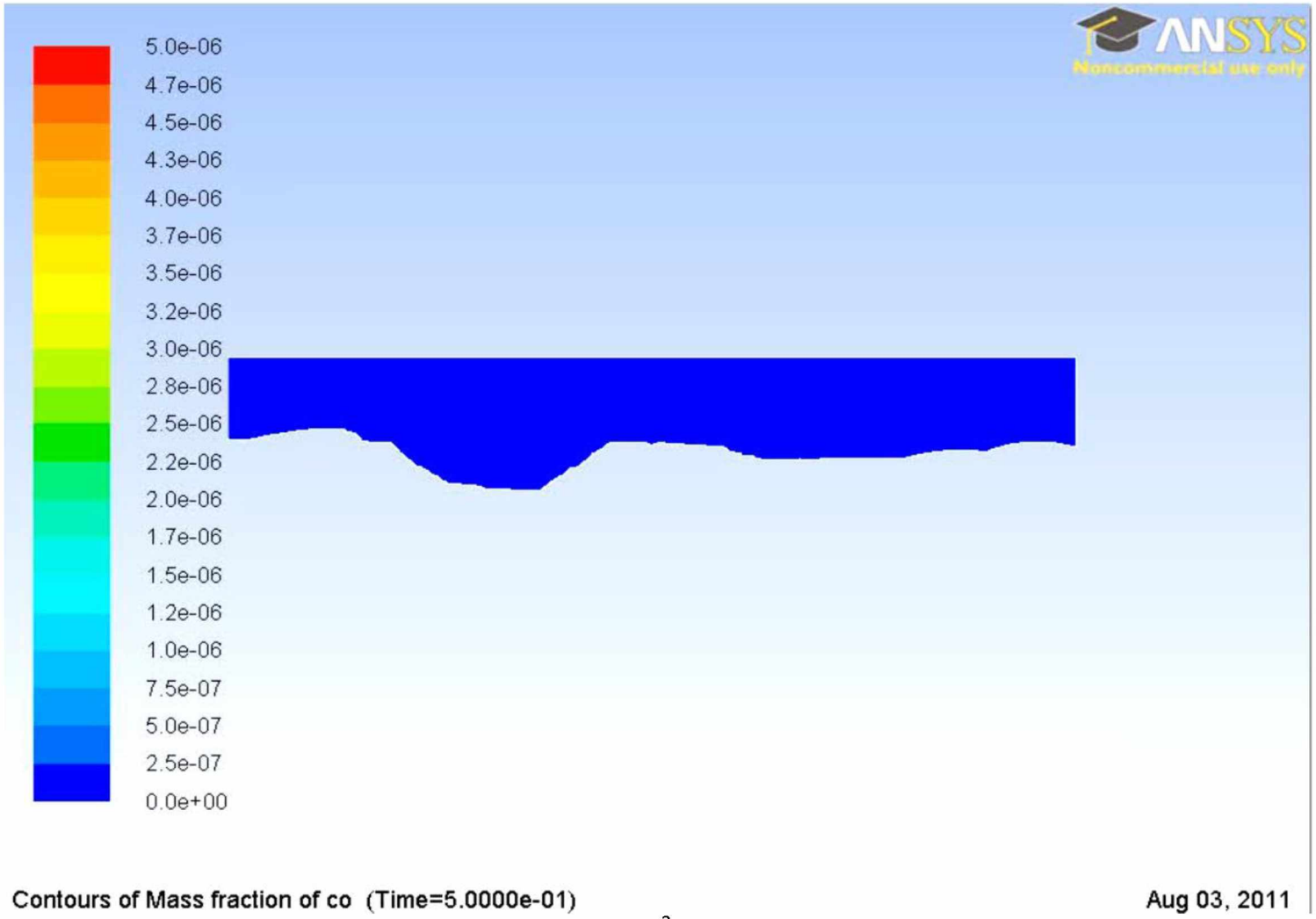

Figure 5.9: CO Concentration Contours with a 556 m^3/s Fan Located Opposite the Source (Time ≈ 0 Hrs.)

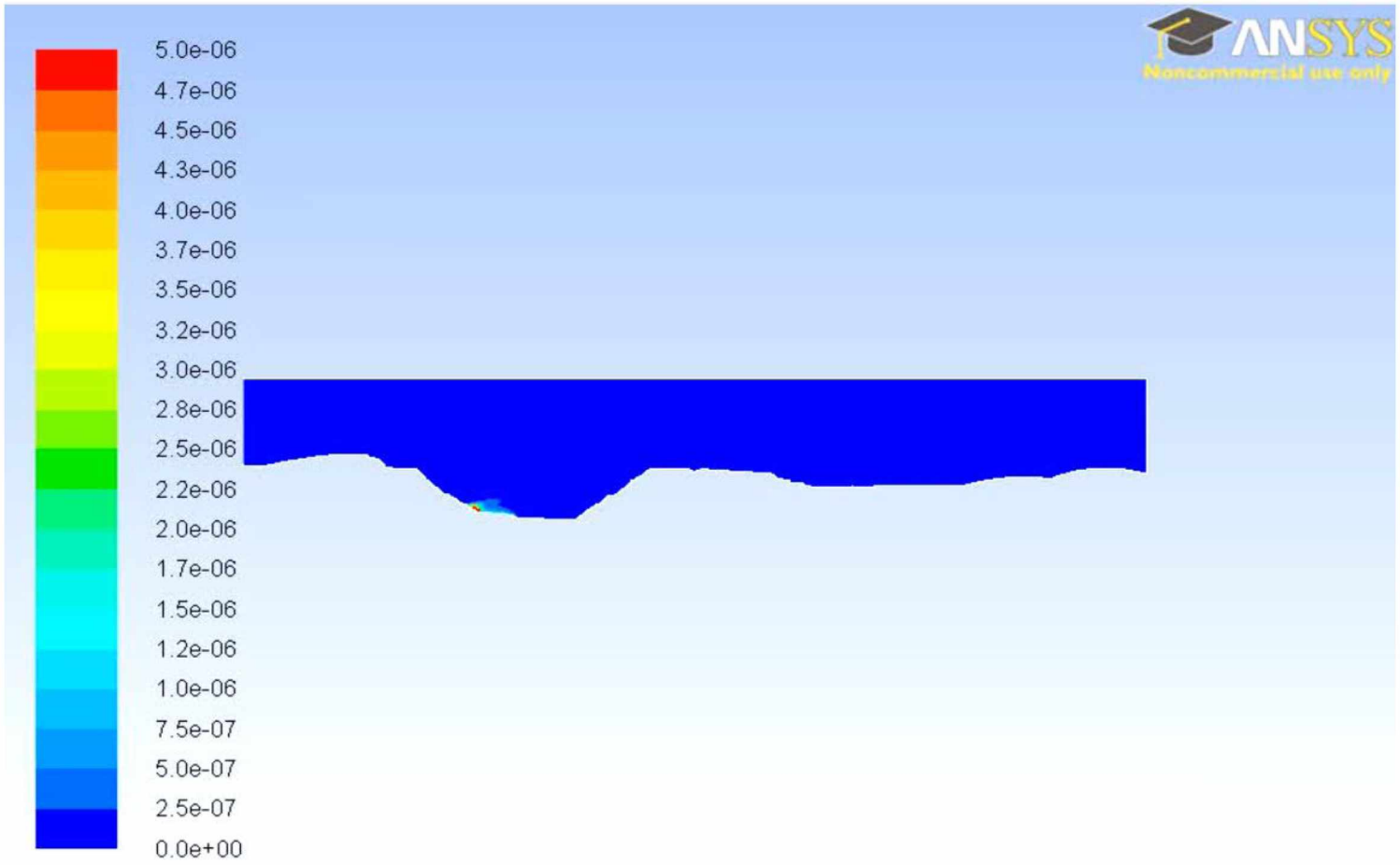

Figure 5.10: CO Concentration Contours with a 556 m^3/s Fan Located Opposite the Source (Time ≈ 4.0 Hrs.)

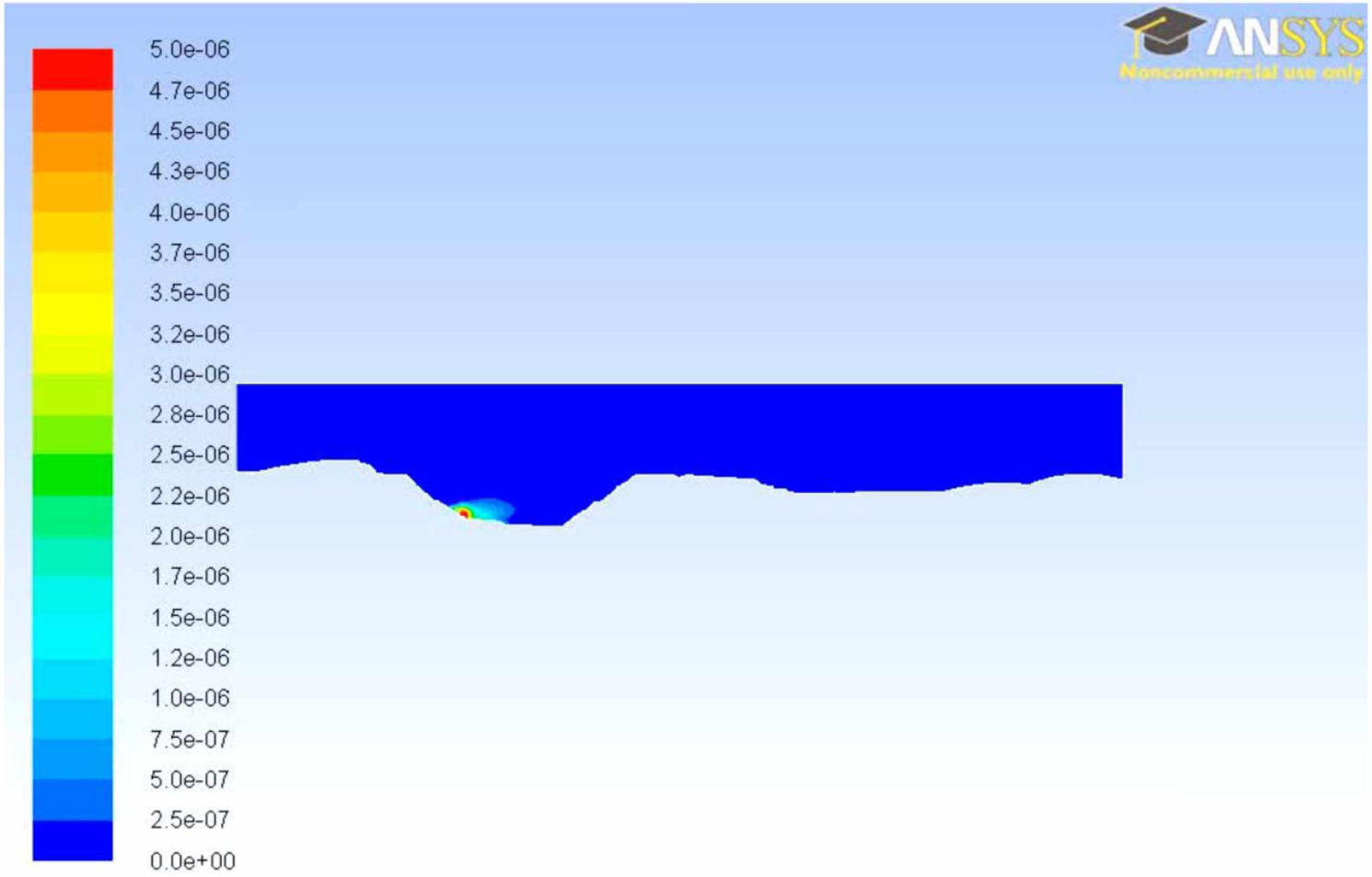

Figure 5.11: CO Concentration Contours with a 556 m^3/s Fan Located Opposite the Source (Time ≈ 8.1 Hrs.)

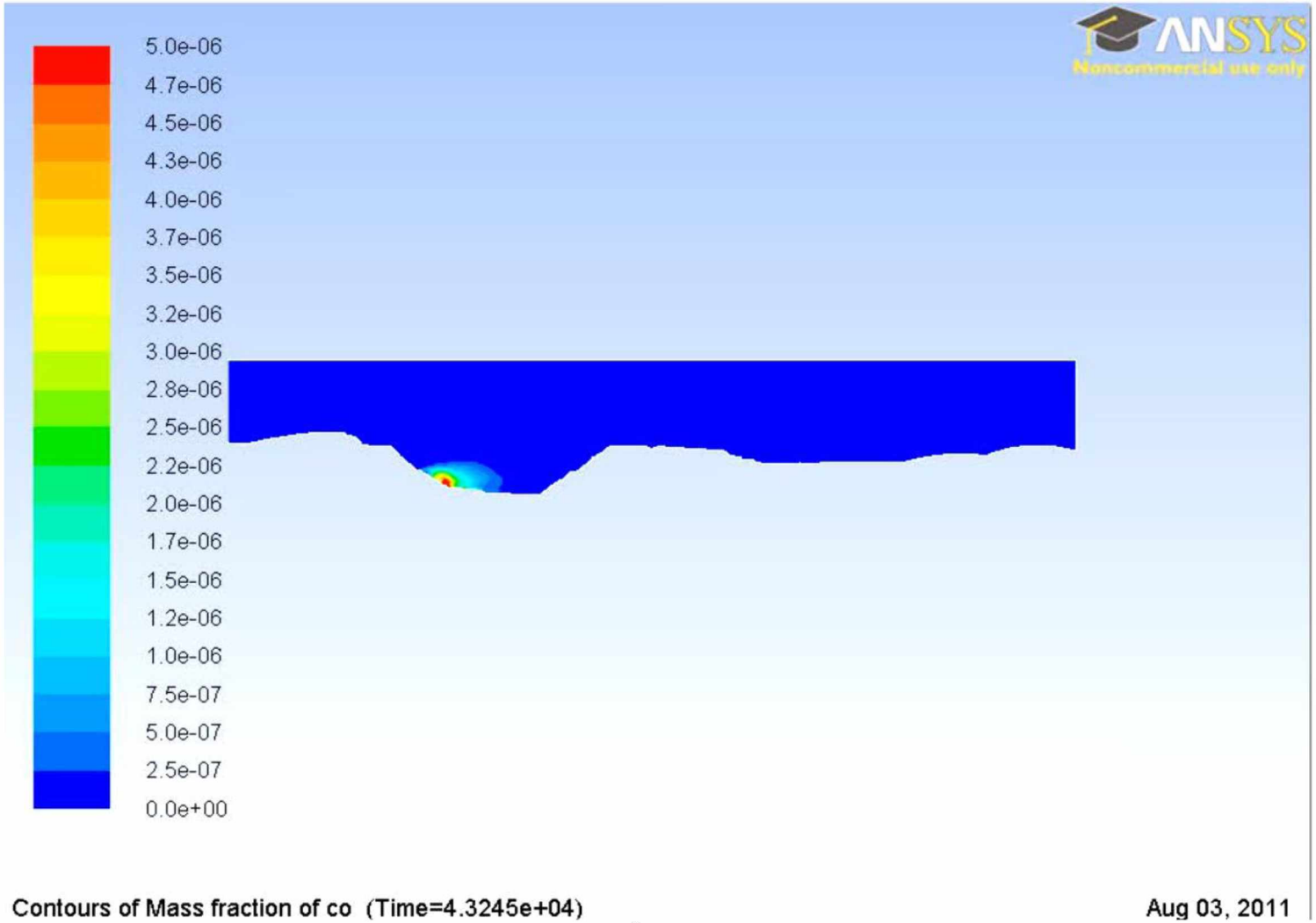

Figure 5.12: Concentration Contours with a 556 m^3/s Fan Located Opposite the Source (Time ≈ 12.0 Hrs.)

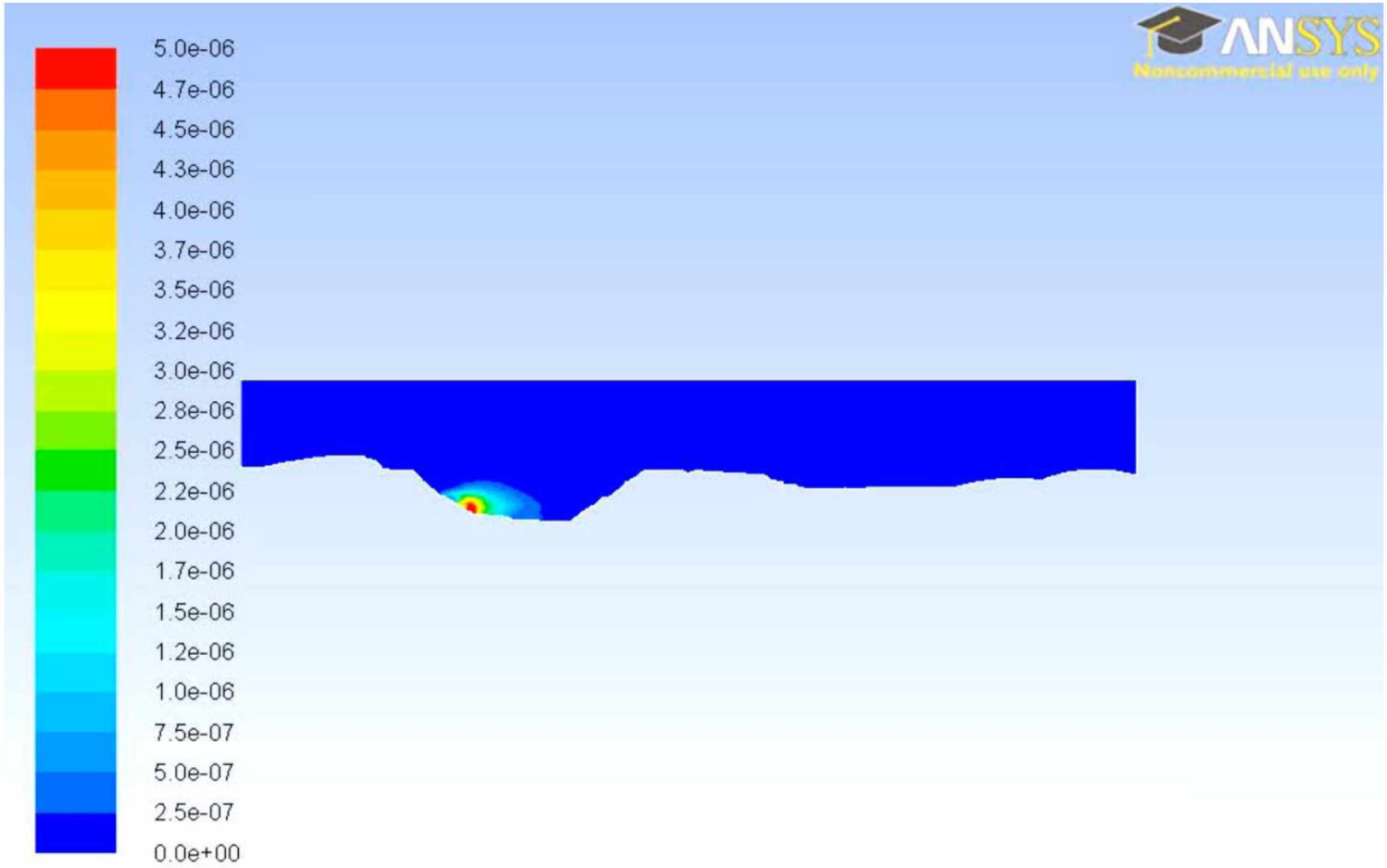

Figure 5.13: Concentration Contours with a 556 m^3/s Fan Located Opposite the Source (Time ≈ 16.1 Hrs.)

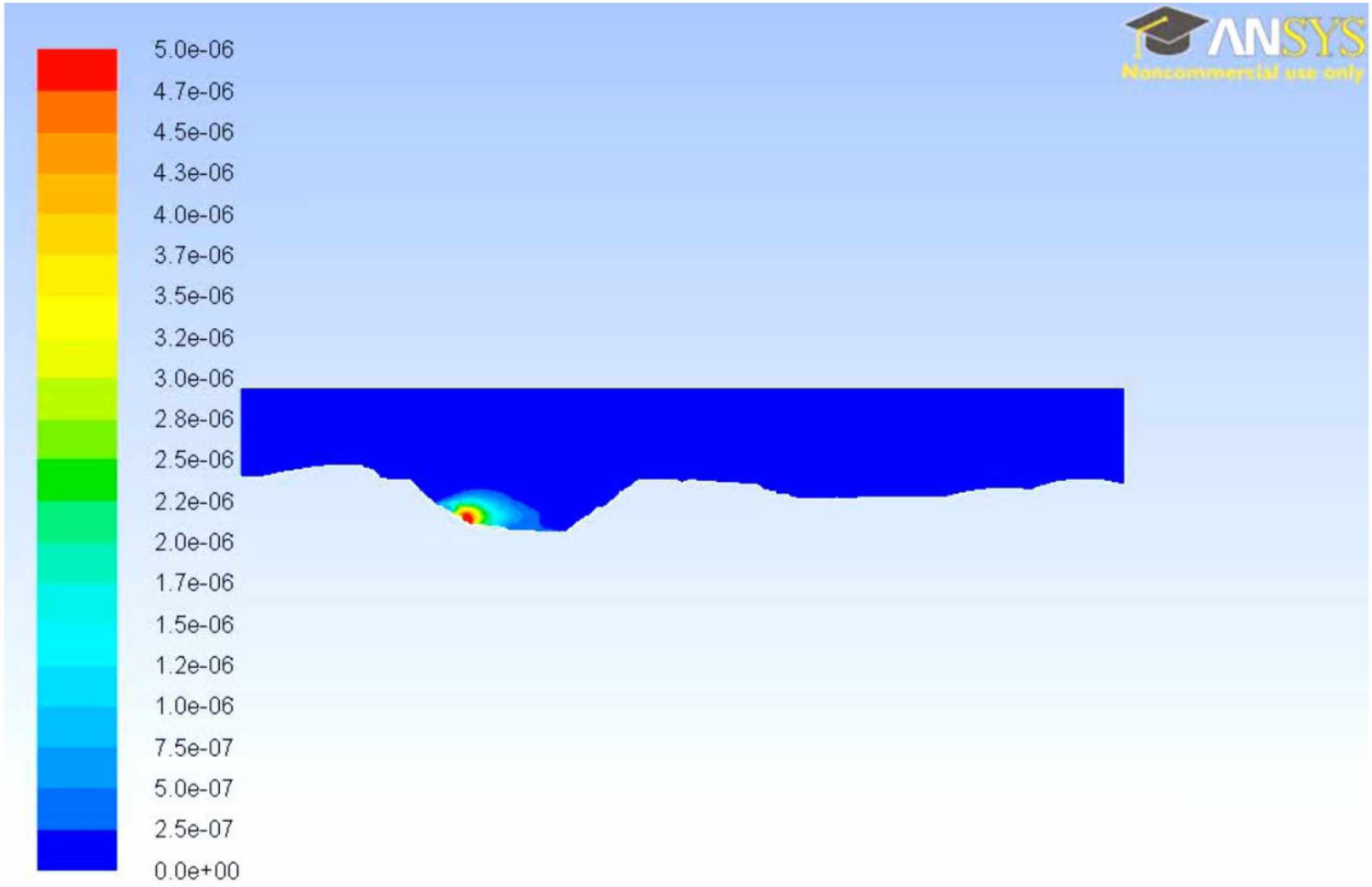

Figure 5.14: Concentration Contours with a 556 m^3/s Fan Located Opposite the Source (Time ≈ 18.0 Hrs.)

5.4 Exhaust Fans—Multiple Fans, Multiple Sources (142 m^3/s)

The selected mine modeled in this research, typically operates a two unit truck-shovel fleet. Each shovel generally works on a separate bench. To model the conditions at the mine site more accurately, two source terms located at different elevations were incorporated into the model. A 142 m^3/s (300,000 cfm) sink (i.e., exhaust fan) was located adjacent to each pollutant source to see if the pollutant concentrations in the pit could effectively be reduced. Figure 5.15-Figure 5.20 show the results from this model study. As can be seen from the figures, the two 142 m^3/s fans are not able to prevent contaminants from building up in the pit.

Figure 5.21 shows the CO concentration along a vertical cross section in the 2010 pit. The ventilation fans do provide some dilution of the contaminants near the ground surface. However, the volume of air moved by the fans is not sufficient to prevent contaminants from building up in the pit. Figure 5.22 compares the contaminant concentrations in the 2010 pit along a vertical cross section with and without exhaust fans. The simulation predicts that the two 142 m^3/s will reduce peak CO concentration near the ground surface by approximately 1.3 ppm. Peak NO_2 concentrations are reduced by approximately 0.6 ppm near the surface (Figure 5.23). At approximately 60 m above the ground surface, simulation predicts that contaminant concentrations will be higher with mechanical ventilation than without.

Figure 5.24 shows the concentration of CO along a horizontal cross section in the pit with the two 142 m^3/s running. The fans reduce CO concentration near the pollutant

sources, but CO concentrations at the east end of the pit are actually elevated as contaminated air is pulled towards the fan. Figure 5.25 compares the NO_2 concentrations in the 2010 pit along a horizontal cross section with and without exhaust fans. A significant reduction in NO_2 concentration can be seen in the area surrounding the pollutant sources (approximately 7 ppm NO_2). In this case, the exhaust fans are able to provide enough local dilution to bring the NO_2 concentrations at the pollutant sources in compliance with TLVs. NO_2 concentrations in the eastern portion of the pit are approximately 0.5 ppm higher than in the base case without mechanical ventilation.

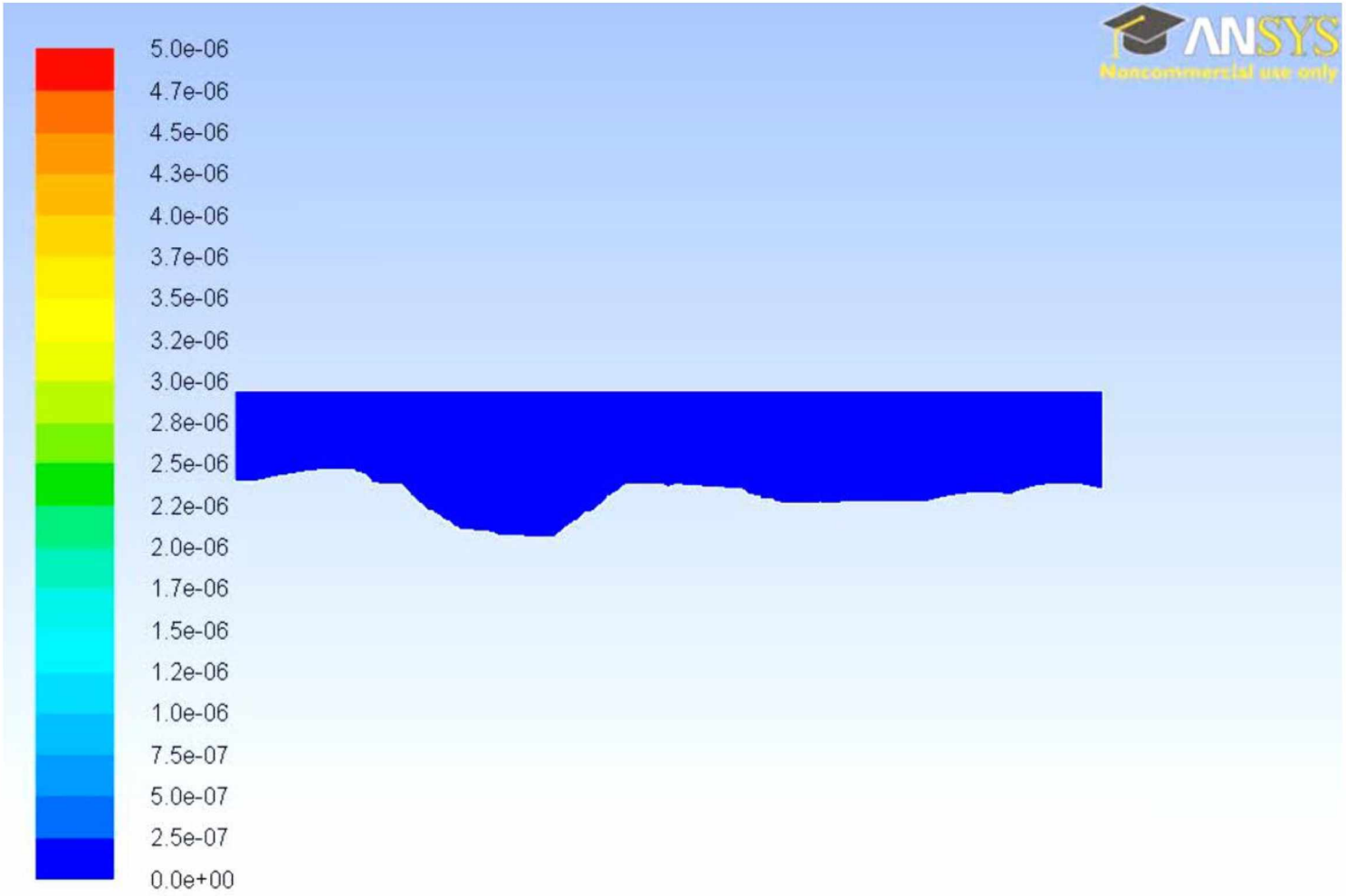

Figure 5.15: Concentration Contours with Two Sources and Two Sinks (Time ≈ 0 Hrs.)

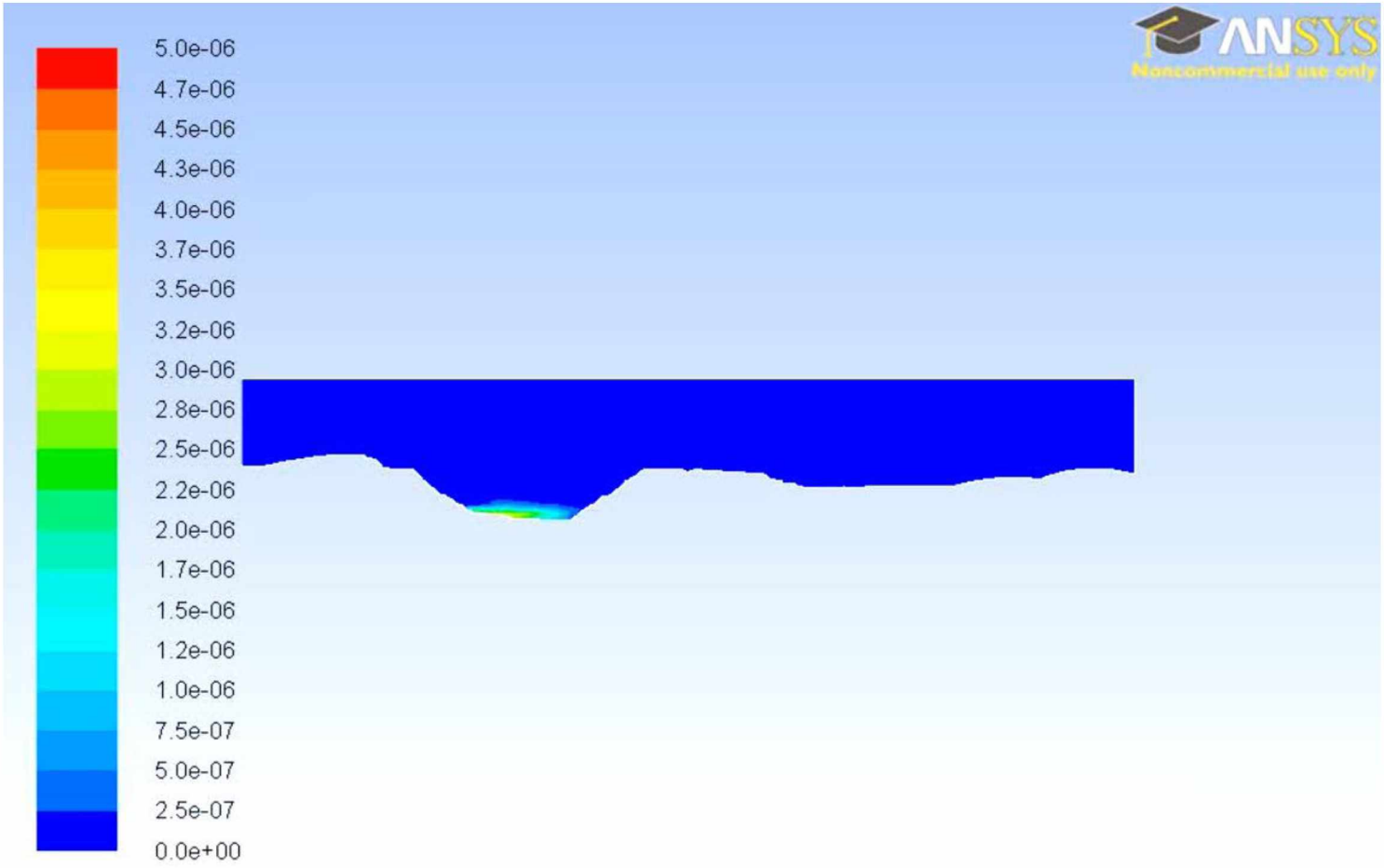

Figure 5.16: Concentration Contours with Two Sources and Two Sinks (Time ≈ 4.1 Hrs.)

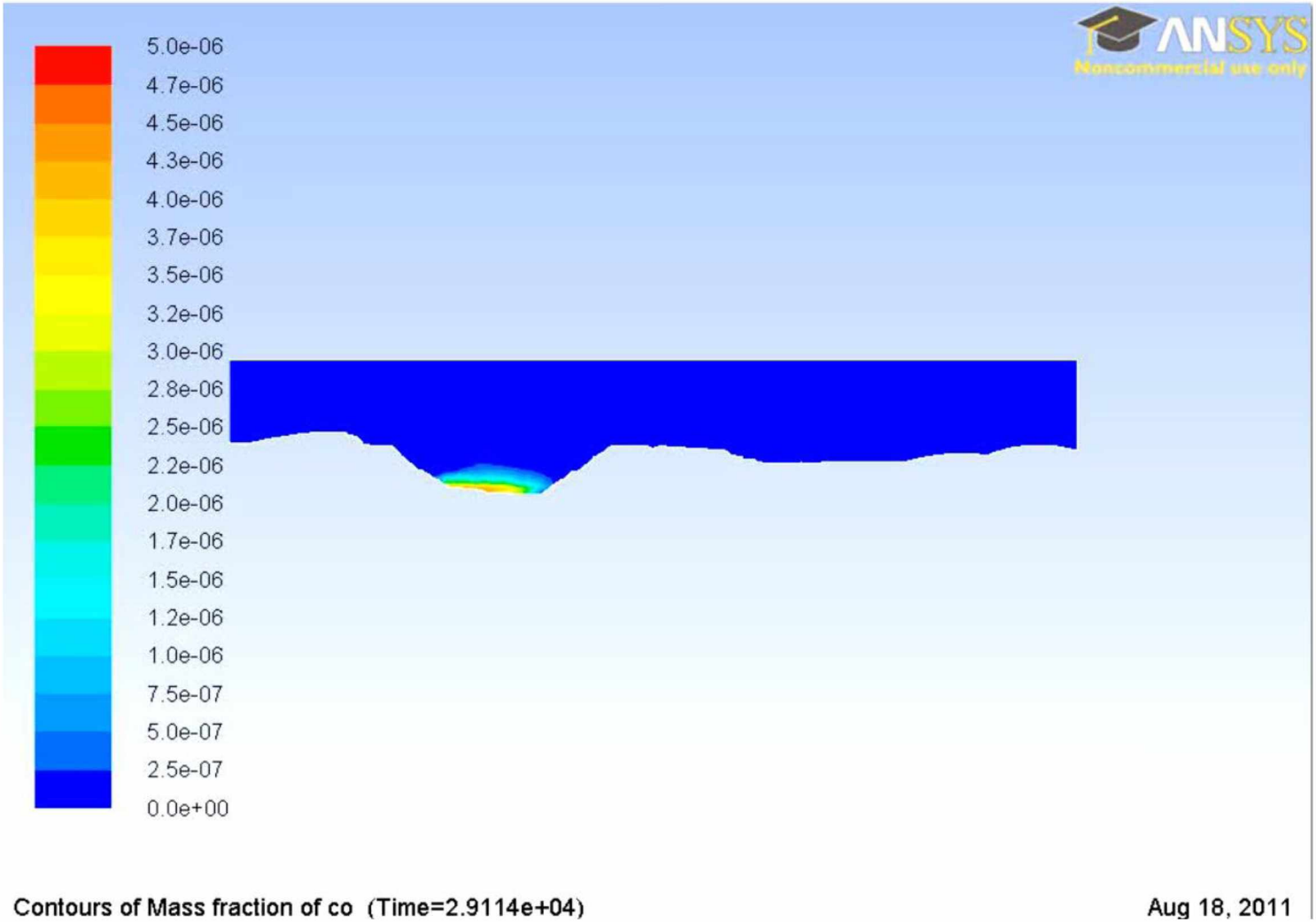

Figure 5.17: Concentration Contours with Two Sources and Two Sinks (Time ≈ 8.1 Hrs.)

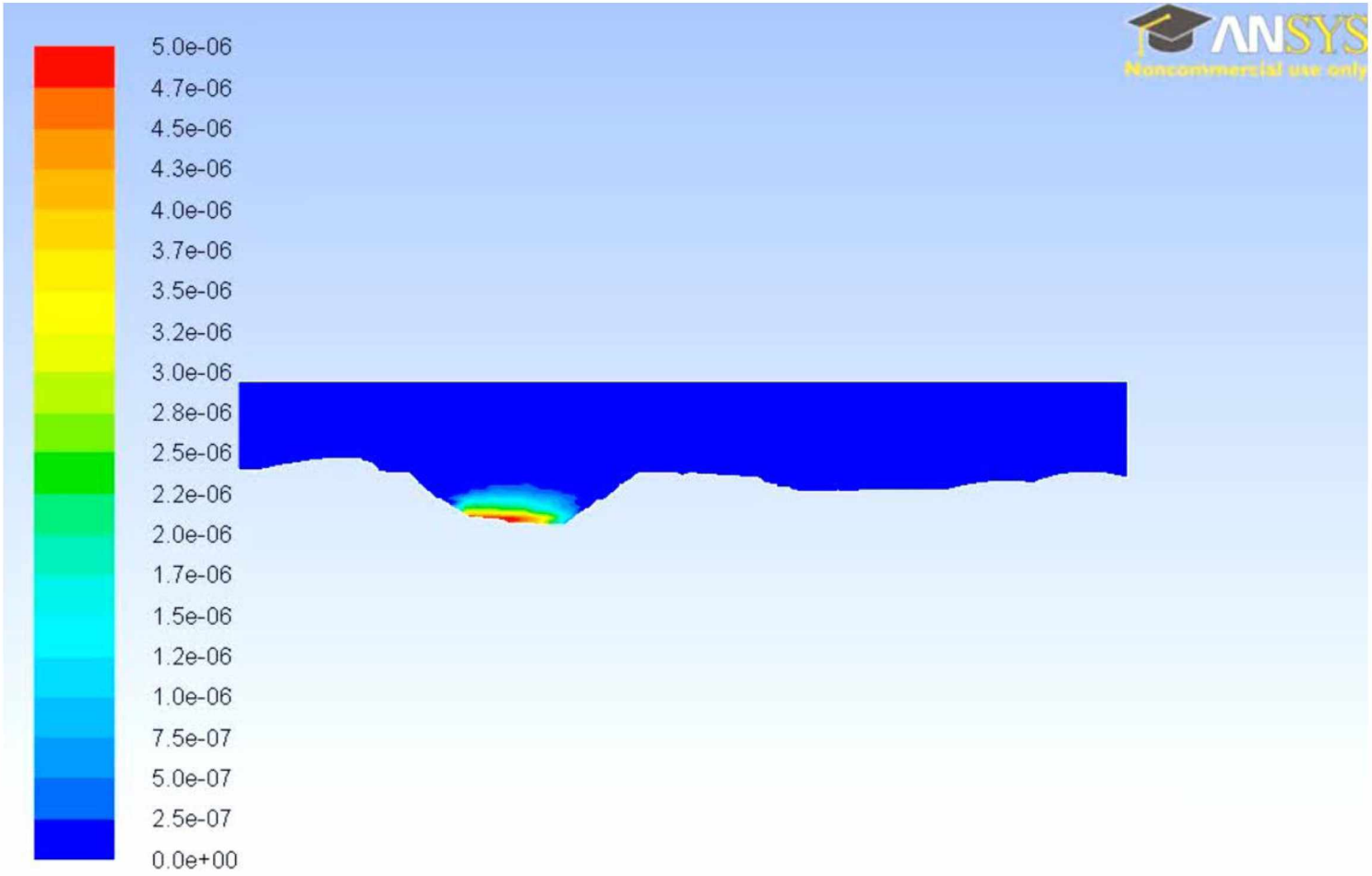

Figure 5.18: Concentration Contours with Two Sources and Two Sinks (Time ≈ 12.0 Hrs.)

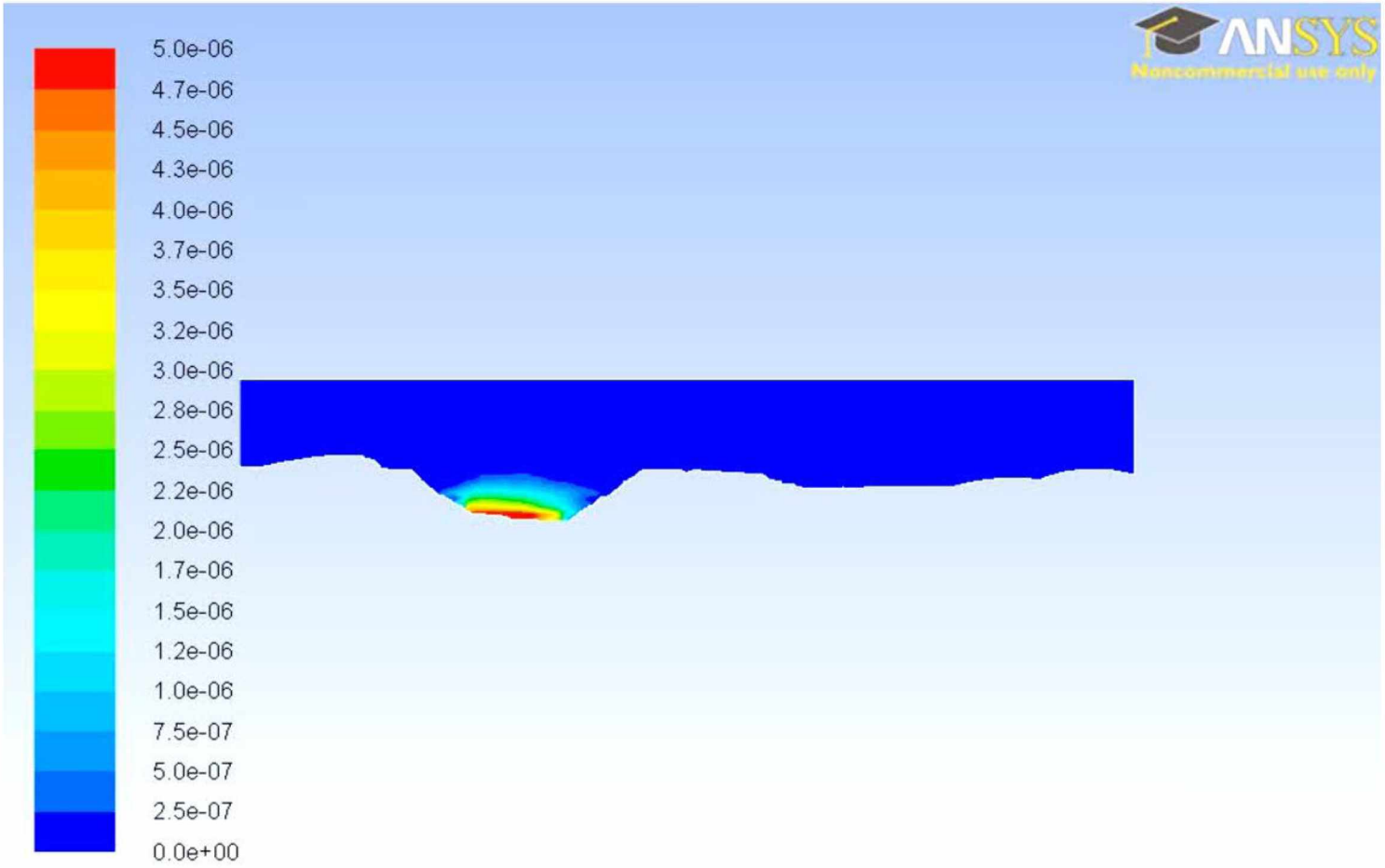

Figure 5.19: Concentration Contours with Two Sources and Two Sinks (Time ≈ 16.0 Hrs.)

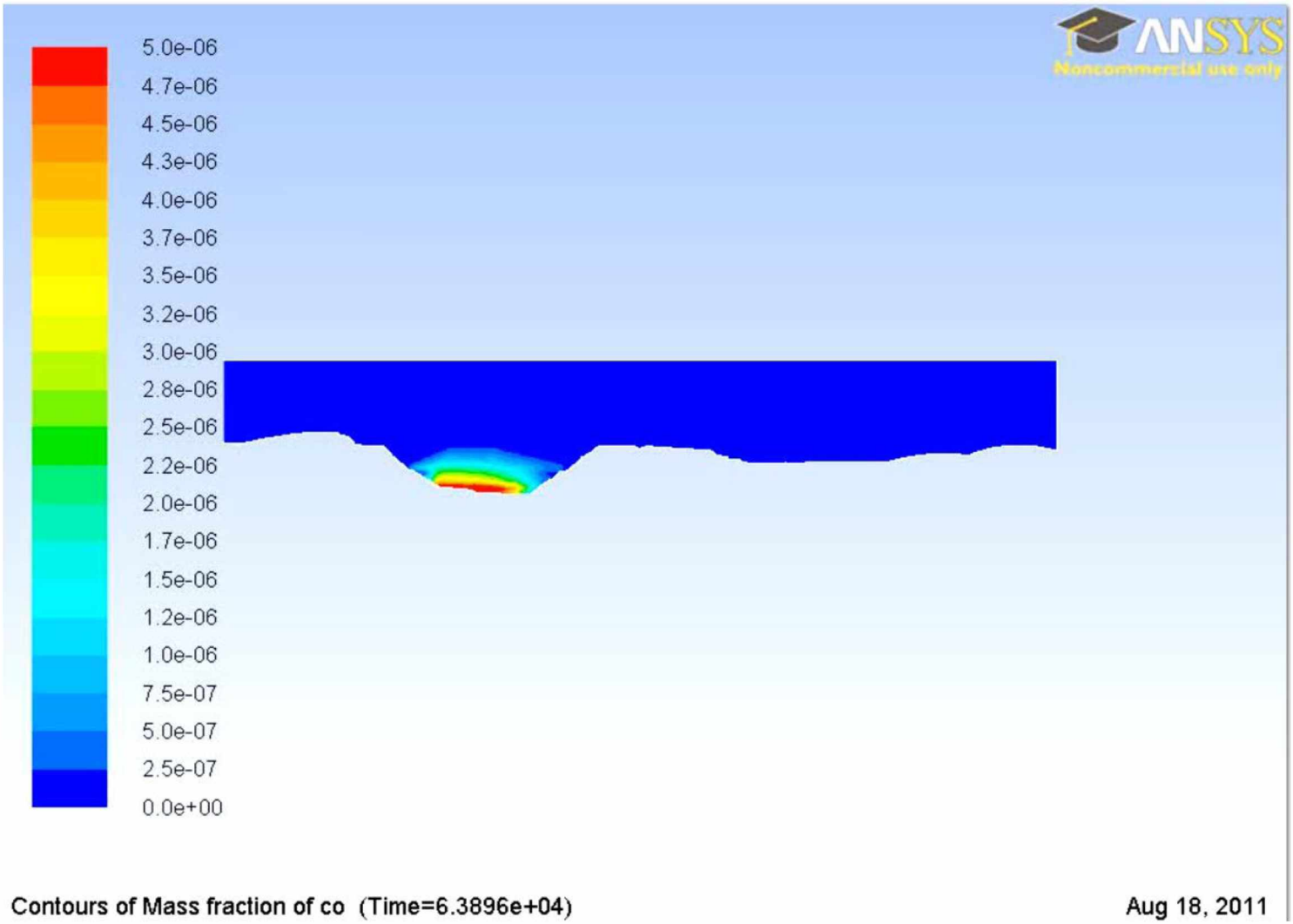

Figure 5.20: Concentration Contours with Two Sources and Two Sinks (Time ≈ 18.0 Hrs.)

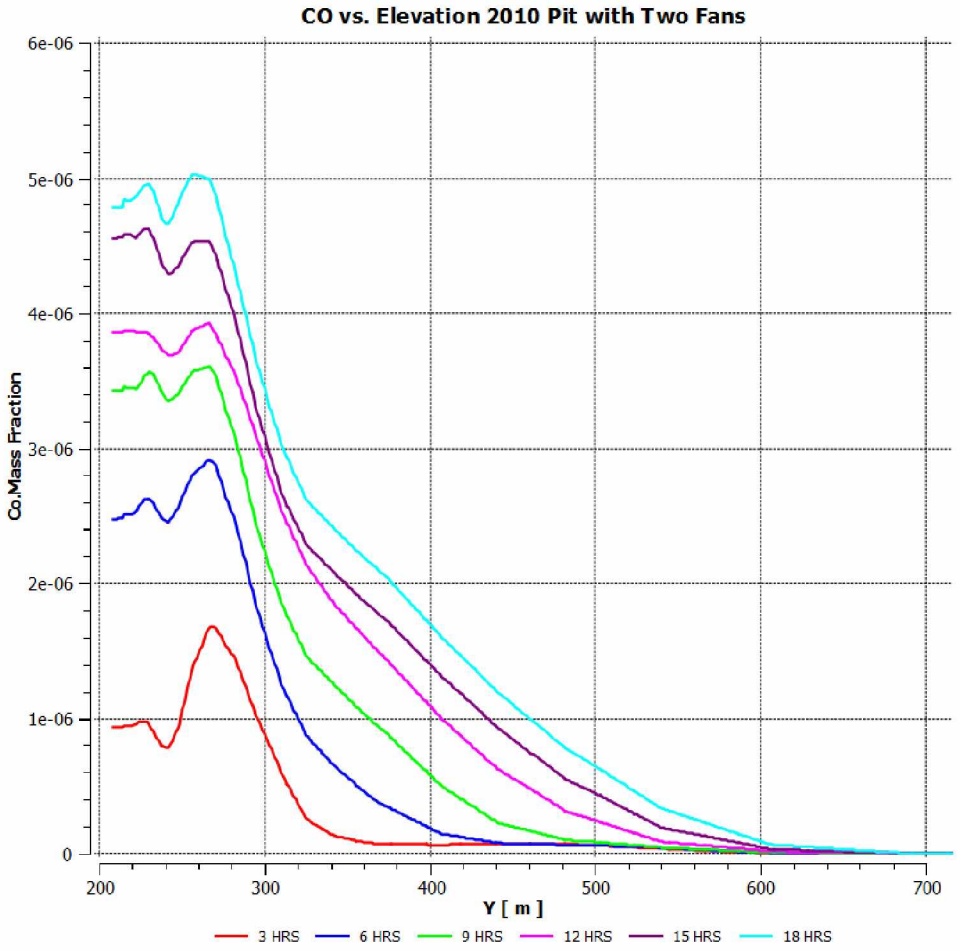

Figure 5.21: CO Concentration in the 2010 Pit with Two 142 m^3/s Fans (3 Hour Intervals)

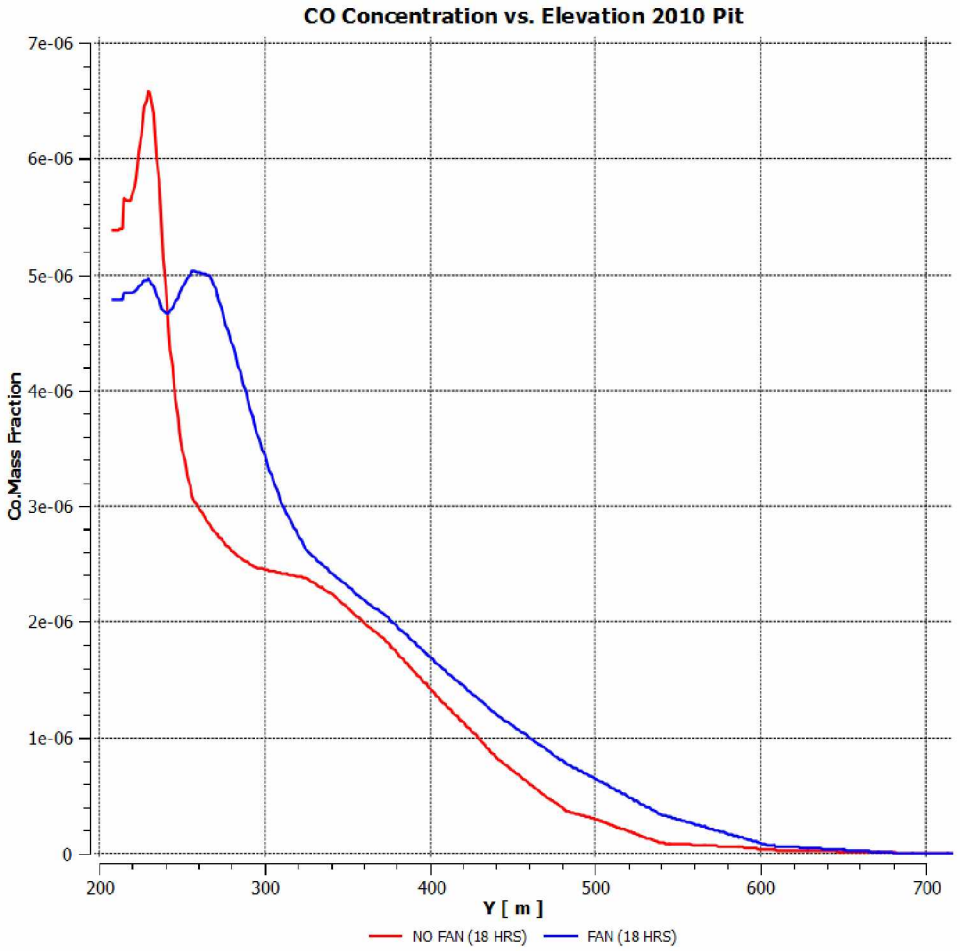

Figure 5.22: CO Concentration in the 2010 Pit with and without Ventilation (18 Hrs)

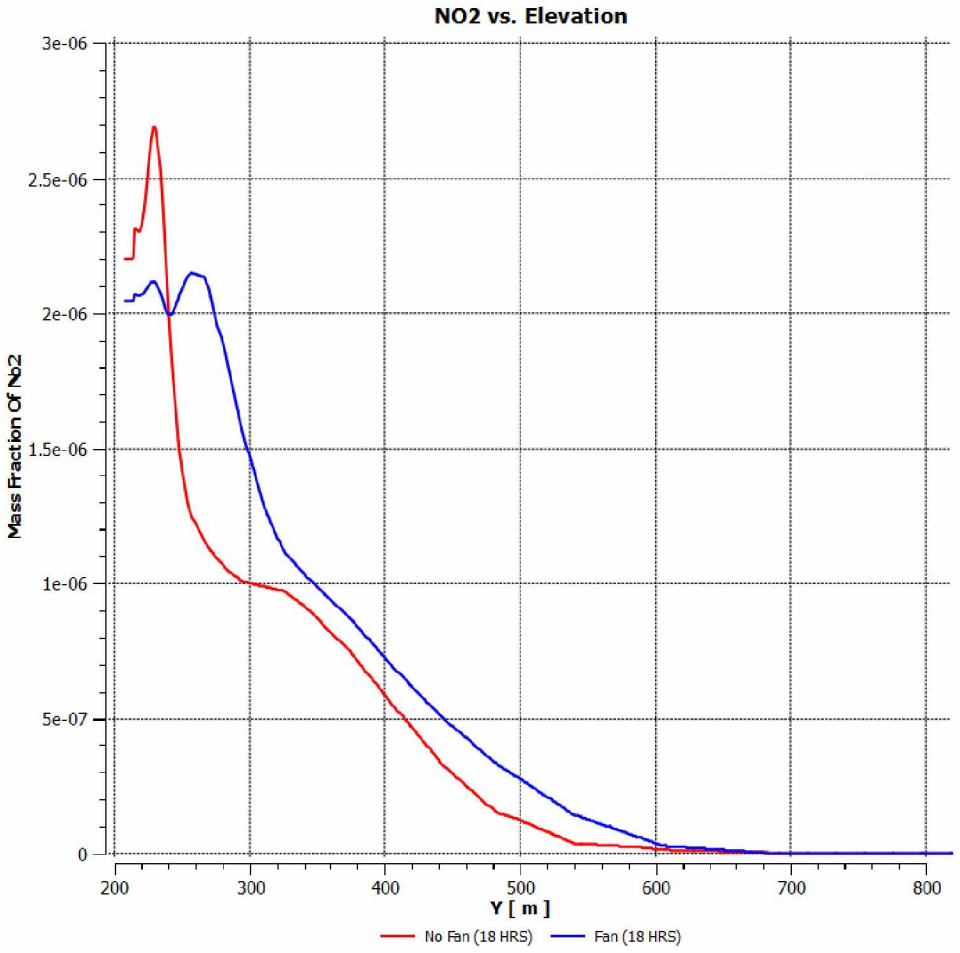

Figure 5.23: NO_2 Concentration in the 2010 Pit with and without Ventilation (18 Hrs)

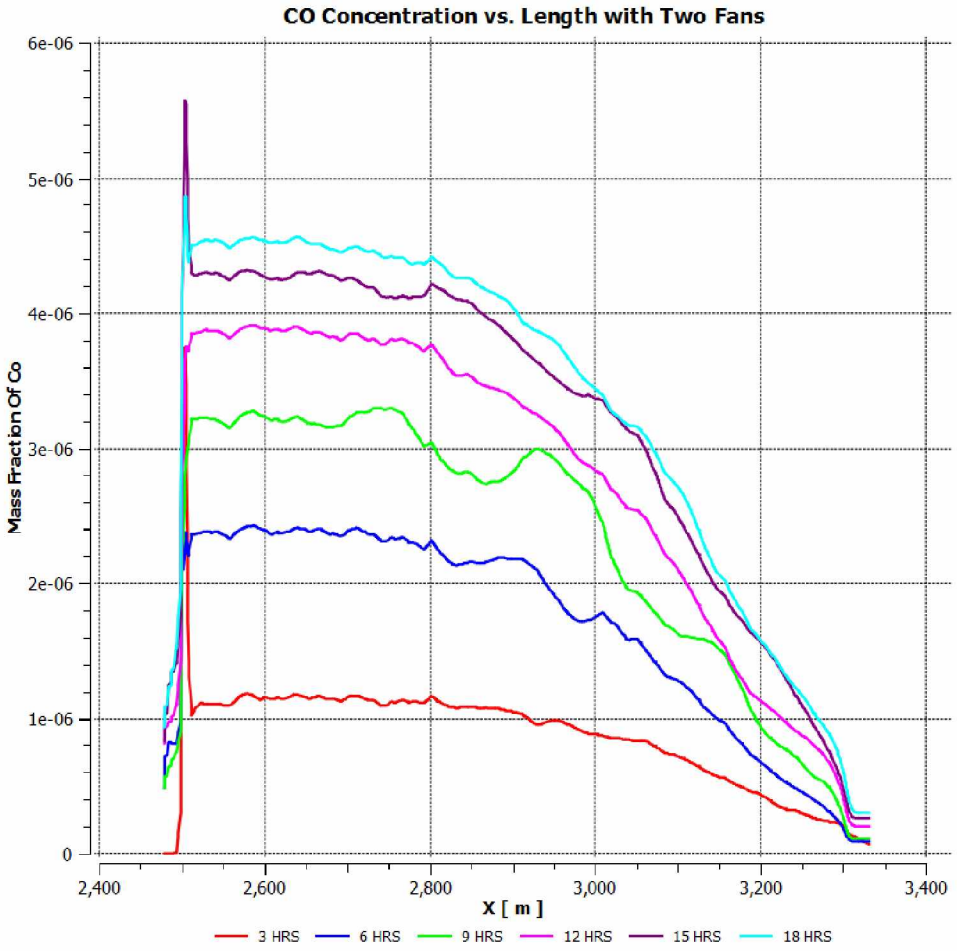

Figure 5.24: CO Concentration in the 2010 Pit with Two 142 m^3/s Fans (3 Hour Intervals)

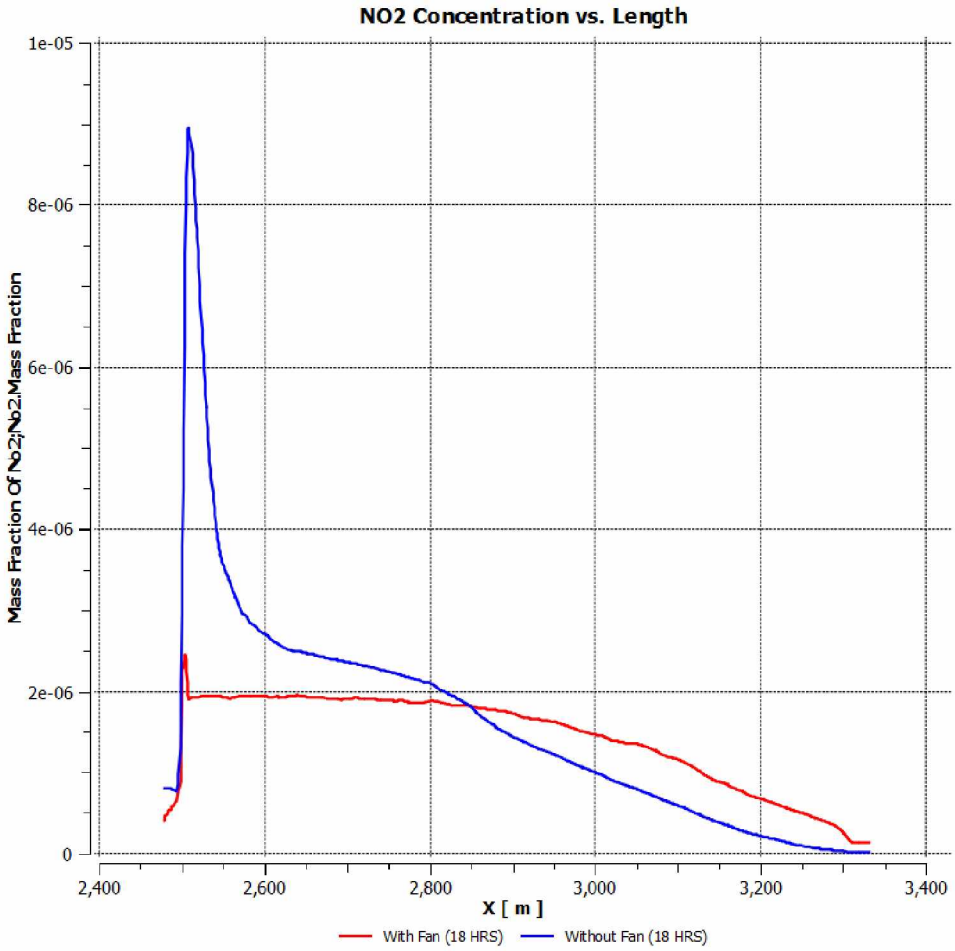

Figure 5.25: NO_2 Concentration in the 2010 Pit with and without Ventilation (18 Hrs)

5.5 Exhaust Fans—Multiple Fans, Multiple Sources (284 m^3/s)

In the final mitigation scenario considered in this research, the capacity of the two exhaust fans in the two source model was increased to 284 m^3/s (600,000 cfm) for a combined total of 556 m^3/s (1.2 million cfm) of airflow. It should be noted that supplying this volume of ventilating air would most likely be impractical in an industrial setting.

Figure 5.26 shows the CO concentration along a vertical cross section in the 2010 pit for the two 284 m^3/s fans. Again, it can be seen from the figure that the two fans cannot prevent the build-up of contaminants in the pit when two truck-shovel fleets are operating. Figure 5.27 compares the contaminant concentrations in the 2010 pit along a vertical cross section for the three cases: 1) No fans, 2) Two 142 m^3/s fans, and 3) Two 284 m^3/s fans. Compared to the 142 m^3/s fans, the larger fans reduce peak CO concentrations by an additional 0.6 ppm near the ground surface. Peak NO_2 concentrations are reduced by an additional 0.5 ppm near the surface when the larger fans are used (Figure 5.28).

Figure 5.29 shows the concentration of CO along a horizontal cross section in the pit with the two 284 m^3/s fans. The larger fans have the effect of homogenizing the contaminant concentrations; the concentration of NO_2 is nearly constant along the length of the cross section. Figure 5.30 compares the NO_2 concentrations in the 2010 pit along a horizontal cross section for the three cases discussed above. The larger fans further reduce the peak NO_2 concentration. However, the larger fans do not seem to

provide a significant improvement in the local dilution of contaminants. The smaller fans reduced peak NO_2 concentrations by 7 ppm. Doubling the fan capacity reduces peak NO_2 concentration by 7.5 ppm, an increase of only 0.5 ppm NO_2.

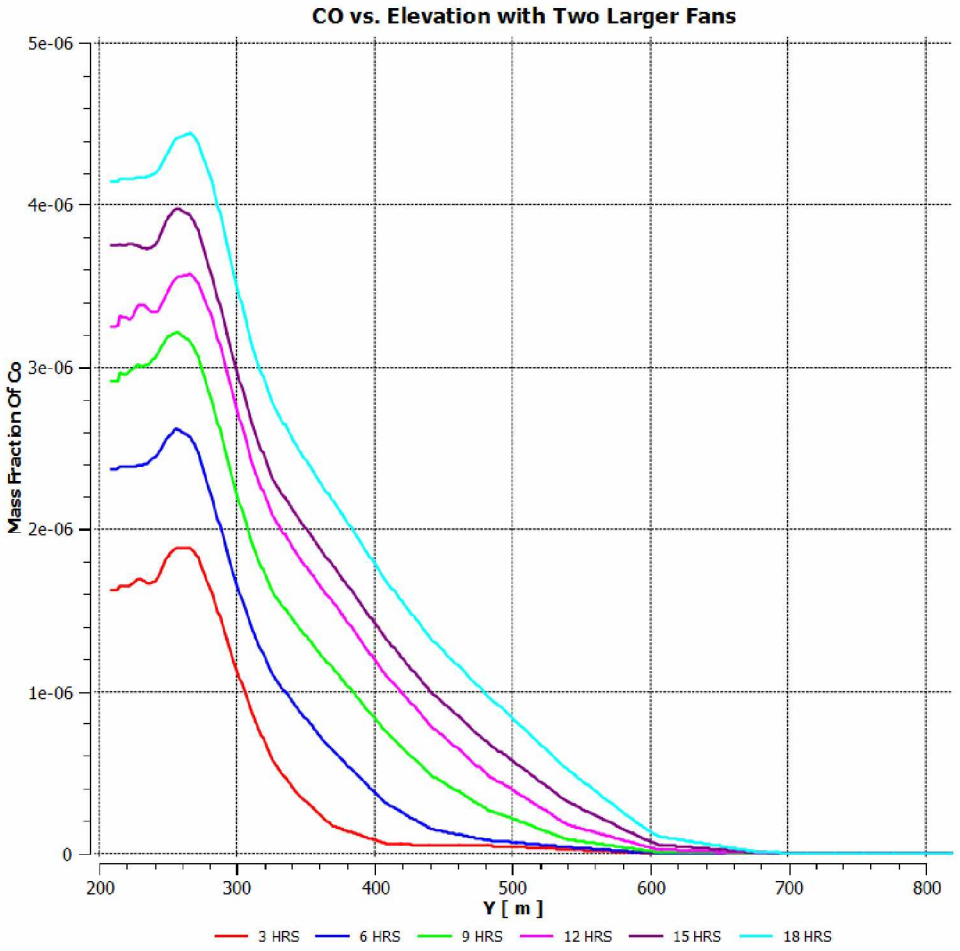

Figure 5.26: CO Concentration in the 2010 Pit with Two 284 m^3/s Fans (3 Hour Intervals)

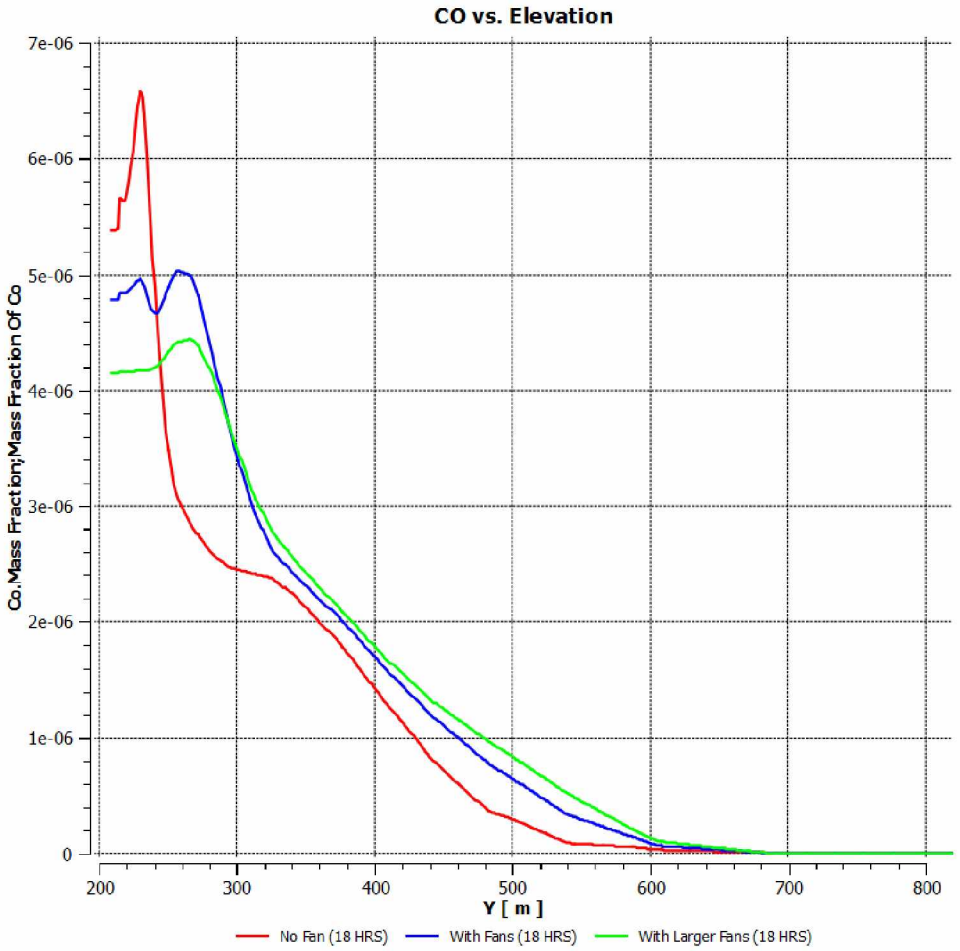

Figure 5.27: CO Concentration in the 2010 Pit with and without Ventilation (18 Hrs)

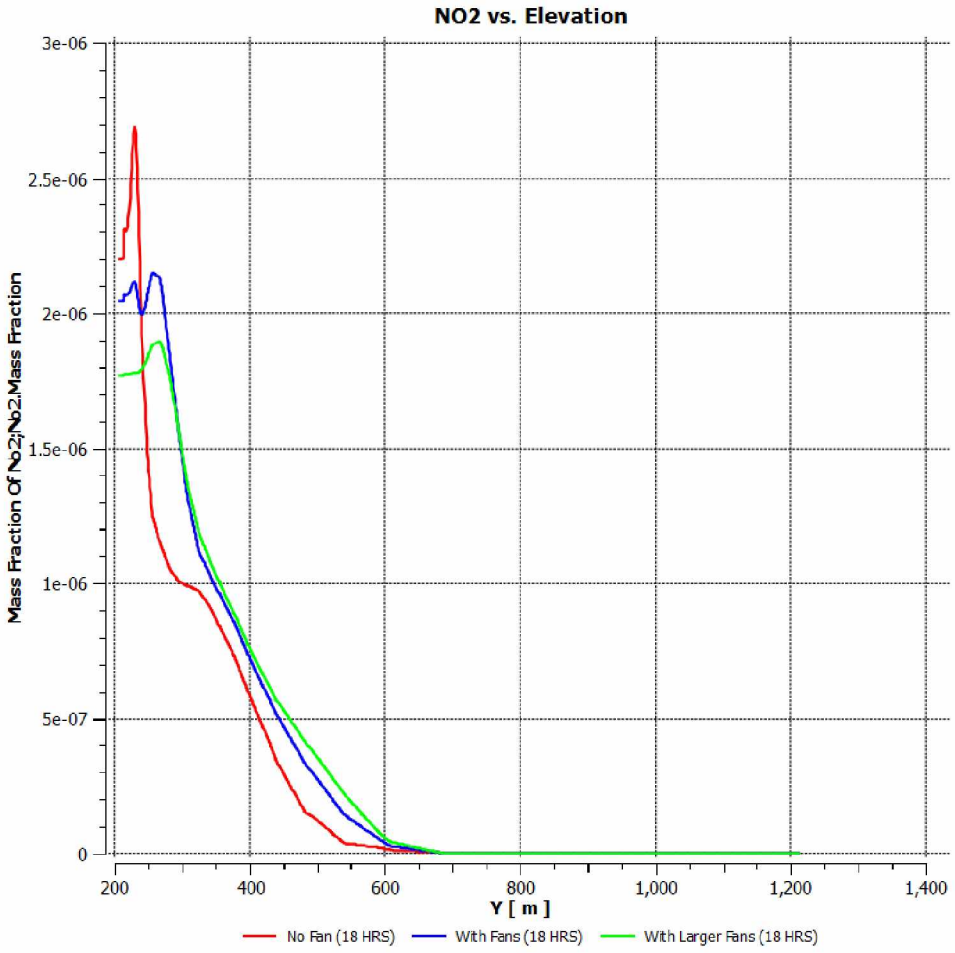

Figure 5.28: NO_2 Concentration in the 2010 Pit with and without Ventilation (18 Hrs)

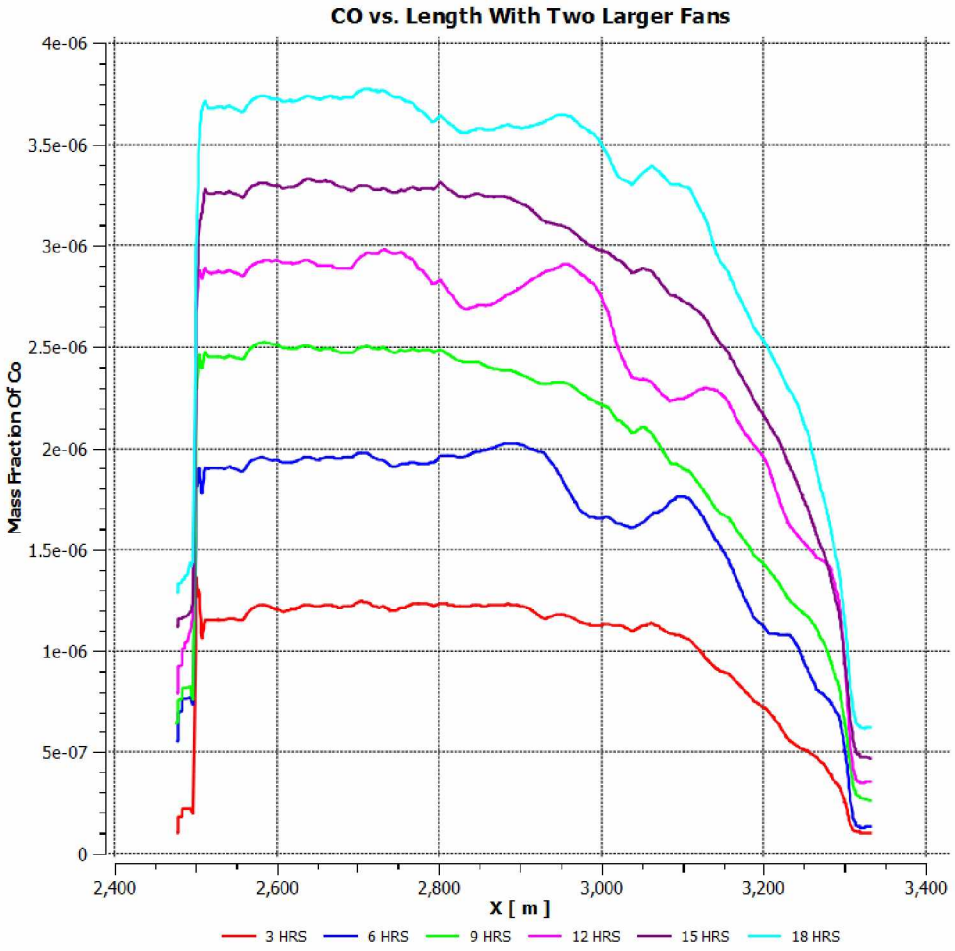

Figure 5.29: CO Concentration in the 2010 Pit with Two 284 m^3/s Fans (3 Hour Intervals)

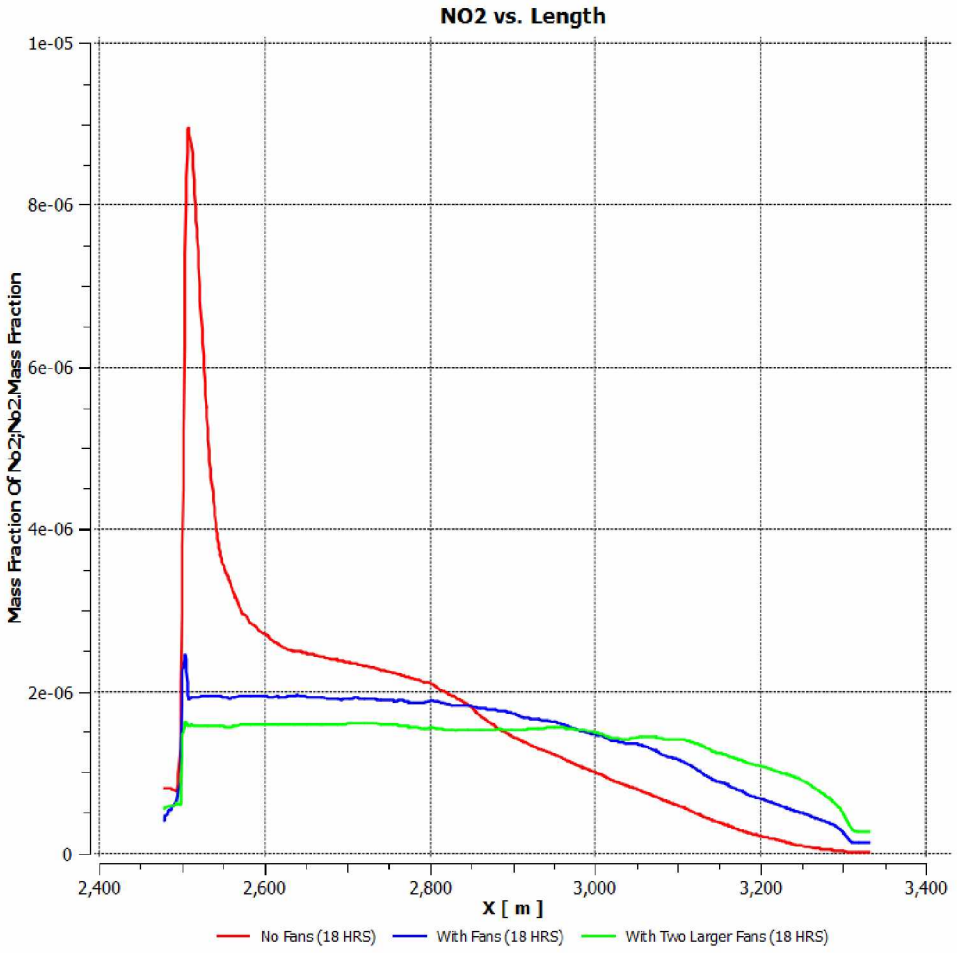

Figure 5.30: NO_2 Concentration in the 2010 Pit With and without Ventilation (18 Hrs)

Chapter 6: Summary, Conclusions, and Recommendations for Future Work

6.1 Summary and Conclusions

The concentrations of pollutants within the pit is a concern to worker health and safety, but this issue has received very little attention in the published literature. CFD modeling has been widely used in atmospheric pollution studies in urban areas. However, none of those models or studies including those models has addressed ventilation design for deep, open pit mines in general and especially in arctic or sub-arctic conditions. Pollutant transport and dispersion in deep open pit mines is complex, and any solution requires a good understanding of the interaction of the ABL, heat transfer in cold regions, aerodynamic movement of air, air inversion processes, meteorology, pollutant sources, and application of fans in open pit mines.

The atmosphere in an open pit mine is highly dependent on the mine geometry, mesoscale meteorological processes, the air inversion process, pollutant sources, and the application of fans or other mitigation measures.

Ventilation design for open pit mines requires knowledge of the quantity of the pollutants that are liberated into the pit from various sources. The most important items in the total balance of pollutants in open pit mines are the stationary point sources (drilling rigs, excavators, loading machines) and moving sources (such as trucks). The transport of admixtures from these sources in an open pit mine is directly related to the aerodynamics of the airflow in the open pit. Evaluation of the atmospheric conditions in an open pit mine, thus, requires a determination of the

concentration of admixtures. CFD is an effective tool for simulating the transport and dispersion of pollutants in deep open pit mines under arctic air inversion. The CFD techniques are rather complex, but CFD is capable of modeling complex geometries, thermal effects, and flow conditions. The meteorological conditions within the open pit are significantly affected by the temperature, wind velocity and solar radiation. The complex geometry, uncontrolled wind flows and other conditions (sources of pollutants) within the open pit mine makes it extremely difficult to model the transport and dispersion of pollutants within the pit.

Appropriate mathematical model is needed for this complex interactions. Meshing a large, highly irregular geometry, such as an open pit mine, is a challenge. The sharp edges and irregular boundaries of the model domain can result in poor quality mesh elements. A quality mesh is an essential first step in obtaining a quality CFD analysis. It is important to refine the mesh in areas with large flow gradients. Selection of an appropriate mesh is a trial and error process. A refined mesh is required to capture the large velocity, heat flux, and concentration gradients in these particular areas. It appears that a triangular element is well suited for meshing a two-dimensional profile of an open-pit mine. Modeling turbulence is critical to problems in open pit mine ventilation. The natural wind flow in open pit mines is often recirculatory. The geometry of an open pit mine naturally generates large amounts of mechanical turbulence. Turbulence is important from a modeling perspective because turbulence

affects the values of mass diffusion coefficients, convective heat transfer coefficients, and many other parameters.

A two-dimensional (2D) model for the flow of air in an actual, deep, open-pit mine in the arctic and the characteristics of pollutant distribution was modeled. The transport and dispersion of pollutants were investigated. One of the goals for the 2D model development and analysis was to characterize the parameters and values of the governing parameters. In the model results, various trends were observed with respect to both the recirculatory patterns and the distribution of the pollutants. Though the 2D model shows significant features of the patterns of recirculatory airflow and pollutant transport, it fails to provide a realistic assessment because of the lack of the third dimension. Thus, flow characteristics and peculiarities of the actual mine could not be captured with this model. In the absence of the 3-D geometry, it is possible that the model could not be properly scaled to the flow regime.

The effect of depth, wind velocity, and pit slope angle on the recirculation within open pits was studied. In general, the flow regime in each open pit model transitions from a laminar region at the top of the pit to turbulent flow at the bottom of the pit. The size of the turbulent eddies vary as a function of velocity, pit depth, and slope angle. Modeling heat flux at the pit boundary is necessary in order to simulate an atmospheric inversion. A modified modeling approach has allowed for model convergence under non-neutral atmospheric conditions. A fully compressible CFD model (which uses the ideal gas law to determine density) is complex, and convergence problems are very

common. An alternative to the fully compressible approach is to use the incompressible ideal gas law to determine the air density. The alternative approach modifies the ideal gas law by assuming a constant operating pressure. The density is then calculated solely as a function of temperature. Model convergence is much more easily achieved when the incompressible ideal gas law is used as opposed to a fully compressible model.

The microclimate that is created in the deep open pit mines due to the influence of external ABL and the contributions of mechanical and thermal forces significantly influences the recirculatory zone and transport and dispersion of the pollutants within the pit. The numerical results show that fairly strong turbulence exists in the pit, which is possibly caused by the interaction of the non-linear and diffusion terms in the governing equations. Lack of ventilation air and negative thermal energy are the primary reasons for stable stratification of the pollutant admixture accumulation in the pit.

A variety of different exhaust fan configurations were modeled to determine if mechanical ventilation could successfully clear the pit of contaminants during an inversion. The ventilation scheme was largely ineffective at removing polluted air from the pit during the inversion. Positive results were seen for a very large fan volume (1.2 million cfm), but supplying this quantity of air to the pit is probably impractical.

6.2 Future Work

Many of the shortcomings of this research would be mitigated by a geometrical three-dimensional (3D) model, which, in addition to providing a third dimension to the

model space, would also resemble the actual mine geometry, thus capturing the geometry-initiated inflections of both the velocity and the pollutant fields.

There may be several conceivable remediation techniques, including an exhaust fan and duct system, a push-pull ventilation system (in which a forcing and an exhaust fan could be used in tandem), or addition of extra heat near the pit bottom. Some of these techniques may be studied be using the 3D models.

This research focused solely on gaseous transport and dispersion. The generation and transport of aerosols is also of significant interest to the mining industry. Exposure to particulates in the mine atmosphere—such as dust and DPM—can result in chronic diseases in miners. Future research into the transport and dispersion of aerosols under arctic air inversion would be of great interest to the mining community.

Chapter 7: References

Allwine, K.J., X. Bian, C.D. Whiteman, and H.W. Thistle, "Valdrift – A Valley Atmospheric Dispersion Model," Journal of Applied Meteorology, Vol. 36, pp. 1076-1087, 1997.

Aloyan, A.E., A.A. Baklanov, and V.V. Penenko, "Fictitious Regions in Numerical Simulation of Quarry Ventilation," Soviet Meteorology & Hydrology, Vol. 7, pp. 32-37, 1982.

ANSYS, Inc. (2009), ANSYS Fluent Theory Guide, ANSYS, Inc.

ANSYS, Inc. (2009), ANSYS Fluent User's Guide, ANSYS, Inc.

ANSYS, Inc. (2009), ANSYS Meshing User's Guide, ANSYS, Inc.

Baklanov, A., "Application of CFD Modelling in Air Pollution Problems: Possibilities and Gaps," Environmental Monitoring and Assessment, Vol. 65, No. 1-2, pp. 181-189, 2000.

Baklanov, A.A., " Determining the Propagation of Impurity in the atmosphere of a Pit on the Basis of Mathematical Modeling," Soviet Mining Science, Vol. 20, No. 5, pp. 402-407, 1984.

Baklanov, A.A., "A Method for Evaluating the Energy Characteristics of the Air in an Open pit Mine," Soviet Mining Science, Vol. 22, No. 1, pp. 66-70, 1986.

Baklanov, A.A. and O.Y. Rigina, "Effectiveness of Cascade Ventilation Systems for Open pit Mines," Soviet Mining Science, pp. 152-157, 1993 (In Russian).

Bandopadhyay, S., and V.Y. Izaxon, Health and Safety Problems in Mining in the Arctic," Proceedings of the 8th International Symposium on Mining in the Arctic, Melinikov and Reshetnyak (eds.), Mining Institute of the Kola Science Center, Russian Academy of Sciences, pp. 139-156, 2005.

Bandopadhyay, S., and R.V. Ramani, "Computer aided Analysis of Exhaust Dispersions in Underground Airways," The Canadian Institute of Mining and Metallurgical Bulletin, Vol. 76, No. 858, pp. 69-74, October 1983.

Bandopadhyay, S., and R.V. Ramani, "Convection Diffusion Equations in Mine Ventilation Planning," Proceedings of the 3rd International Mine Ventilation Congress, The Institution of Mining and Metallurgy, The Institution of Mining Engineers, England, M.J. Howes and M.J. Jones (eds.), pp. 397 -404, 1984.

Bandopadhyay, S., and R.V. Ramani, "Mine Planning with Diesel Powered Equipment Ventilation Considerations," Proceedings of the 2nd U.S. Mine Ventilation Symposium, P. Mousset Jones (Editor), A.A. Balkema, pp. 627-636, 1985.

Bandopadhyay, S., and R.V. Ramani, "Mass Transfer Problems in Mine Ventilation: Some Solution Strategies," Proceedings of the 4th International Mine Ventilation Congress, A.D.S. Gillies (ed.), Australian Institute of Mining and Metallurgy, pp. 73-83, July, 1988.

Bell, M.L., D.L. Davis and T. Fletcher, "A Retrospective Assessment of Mortality from the London Smog Episode of 1952: the Role of Influenza and Pollution," Environmental Health Perspectives, January, pp. 6-8, 2004.

Belousov, V.I., "Natural Dynamic Ventilation of Open pit Mines," Soviet Mining Science, Vol. 21, No. 3, pp. 264-267, 1985.

Belousov, V. I., "Ventilation of Open pit Mines by Controlling the Boundary Layer of the Wind Stream," Vol. 25, No. 3, pp. 267-270, 1990.

Belousov, V. I, "Breeze Circulation in Open Pit Mines," Journal of Mining Science, Vol. 31, No. 3, pp. 216-220, 1995.

Blocken, B., T. Stathopoulos and J. Carmeliet, "CFD Simulation of the Atmospheric Boundary Layer: Wall Function Problems," Atmospheric Environment, Vol. 41, No. 2, pp. 238-252, 2007.

Bowling, S. A., "Climatology of High Latitude Air Pollution as Illustrated by Fairbanks and Anchorage, Alaska," Journal of Climate and Applied Meteorology, Vol. 25, pp. 22-34, 1986.

Collingwood, W., K. Raj, A. Choudhury, and S. Bandopadhyay, "CFD Modeling of Air Flow in an Open Pit Mine", Mining Engineering, Vol. 64, No. 2, pp. 44-50, 2012.

Dmitriev, M. T., and A.S. Shadrin, "Formation of Photochemical Smog in Open Pits," Soviet Mining Science, Vol. 2, March-April, pp. 97-100, 1973.

Doran, J. C., and T. W. Horst, " An Evaluation of Gaussian Plume-depletion Models with Dual-tracer field Measurements," Atmospheric Science, Vol. 19, pp. 939-951, 1985.

Fomin, A. A., "Modeling of Natural Convection in an Open Pit," Fluid Dynamics, Vol. 31, No. 4, pp. 490-496, 1996.

Hartman, B., and G. Wendler, "Climatology of the Winter Surface Temperature Inversion in Fairbanks, Alaska," 85th AMS Annual Meeting, San Diego, CA, American Meteorological Society, JP2.26, pp. 2767-2773, 2005.

Holty, J. G, "Air Quality in a Subarctic Community, Fairbanks, Alaska," Arctic, Vol. 26, pp. 292-302, 1973.

Jacob, D. J., "Introduction to Atmospheric Chemistry," Princeton University Press, pp. 14-15, 1999.

Jacobson, M.Z., "Fundamentals of Atmospheric Modeling," Cambridge University Press, New York, 2005.

Kantipudi, Rohini, E.C. Nsofor, Y.P. Chugh and V.K. Kollipara, "CFD Modeling of Airflow Distribution Around a Room-and-Pillar Mining Face Area," Proceedings of the Ninth International Mine Ventilation Congress 2009, edited by D.C. Panigrahi, Dhanbad, Mohan Primlani, Oxford and IBH Publishing Co. Pvt. Ltd., New Delhi, India, 2009.

Lowndes, I.S., S.A. Silvester, S.W. Kingman and D.M. Hargreaves, "The Application of an Improved Multi-scale Computational Modelling Techniques to Predict Fugitive Dust Dispersion and Deposition Within and from Surface Mining Operations", 12th

U.S./North American Mine Ventilation Symposium 2008, K.G. Wallace, ed. Reno, NV, University of Nevada, Reno, 2008.

Mölders, N. and G. Kramm, "A Case Study on Wintertime Inversions in Interior Alaska with WRF," Atmospheric Research, Vol. 95, pp. 314-332, 2010.

Peng, X., and G.R. Lu, "Physical Modeling of Natural Wind and its Guide in Large Open Pit Mines," Journal of Wind Engineering and Industrial Aerodynamics; pp. 54-55 and 473-481, 2005.

Purusotham, T. and S. Bandopadhyay, "Analyzing Shock Losses at Air-Crossings in a Mine Ventilation Network using CFD Simulations," Proceedings of the 13th U.S./North American Mine Ventilation Symposium 2010, edited by Stephen Hardcastle and D.L. McKinnon, Omnipress Sudbury, Ontario, Canada, 2010.

Reed, W.R., "Significant Dust Dispersion Models for Mining Operations," NIOSH IC 9478, Pittsburgh, PA, 2005.

Reichardt, P.B. and S.K. Reidy, "Atmospheric Polycyclic Aromatic Hydrocarbons: an Aspect of Air Pollution in Fairbanks, Alaska," Arctic, Vol. 33, No. 2, pp. 316-325, 1980.

Sharan, M., and M. Modani, "A Two-dimensional Analytical Model for the Dispersion of Air Pollutants in the Atmosphere with a Capping Inversion," Journal of Atmospheric Environment, Vol. 40, No. 3, pp. 3479-3489, 2006.

Shi Yong, X., S. Feng, and F. S. Wei, "Three-Dimensional Nonhydrostatic Numerical Simulation for the PBL of an Open Pit Mine," Boundary Layer Meteorology, Vol. 94, pp. 197-224, 2000.

Skobunov, V.V., "Dissipation of Admixtures from Point Sources," in Air Pollution in Mines—Theory, Hazards, and Control, Academy of Sciences of the USSR Mining Institute, 1962.

Stephens, M. and F. Calizaya , "A Study of Leakage Flow in a Laboratory Model and Using CFD," Proceedings of the 13th U.S./North American Mine Ventilation Symposium 2010, edited by Stephen Hardcastle and D.L. McKinnon, Omnipress, Sudbury, Ontario, Canada, 2010.

Stull, R.B. "An Introduction to Boundary Layer Meteorology", Kluwer Academic Publishers, Netherlands, 2003.

Tandon, N., and R. Bhaskar, "Numerical Fluid Modeling for Idealized and Actual Geometry of a Large Open pit Mine," Proceedings of the 91st Annual Meeting and Exhibition of Air and Waste Management Association, San Diego, CA, (98-MA3A-04 (A71)), 1998.

Taylor, G.I., "Diffusion by Continuous Movements," London Mathematical Society, Vol. 20, pp. 196-211, 1921.

Tran, H.Q.N, and N. Mölders, "Investigations on Meteorological Conditions for Elevated PM2.5 in Fairbanks, Alaska, Atmos. Res. 99: 39-49, 2011.

TRC Environmental Consultants, Inc., "Dispersion of Airborne Particulates in Surface Coal Mines—Data Analysis." EPA-450/4-85-001, US EPA, NC, 1985.

Vershinin, A.A., "Comparative Assessment of Schemes for Artificial Ventilation of Quarries," Vol. 12, No. 6, pp. 627-630, 1976.

Wallace, J. and P.V. Hobbs, Atmospheric Science: An Introductory Survey, Elsevier, Burlington, MA, 2006.

Warner, T.T., R.A. Peterson, and R.E. Treadon, "A Tutorial on Lateral Boundary

Conditions as a Basic and Potentially Serious Limitation to Regional Numerical Weather Prediction," Bulletin of the American Meteorological Society, Vol. 78, No. 11, pp. 2599-2617, 1997.

Wendler, G. and K.O.L.F. Jayaweera (1972), "Some Measurements of the Development of the Surface Inversion in Central Alaska during Winter," Pure and Applied Geophysics, Vol. 99 (1), pp. 209-221.

White, F.M. , Viscous Fluid Flow, McGraw-Hill, New York, N.Y, 2006.

Winges, K.D., Fugitive Dust Model (FDM) User's Guide (Revised), Vol.1, User's Instructions, US EPA/910/988/202/R, 1990.